THE DEVELOPMENT AND ORGANIZATION OF DENDRITES OF MOTONEURONS IN LARVAL ZEBRAFISH

A Disseration

Presented to the Faculty of the Graduate School

of Cornell University

In Partial Fulfillment of the Requirements for the Degree of

Doctor of Philosophy

by

Sandeep Kishore

January 2011

THE DEVELOPMENT AND ORGANIZATION OF DENDRITES OF MOTONEURONS IN LARVAL ZEBRAFISH

Sandeep Kishore, Ph.D.

Cornell University 2011

The work described here focuses on novel patterns of motoneuron dendritic organization and dendritic development in relation to the recruitment patterns of spinal motoneurons that drive swimming in larval zebrafish. I first looked at the dendritic organization of motoneurons in freely swimming fish and tracked its emergence in relation to the maturation of locomotor behavior. I used transient expression of fluorescent proteins to visualize the dendritic structure of motoneurons in zebrafish larvae at a stage when they have been swimming freely for a few days. My work showed that there is a dendritic topography related to the recruitment of motoneurons at different locomotor speeds that emerges by the time fish first begin to swim, and is maintained even as dendrites grow after the onset of spontaneous swimming. Since neuronal activity is thought to influence dendritic structure, I then studied the structural dynamics of dendritic arbors of individual motoneurons in larval zebrafish soon after they begin swimming. I found a systematic relationship between the location of a spinal motoneuron and the dynamics of its dendritic arbor – youngest, ventral motoneurons are least dynamic whereas increasingly older and more dorsal motoneurons are more dynamic. This is contrary to the idea that dendrites of younger neurons are more dynamic than dendrites of older neurons because younger ones are growing more. I then asked if this pattern of dendritic dynamics is related to the systematic variation of excitability of motoneurons described recently. I tested this possibility genetically by expressing Kir2.1 to suppress excitability of individual

motoneurons. This led to a dramatic increase in the dynamics of ventral motoneurons, which became more dynamic than more dorsal ones. My results suggest that a naturally occurring dorsoventral gradient of excitability may contribute to the variation in dendritic dynamics. The patterns of dendritic organization and development I describe may also be applicable to other interneuron types in the spinal cord and hindbrain.

BIOGRAPHICAL SKETCH

Sandeep Kishore received his undergraduate degree in Biochemistry at University of Delhi. It was at during this time that he developed a broad interest in biology and evolution. This interest slowly morphed, first, into an interest in understanding how the nervous system evolved, and subsequently, in understanding how the nervous system works.

In August 2002, he joined the doctoral program for Neurobiology and Behavior at Stony Brook University. In June 2003, he joined the lab of Dr. Joseph Fetcho, and in May 2004, he received his Masters degree in Neurobiology and transferred to the doctoral program for Neurobiology and Behavior at Cornell University in August 2004. He has been in Dr. Fetcho's lab at Cornell during his time at Cornell.

TABLE OF CONTENTS

LIST OF FIGURES

CHAPTER 1

INTRODUCTION

Precise connectivity between neurons is critical for processing sensory input correctly and for generating appropriate motor output. The mechanisms that determine connectivity in sensory circuits are understood in some detail. In contrast, how spinal motor networks are wired up is largely unknown. In sensory circuits, topography in the distribution of axons and dendrites provides a first layer of specificity in connectivity. Determining the mechanisms that establish this topography has provided insights into how sensory circuits are wired [1, 2]. The discovery of anatomical topography in motor circuits can similarly simplify the task of understanding how connectivity is established in motor circuits. This thesis takes advantage of the recent description of an orderly organization of motoneuron somata related to their recruitment at different swimming speeds, to look for patterns of dendritic organization and dendritic development related to soma position as the locomotor behavior of zebrafish develops.

The experiments described in this dissertation focus upon the following questions: Are dendrites of motoneurons innervating axial musculature topographically organized? When does this topography emerge in relation to the maturation of locomotor behavior? Does this topography emerge due to targeted dendritic growth or as a consequence of selective pruning from an initially exuberant structure? Finally, are the dendritic dynamics underlying dendritic growth influenced by the intrinsic excitability of motoneurons? We chose to address these questions in the spinal motor network of larval zebrafish. The goal of these experiments is twofold: first, to determine if an anatomical topography underlies a recently discovered age

related functional organization in relation to swimming speed in larval zebrafish [3] and, second, to explore the emergence of this topography in relation to the development of motor behavior [4] in larval zebrafish. The discovery of an age and functional-related anatomical topography for swimming circuits in larval zebrafish lays the foundation to search for similar patterns of dendritic organization in motor circuits of other vertebrates. It also sets the anatomical framework to test for genetic and activity dependent mechanisms that determine wiring in motor networks.

Much of our current understanding of how central circuits wire up is derived from experiments that seek to understand how axonal and dendritic topography is established and maintained in sensory circuits. I first review seminal experiments that led to the current thinking about wiring in sensory circuits, followed by a review of the literature on dendritic organization and development, and the mechanisms that influence dendritic development in sensory circuits. I then review the literature on how central motor networks are wired up in invertebrates and in vertebrates. Finally, I discuss how the discovery of an age-related topographic organization of spinal motor networks in larval zebrafish, in combination with the technical advantages of zebrafish larvae, provides an opportunity to understand how vertebrate spinal circuits are wired up.

Circuit Formation in Sensory Systems

Historically, two classic experiments have shaped the broad framework within which wiring hypotheses have been developed and tested. In the 1940s, Roger Sperry performed experiments in which he surgically cut the optic nerve, rotated the eye in newts 180 degrees and studied their visuomotor behaviors after the nerve regenerated. After the surgery, the newt motor behavior in response to a lure was as if their visual

world were back to front and upside-down [5]. Sperry proposed that when the axons of the rotated eye regenerated they projected back to their original targets instead of "correcting" for the altered representation of visual space. This led Sperry to postulate that molecular gradients exist across the retina and the tectum which determine where in the tectum retinal axons would terminate. This idea of wiring determined by molecular cues has since come to be known as the chemoaffinity hypothesis.

In sharp contrast to the notion of a "hard-wired" brain, Hubel and Wiesel performed experiments in cats which revealed that sensory experience can also have a profound role in the the organization of developing circuits. Hubel and Wiesel first showed that visual cortical neurons in normal cats can be categorized as: a. responding to visual stimulus from the ipsilateral eye or the contralateral exclusively (monocular); b. responding to visual stimuli from both eyes (binocular) [6]. In a subsequent set of experiments, Hubel and Wiesel showed that suturing one eye shut early in development for several months led to a dramatic alteration in the response properties of visual cortical neurons such that most visual cortical neurons now responded exclusively to the open eye [7]. These early studies by Sperry and, Hubel and Wiesel, appear to have led to a conceptual dichotomy where activity dependent mechanisms and molecular cues were thought to be mutually exclusive in circuit formation.

Hubel and Wiesel also showed that cortical neurons in Layer 4 of the visual cortex in monkeys were largely monocular in their response properties and these neurons were organized in a series of alternating columns; any given column contained neurons that responded exclusively to visual input to one of the eyes [8]. This organization came to be known as ocular dominance columns and this functional organization of neurons was shown to be a result of the axonal organization from thalamic afferents to layer 4. Hubel and Wiesel subsequently showed that ocular

dominance columns were disturbed in response to monocular deprivation; columns that represented the open eye became much wider compared to the columns of the deprived eye [9, 10]. They thus showed that activity dependent changes in the functional properties of neurons had an anatomical correlate. Several studies since then have used the topographic organization of axons as a way to test wiring hypothesis. Work in several other systems showed that sensory axons are topographically organized and understanding the mechanisms that lead to the topographic organization of circuits provides insights into how neuronal circuits are wired up. Topographically organized circuits are also known as topographic maps.

Based on decades of experiments on the topographic organization of axons in different sensory circuits in different model systems, there are two models of map formation. The first model based on data from several systems argues that axons initially overgrow and form exuberant connections and final topography is achieved by the elimination of inappropriate axonal projections [11]. A second model of map formation suggests that the targeting of axons is precise from the onset, and the initial topography of axons is highly precise without need of refinement [12]. It is now generally accepted that many maps are quite precisely organized before the onset of function and subsequent neuronal activity is necessary to maintain and tweak the circuit in the face of continued synaptogenesis after birth [13].

Though the initial understanding of map formation came largely from studying axonal organization and development, work on dendritic structure and development lagged behind largely because of inaccessibility of postsynaptic neurons located deep in the brain. It was unclear if dendrites of postsynaptic neurons were organized topographically. It was also unknown if the dendrites were passive players in

establishing precise connectivity or if genetic programs and neuronal activity influence their patterns of arborization.

Dendritic organization and development in sensory systems

Clear data that dendrites, and not just axons, are organized spatially first came from studies on the structure of retinal ganglion cells. These studies showed that dendrites of on- and off-retinal ganglion cells occupied distinct lamina in the retina and were spatially segregated from each other [14]. Subsequent work in the somatosensory cortex [15], visual cortex [16] and olfactory bulb [17] showed that dendritic organization is a common organizational feature of first order post-synaptic neurons in many sensory circuits. Cells in layer 4 of the somatosensory cortex of rodents are anatomically clustered as "barrels" such that they reflect the arrangement of whiskers on the snout [30]. Dendrites of layer 4 cells in the somatosensory cortex are oriented such that they remain within the topographic boundaries of the barrel – cells at the edge of the barrel have asymmetric dendritic trees that are oriented such that most of the tree is localized to one barrel [15]. In the cat visual cortex, dendrites of layer 4 spiny stellate cells at the edges of ocular dominance columns preferentially arborize within one column [16]. In the olfactory system, dendrites of mitral cells are confined to single glomeruli [17]. Thus, dendritic and axonal organization confers a layer of specificity in the connectivity of many sensory circuits.

Whether dendritic organization is precise from the onset or whether it is achieved by the selective elimination of inappropriate branches from initially exuberant growth has been the focus of several decades of experiments. The precise adult laminar organization of retinal ganglion cell dendrites has made retinal circuits a model system of choice for studying dendritic development. Based on analyzing

morphological data at different developmental time points, Chalupa and colleagues proposed that dendrites of retinal ganglion cells are not stratified early in development, and achieve stratification by the elimination of inappropriate branches. This was reflected in the functional response properties of retinal ganglion cells. RGCs early in development receive input from 'ON' and 'OFF' bipolar cells, but respond only to 'ON' or 'OFF' in parallel with the stratification of dendrites [18, 19]. Dendritic refinement is similarly observed in mitral cells in the olfactory bulb, which initially have multiple primary dendrites that contact multiple adjacent glomeruli during development [17]. However, they lose all but one of the primary dendrites and associate with a single glomerulus as adults. Thus, until recently, based on these and other similar studies, excessive and inappropriate growth followed by the pruning of wrong branches has been the dominant model of establishing dendritic organization in sensory circuits.

Recent work shows that, in many cases, dendritic organization may be more precise than previously suggested and could be achieved by targeting dendrites to their right location from the onset. The first paper to show evidence of dendritic targeting came from the *Drosophila* olfactory system [20]. A series of experiments showed that dendrites of antennal lobe neurons are targeted to their precise location early in development. Subsequent work showed that dendritic targeting occurs in vertebrates as well. By monitoring the same retinal ganglion cells in larval zebrafish *in vivo* during development over several days, Mumm and colleagues showed that the dendrites of many retinal ganglion cells specifically arborize in their target layer [21]. Though some cells show branch pruning, dendritic targeting was the primary mechanism of achieving anatomical organization of RGC dendrites in larval zebrafish retina. A subsequent study suggests that dendritic targeting might be the primary

mechanism of organizing RGC dendrites in mouse retina as well [22]. These observations are in sharp contrast to all previous studies of vertebrate RGC dendrites.

A recent study that used genetic techniques to label specific RGC subtypes might help to reconcile the disparate observations from previous experiments [23]. Sanes and colleagues show that different RGC cell types in the mouse retina appear to have different programs of developmental growth – while some cell types are targeted to the correct lamina, other cell types have initially diffuse dendritic arbors that are pruned to achieve their correct stratification pattern. How neural activity and genetic mechanisms might influence these patterns of dendritic growth and distribution has been an area of intense scrutiny.

Role of molecular cues in determining dendritic arborization

The most extensive work on identifying molecules involved in dendritic targeting has come from Liqun Luo's lab by studying the *Drosophila* olfactory system. By performing a systematic clonal analysis using the MARCM technique [24], they showed that the glomerular choice of PN dendrites correlated with the lineage and birth time of the projection neurons [25]. They further showed that this glomerular organization of dendrites was achieved before the arrival of ORN axons [26]. Using imaging and pioneering genetic techniques, Liqun Luo's lab has identified a large number of molecules that target projection neuron dendrites to the correct glomerulus in the antennal lobe. While a detailed discussion of these molecules is beyond the scope of this review, the molecules implicated can broadly be classified as an ensemble of transcription factors [20], guidance molecules [27] and cell surface molecules [28]. It remains to be seen if and how the expression of guidance molecules and cell surface molecules implicated in targeting are related to the transcription factor

code, and ultimately how the transcription factor code is related to the lineage and age of projection neurons.

Given that many of these molecules have vertebrate homologs, it is plausible that molecules that play a role in dendritic targeting in *Drosophila* are involved in the organization of dendrites in vertebrates as well. Recent work shows that Dscam and Sidekick proteins are involved in specifying laminar connections in the chick retina [29]. Sophisticated genetic techniques such as those used in *Drosophila* will likely reveal the molecules involved in dendritic targeting among vertebrates.

Role of afferent activity in regulating dendritic development.

The role of neuronal activity in regulating the growth and structure of dendrites has been studied extensively. Experiments that test the role of neuronal activity in the formation of dendritic structure have explored the effects of deafferentation of sensory input, the effects of altered sensory input, the consequences of pharmacological block of excitation, or, more recently, genetic perturbation of excitatory input.

Deafferentation experiments lead to the atrophy of deafferented dendritic arbors which suggests that the maintenance of dendritic structure is dependent on synaptic input . Since the atrophy is localized to parts of the dendritic arbor that originally received the input, it suggests that the role of activity in influencing dendritic structure is mediated locally. However, a major caveat of these experiments is that these effects can also be interpreted as a consequence of a lack of trophic support from sensory afferents.

Another line of evidence for the role of neuronal activity in influencing dendritic structure comes from experiments that alter the sensory environment and

result in altered dendritic distribution without affecting overall growth of the dendritic arbor. Cells in layer 4 of the somatosensory cortex of rodents are anatomically clustered as "barrels" such that they reflect the arrangement of whiskers on the snout [30]. Dendrites of layer 4 cells in the somatosensory cortex in mice are oriented such that they remain within the topographic boundaries of the barrel – cells at the edge of the barrel have asymmetric dendritic trees that are oriented such that most of the tree is localized to one barrel, whereas dendritic trees of cells located towards of the center of the barrel do not show an orientation bias. Removing a row of whiskers early in development results in the formation of a giant barrel, and cells that would have been at barrel boundaries in normal mice are now at the center of these giant barrels. Interestingly, these cells now have radially symmetric dendritic arbors suggesting that arbor orientation can be influenced by changing sensory input [31, 32].

The orientations of dendritic arbors of cells in visual circuits have also been shown to be sensitive to afferent organization. The normal frog tectum receives input exclusively from the contralateral eye. Frog tecta can be experimentally made to receive input from 2 eyes by adding a third primordium during embryonic stages. Amazingly, afferents from the 2 eyes segregate within the tectum to form alternating stripes similar to ocular dominance columns in cats and primates [33, 34]. Katz and Constantine-Paton investigated if the dendritic structure of neurons in these altered tecta were different from dendritic arbors in normal tecta [35]. Dendritic arbors of some cells were seen to abruptly terminate at the borders between stripes, and these cells typically had small, highly branched arbors. Another category of cells had "clumps" of dendrites in stripes from both eyes but individual dendrites were restricted to a single stripe. Finally, there were several cells whose dendritic arbors did not appear to be influenced by stripe boundaries. This study suggested that afferent

activity modulates dendritic structure of some cells and not others. The sensitivity of dendritic structure of some cell types but not others to sensory manipulation can be better explained if their sources of presynaptic input and patterns of recruitment during function were better understood.

Several groups have attempted to understand if the effect of afferent activity is mediated by excitatory neurotransmission. Pharmacological blockade of glutamatergic neurotransmission in the retina prevents dendritic stratification that is normally observed in retinal circuit formation [19]. More direct evidence linking neurotransmission, sensory activity and dendritic growth came from a series of experiments done in Hollis Cline's lab [36]. Sin and colleagues clearly demonstrated increased dendritic growth of optic tectal neurons *in vivo* in response to visual activity. They further showed that this growth was blocked by exposure to APV and CNQX, NMDA-receptor and AMPA-R antagonists respectively, clearly showing that sensory activity induced changes in dendritic arbor growth are mediated by glutamatergic neurotransmission.

The role of neurotransmission has also been tested by genetically knocking out molecules involved in synaptic transmission. Remarkably, completely abolishing neurotransmission throughout development by genetically knocking out Munc-18-1, a protein needed for synaptic release, did not prevent circuit formation in different parts of the brain of mice [37]. However, after the initial formation of circuits, these mutant mice show extensive apoptosis of neurons. This study strongly suggests that synaptically mediated neurotransmission is not necessary for early circuit formation but necessary for subsequent maintenance and perhaps refinement of circuits.

Recent work using targeted genetic techniques unambiguously tested the role of afferent activity in regulating dendritic structure [38]. Retinal ganglion cells (RGCs) either receive input exclusively from ON or OFF bipolar cells (ON or OFF RGCs) or make similar numbers of synapses with both on different parts of the dendritic arbor (ON-OFF RGCs), a choice they make during the development of retinal circuits. Previous work had suggested that this choice is mediated by pruning inappropriate dendritic branches that bore less active inputs. By driving the expression of tetanus toxin light chain (TeNT) in ON bipolar cells, Kerchensteiner and colleagues genetically abolished glutamatergic transmission selectively in ON bipolar cells. TeNT is a bacterial protease that cleaves vesicle-associated membrane protein 2 (VAMP2) and inhibits vesicle fusion. This absence of presynaptic drive from ON bipolar cells only resulted in reduced synapse formation between ON bipolar cells and ON RGCs, but did not result in the pruning of dendritic branches that contained fewer synapses. This set of experiments shows that, at least in mammalian retinal circuits, glutamatergic transmission only regulates synapse formation but not synapse elimination or dendritic refinement. The authors suggest that different rules might guide activity-dependent development of different circuits and that this might be determined by distinct architectures of early neural circuits. Since some circuits show laminar architecture, the rules that determine activity dependent development in laminar circuits might be different from rules that determine topographic circuit organization in more continuous maps.

Dendritic dynamics during development

Static images of dendrites at early developmental stages in many systems showed fine protrusions, called filopodia, extending from the main dendritic branch (reviewed in [39]). The density and numbers of filopodia were observed to reduce later in

development concurrent with an increase in spine number. Their structural similarity to spines, and developmental appearance before spines led to the idea that filopodia could be precursors to spines. Their elongated morphology also suggested that filopodia could serve to facilitate contact between axons and dendrites. It was proposed that the presence of filopodia could simply be a passive mechanism to increase the dendritic cross-section of a neuron and hence increase the probability of contact with an ingrowing growth cone. Alternatively, filopodia could actively seek to initiate contact with nearby axonal shafts or growth cones [40]. The synaptotropic hypothesis states that synaptic contact in developing nervous systems are initiated by dendritic filopodia and the stabilization of a subset of these filopodia leads to dendritic arbor growth and provides the substrate for subsequent dendritic growth. While golgi staining and electron microscopy could provide static images, these hypotheses could not be directly tested without the ability to simultaneously image interactions between developing axons and dendrites in real time at a high spatial resolution. The advent of new imaging techniques such as multiphoton and confocal microscopy, in combination with the availability of novel dyes, paved the way for real time imaging of small neuronal structures in living tissue on the time scale of seconds to minutes.

The first study of dendritic dynamics using novel imaging techniques came from Stephen Smith's group [41]. Using time-lapse fluorescence confocal microscopy to directly visualize dendritic branches and spines of pyramidal neurons in developing hippocampal tissue slices, Daley and Smith demonstrated that during early development, filopodial structures on dendrites extend and retract rapidly on the time scale of minutes [41]. They also showed that as dendritic arbors mature, filopodia are replaced by relatively more stable spine-like structures, that nevertheless show changes in length and shape over a time scale of minutes. This pioneering study

revealed the highly dynamic state of developing dendrites and challenged the notion that dendrites are passive structures in synapse formation. Subsequent real time imaging studies, in vitro, of retinal ganglion cells [42], Purkinje cells [43], and cortical neurons [41, 44] and, *in vivo,* of developing tectal neurons in Xenopus larvae*,* provided compelling evidence that rapid dendritic dynamics is pervasive in developing nervous systems [45].

Several early experiments in the mammalian CNS were focussed on the relationship between dendritic filopodia and the formation of spines [41, 44]. However the demonstration that developing aspiny neurons, like retinal ganglion cells and tectal neurons in Xenopus, are highly dynamic suggested that dendritic filopodial dynamics serves a more general function in developing circuits than the formation of spines. The demonstration that developing dendrites are highly dynamic raised three related questions that have been the focus of subsequent experiments: What is the precise role of filopodial dynamics? What are the cellular mechanisms that determine how, when and where filopodia originate? How do filopodia interact with molecules and neuronal activity implicated in wiring the nervous system?

The first data to hint at the function of filopodia came from studies that simultaneously visualized dendrites and functional presynaptic boutons (using FM4-64) in hippocampal cell cultures [46]. This study was the first to observe dendritic filopodia initiating contact with neighboring axons which eventually resulted in the formation of a presynaptic bouton at the site of contact. *In vivo* time lapse two photon imaging in developing zebrafish suggested transient interactions between the Mauthner axon growth cone and filopodia of primary motor neurons [47]. This transient interaction led to the formation of a varicosities at the site of putative contact between the axon and dendrite, and based on electron microscropy data that showed

the presence of synaptic vesicles at thicker regions of the axon, the authors proposed that the varicosities are, in fact, a nascent synapse. Their work thus provided more evidence that the axonal and dendritic filopodial interactions were the sites of synaptogenesis. Finally, recent high resolution confocal imaging clearly shows that dendritic filopodia initiate contact with presynaptic neurons [48]. Taken together these studies strongly suggest that dendritic filopodia play an active role in initiating contact with potential pre –synaptic partners.

However, none of these studies provided evidence for the 'synaptotropic' hypothesis of dendrite development. Indirect evidence comes from Hollis Cline's lab: experiments done over the years to impair excitatory synapse formation lead to shorter and less complex dendritic arbors (reviewed in [49]). The most compelling experiments to provide support for the synaptotrophic hypothesis were done in the larval zebrafish optic tectum in Stephen Smith's lab [50]. In these experiments, single optic tectal neurons were co-labeled with a cytosolic red fluorescent protein to label the dendritic structure and PSD95-EGFP, a GFP-tagged form of a synaptic protein found at excitatory synapses, to visualize excitatory synapse formation. Simultaneous time lapse imaging of the dendritic arbor and putative synapses over the course of hours revealed that the stability of newly formed filopodia correlated with postsynaptic assembly on those filopodia. Filopodia that did not bear any synapses were retracted and synapse elimination was followed by filopodial retraction. They also showed that new filopodia emerged near existing synapses. These observations provide the best evidence for the synaptotrophic hypothesis. It remains to be seen if this is a general model for dendritic growth.

Since several lines of evidence suggest that dendritic filopodia actively seek to make connections, another line of inquiry attempted to understand if dendritic

filopodia originated in response to extracellular cues in the environment. Neural activity is pervasive in developing neural circuits and is thought to play a role in circuit formation. This motivated several groups to determine what role afferent activity and neurotransmission might play in the genesis of dendritic filopodia. Work done in developing CA1 hippocampal neurons [51] provides strongest evidence that filopodial dynamics is influenced by afferent activity and neurotransmission. Svoboda and colleagues used two-photon microscopy to image filopodial dynamics of CA1 dendrites in culture while simultaneously providing electrical stimulation close (about 3-10 um) to the dendrite. Using this experimental setup, they observed an increase in the numbers dendritic filopodia in response to tetanic stimulation, as compared to controls without any electrical stimulation. Furthermore this increase in filopodial numbers was blocked in the presence of APV, a specific antagonist for NMDA receptors. These experiments suggested that neurotransmitter release due to afferent stimulation could lead to new filopodia.

More evidence to support this idea has emerged from studies that block glutamatergic neurotransmission and show a significant decrease in filopodial numbers and motility [52, 53]. In another experiment, focal glutamate application led to an increase in dendritic shaft filopodia in pyramidal neurons from the mouse neocortex [54]. Recent experiments show that blocking GABA transmission leads to a decrease in branch formation in developing tectal cell dendrites [55].

All of these experiments strongly suggest that neurotransmission influences filopodial dynamics. However, filopodial dynamics are never entirely abolished when synaptic transmission or neuronal activity are blocked. Hence, other extracellular and cell autonomous factors probably play a role in dendritic filopodial dynamics. BDNF [56] and EphrinB [57] have also been shown to influence the rate and extent of

dendritic filopodial dynamics providing a link between growth and guidance molecules and dendritic structure. It is thus likely that the extent and location of filopodial dynamics is influenced both by the molecules and neuronal activity implicated in neural development.

The first insights into the mechanism by which neurotransmission influences filopodial dynamics came from experiments done in Rachel Wong's lab. By loading retinal ganglion cells with calcium indicator dyes during a period of synaptogenesis, they were able to simultaneously monitor dendritic calcium dynamics and dendritic structure [58]. Two forms of spontaneous calcium transients were observed: global calcium increase throughout the cell, and local calcium 'flashes' restricted to parts of the dendritic arbor. By performing the experiments in a zero calcium environment, they showed that calcium influx was necessary for global and local events. They also showed that blocking cholinergic transmission reduced the frequency of local calcium transients. Blocking release of internal calcium stores using thapsigargin and 2-APB reduced local calcium transients. All of these pharmacological conditions also resulted in dendritic retraction suggesting that local calcium activity plays a role in maintaining dendrites during development. Finally, they conclusively demonstrated the role for local calcium events by focally uncaging caged calcium in a zero calcium environment which resulted in local calcium events and prevented dendritic retraction. These experiments clearly showed that the release of neurotransmitters can locally influence the development of dendritic arbors and that this effect is mediated by calcium influx as well as calcium released from intracellular stores.

Subsequent experiments suggest that these local calcium transients can also be mediated by GABA [48]. Furthermore, the duration and frequency of local calcium transients have since been shown to regulate the spontaneous motility of dendritic

filopodia [59] and may even play a role in selecting appropriate presynaptic partners [48, 60]. The latter papers showed that the onset of local calcium transients in dendrites occurs within a minute of initial contact between an axon and a dendrite. They further showed that the occurrence of calcium transients and the stabilization of filopodia were dependent on the neurotransmitter phenotype of the presynaptic axon. Dendritic filopodia never formed long lived contacts with GABAergic axons, but a small fraction of contacts with glutamatergic neurons were stabilized. This is an intriguing finding because it suggests that dendritic filopodia are able to distinguish between presynaptic axons and that this effect is mediated by the nature of local calcium transients. This is on a much shorter time scale than the time taken to establish a functional synapse, which is thought to take 30-120 min (reviewed in [61, 62]). This has led the authors to propose that initial calcium transients in filopodia are mediated by cell adhesion molecules such as integrins. While these experiments clearly establish that calcium dynamics are integral to filopodial dynamics and local dendritic structure, the exact roles of molecules and neuronal activity in these phenomena remain murky.

In summary, dendritic topography is pervasive in sensory circuits. Directed dendritic growth and systematic dendritic retraction during development can both determine the dendritic topography seen in adults and their precise role might vary across species and circuits. Dendritic development is influenced both by molecular programs as well as by patterns of afferent activity. The genetic programs that influence dendritic arborization are a combination of cell-autonomous factors determined by the age and transcription factor phenotype of the neuron as well as the extracellular milieu of guidance molecules. The development of sophisticated imaging techniques in the last two decades has revealed several phenomena involved in

dendritic development. It is now known unequivocally that developing dendrites constantly remodel. Neurotransmitters, growth factors, and extracellular guidance cues can influence their remodeling, and their effects are mediated intracellularly by calcium influx. These findings dramatically alter the view that dendrites are passive elements in establishing connectivity in neuronal circuits. However, while there are hints as to how to all these events work together to establish appropriate connectivity, a coherent picture that incorporates all of these phenomena into a broader understanding of circuit formation remains elusive.

Mechanisms that establish connectivity in motor circuits

Wiring of motor circuits has been studied both in invertebrates and in vertebrates. While the organization of motor circuits is different between invertebrates and vertebrates, work done in invertebrates, especially *Drosophila*, has revealed novel patterns of dendritic organization, and provides candidate molecular mechanisms that might guide wiring in vertebrates. I will first review recent work done in *Drosophila* and then review our current understanding of wiring mechanisms of vertebrate motor circuits.

Motor neuron dendritic organization and development in *D.melanogaster*

Several recent papers show that motor neuron dendrites form a myotopic map in *Drosophila* – dendrites of motor neurons are distributed differentially in the neuropil, and their location correlates with the target muscles they innervate [63-66]. *Drosophila* larvae generate peristaltic waves of contractions at the end of embryogenesis. The musculature responsible for this movement consists of 30 muscles per half segment and about 36 motor neurons innervate these muscles [65]. The body wall muscles can be further classified into internal and external muscles. In each

segment, external muscles are transverse and have unique anterioposterior positions. In contrast, internal muscles span the width of the segment but have distinct dorsoventral positions.

Using a combination of retrograde dye labeling and genetic labeling, Landraf *et al* showed that dendrites of motor neurons innervating internal and external muscles occupied different regions of the neuropil along the anterioposterior axis [65]. Dendrites of motor neurons innervating the external muscles are anterior, within the same neuromere, relative to dendrites of motor neurons innervating internal muscles. The myotopic map also manifests within the subgroups of motor neurons innervating external muscles and the motor neurons innervating internal muscles. The anterioposterior, but not the dorsoventral, locations of external muscles are mapped centrally along an anterioposterior axis. In contrast, the anterioposterior organization of dendrites from internal motor neurons represents the dorsoventral positions of the muscles they innervate. While the mechanisms underlying this organization are unknown, Landgraf *et al*. showed that this pattern of dendritic organization emerges independently of the presence of target muscles, differentiation of glial cells or competitive interactions between dendritic domains. Cell bodies of motor neurons innervating external and internal muscles appear to be separately clustered anterio-posteriorly as are the motor nerves that carry their axons. Furthermore, the dendrites emerge from the axons at the point where they exit nerve cord. It can be argued that the anterioposterior location of dendrites is simply a "passive" consequence of this organization. The authors of the study address this issue by showing that a motor neuron (DT1) that innervates an external muscle but is clustered with internal muscle motor neurons, nevertheless projects its dendrites to where the external motor neuron dendrites are located. While this is consistent with the idea that the dendritic

organization is not simply a reflection of cell body location, an experimental perturbation that changes dendritic location without affecting cell body location would be much more convincing.

Subsequent work has shown that this myotopic map of internal muscles exists not just along the anterio-posterior axis, but along a mediolateral axis as well [63, 64, 66]. Mauss and colleagues show that the mediolateral position of motor neuron dendrites map to the dorsoventral locations of their target muscles [66]. The medial neuropil is occupied by motor neurons innervating the most ventral muscles and motor neurons innervating progressively more dorsal muscles elaborate their dendrites along a mediolateral gradient such that motor neurons innervating dorsal targets have dendrites in the most lateral parts of the neuropil. This study showed that this topography emerges even when excitatory synaptic input is absent or its location is disrupted. Using genetic manipulation, they went on to show that the myotopic map is determined by midline signaling systems Slit/Robo and Netrin/Frazzled. By perturbing expression levels of Robo and Frazzled cell autonomously, the authors show that mediolateral dendritic organization emerges as a consequence of the opposing actions of Robo and Frazzled. Ectopic expression of Robo prevents dendritic targeting to the midline. Neurons that do not express Robo still require Frazzled expression for midline targeting. The authors conclude that the repulsive behavior of Robo and the attractive behavior of Frazzled are necessary for midline targeting. Finally, using quantitative analysis, this study shows that Robo and Frazzled seem to specifically determine dendritic distribution but not the extent of dendritic growth.

Two studies show that a mediolateral myotopic map exists in the leg neuropil of adult *Drosophila* [63, 64] as well and is also determined by interactions between Slit-Robo and Netrin-Frazzled [64]. In contrast to the Mauss et al study [66], the

myotopic map is a reflection of proximal and distal leg musculature – motor neurons that innervate proximal leg muscles target their dendrites medially and motor neurons that innervate distal muscles target their dendrites laterally. Intriguingly, Brierely and colleagues show that the distinct dendritic domains of neurons are linked to the birth order of the motor neurons. A relationship between the expression of guidance molecules and birth order of neurons is not yet known. It is also not known if this birth order relationship exists for motor neurons innervating the body wall musculature. If so, the birth order of motor neurons could be a unifying determinant of dendritic organization irrespective of the organization of their target muscles.

As discussed above, experiments in sensory systems have suggested that the dendritic distribution of neurons can be influenced by the amount and location of presynaptic inputs. Using a combination of imaging and genetic manipulations, Tripodi et al showed that this is true of motor neuron dendritic arbors in *Drosophila* as well [67]. When the amount of presynaptic input was decreased genetically, motor neuron dendritic arbor increased in length. Conversely, increasing the density of presynaptic inputs, but not the total amount of neurotransmitter released inhibited dendritic growth. Based on several genetic tricks and analysis of branch length, the authors conclude that the motor neuron dendritic branches that contain synapses act as homeostatic devices sensitive to the density of presynaptic input, but this is mediated in an activity-independent manner. They then identify a class of "non-synaptic" branches that are sensitive to activity-dependent neurotransmitter release, and increase in length in the absence of neurotransmitter release. The authors suggest that the role of structural homeostasis is for the dendritic arbor to compensate for naturally occurring animal-to-animal variability in the density of cholinergic terminals. It is

unclear what the roles of these "non-synaptic" dendritic branches is if they do not actually process any synaptic information.

These papers suggest that a mediolateral myotopic dendritic map might be a general feature of the dendritic organization *of* motor neurons in *Drosophila*. Further, this map is likely set up by the opposing effects of Slit and Robo. It has also been demonstrated that motor neuron dendrites change their length in response to the density of presynaptic input and this is mediated by activity independent and activity dependent mechanisms. Since the myotopic map emerges independent of presynaptic activity, it raises the possibility that structural compensation may influence the structure of the myotopic map. Mauss et al [66] do address this question and show that the penetrance of Slit and Robo manipulations is greater before presynaptic innervation. Moreover, in experiments where presynaptic innervation is modulated, dendritic territories appear to be less distinct than in controls. Taken together, map formation in *Drosophila* motor systems bears similarity to the overall model proposed for circuit formation in sensory systems where a genetically determined topographic map emerges before the onset of function and is then subsequently tweaked and maintained by neural activity.

Motor circuit formation in vertebrates

Since differences in anatomy, especially the orientation and distribution of dendritic arbors and axons, suggest differences in wiring, several groups have investigated if there are unique patterns of dendritic distribution in spinal circuits. This effort has almost entirely focused on the dendritic structure of motor neurons. Labeling methods such as cobalt chloride, Golgi, horseradish peroxidase and dye backfills have been used to label motor neuron dendrites. Cullheim *et al.* studied the

spatial dendritic distribution of type identified triceps surae alpha motoneurons in cats, and found no systematic differences between fast-twitch and slow-twitch motoneurons [68]. A few studies have shown that there are differences in the dendritic distribution of motor neurons based on the muscles they innervate. A study of HRP labeled motor neuron dendrites in the lumbar spinal cord of the turtle *Pseudemys scripta elegans,* showed that dorsal dendritic trees of neurons innervating distally positioned musculature (ankle and toe extensors and flexors) contained fewer terminal dendritic branches compared to neurons innervating proximal (hip and knee) muscles [69]. Another study showed qualitative differences in the distribution of dendrites in the lumbosacral motor neuron pools of the chicken [70]. Their data also showed that motor neuron pools that innervate coactive muscles have similar dendritic distribution. While these studies show qualitative differences in dendritic distribution, the functional context in which these differences in dendritic distribution might be relevant is unknown.

An exception to this is work done on sensory-motor connectivity of spinal reflex circuits where anatomy has been looked at in a functional context. This specification of wiring in spinal sensory-motor circuits is the most well understood aspect of how connectivity is established in motor circuits. Connectivity between proprioceptive sensory afferents and motor neurons mediates spinal reflexes. These connections are very specific; a subset of proprioceptive sensory neurons makes monosynaptic connections with motor neurons that supply the same muscle but avoid motor neurons innervating antagonistic muscles. How this specificity is established has been studied in some detail. Using electrophysiology to determine connectivity in the brachial spinal cord of bullfrogs, Lichtman and colleagues showed that sensory axons from the triceps brachii muscle innervate the corresponding triceps motor

neurons but not the subcapularis and pectoralis motor neurons [71]. In a parallel study, using horseradish peroxidase to label the dendritic arbors of the triceps, subcapularis and pectoralis motor neurons, they found no systematic differences in the orientation of their dendritic arbors and concluded that the specificity of connections was not the result of differences in anatomical organization [72].

More recently, this question was revisited in mice [73]. Vrieseling *et al* show that different motor neuron pools in the cervical spinal cord show distinct patterns of dendritic distribution – dendrites of motor neuron pools with dorsomedial cell body positions (Triceps, Pectoralis major) are radially distributed and invade the central gray matter extensively, but dendrites of motorneuron pools with ventrolateral cell body positions (cutaneous maximus (CM), latissmus dorsi (LD)) are restricted to the lateral edges of the spinal cord. This correlated with the patterns of proprioceptive sensory input to these motor neuron pools; while triceps and motor neurons received monosynaptic sensory input from Triceps sensory afferents, CM motor neurons did not. It had been previously reported that CM and LD motor neurons, but not Triceps and Pectoralis Major motor neurons express the transcription factor *Pea3* [74]. Vriesling *et al* showed that in *Pea3* mutant mice CM and LD motor neurons have dramatically different dendritic arborizations that invade the central gray matter extensively. This change in dendritic arborizations correlated with altered sensory motor connectivity such that CM motor neurons now received input from Triceps sensory afferents. While this paper suggests that dendritic patterning is associated with sensory motor connectivity, it cannot be ruled out that these two effects are independent of each other since *Pea3* regulates the expression of several molecules such as plexins and semaphorins which could determine connectivity. A subsequent paper [75] from the same group, in fact, highlights this point – knocking out

recognition molecules sema3e and plexinD1 in subsets of triceps and CM motor neurons and their corresponding sensory afferents was sufficient to alter connectivity between CM afferents and CM motor neurons without altering dendritic patterning. In summary, work done on spinal reflex circuits shows that anatomical differences alone cannot account for the specificity of synaptic connectivity and that complex interactions between recognition molecules determine the patterns of detailed connectivity in this circuit.

Several groups have studied the dendritic development of motoneurons in vertebrates. Using Golgi staining, studies in cats show significant dendritic growth of motoneurons innervating hindlimb muscles during the first 4 to 5 months of postnatal development [76]. The work showed that dendrites of motoneurons are organized as "bundles" in mature cats but the dendritic bundles are absent in newly born kittens and begin to appear at P12 to P14 and continue to grow until the animals are 4 to 5 months old. Electromyograms at similar times show that reciprocal activity between agonist-antagonist muscle pairs only begins to emerge at P12-P14 and is fully mature at 4-5 months. The authors suggest that this behavioral change is related to the development of dendrite bundles. Since several other developmental changes occur during the same time period, it seems highly unlikely that this behavioral change can be attributed to the emergence of dendrite bundles. Moreover, the functional relevance of dendrite bundles is not known. The bundles could simply be a consequence of wiring minimization to maximize connectivity with postsynaptic input. Many subsequent studies done in different vertebrates have confirmed the substantial increase in postnatal dendritic growth in motoneurons innervating different muscle groups [77-79]. While some studies show that dendritic retraction occurs, the extent and functional relevance of retraction is unclear [79]. These studies also suffer from

inferring retraction from very small numbers of representative structures of different neurons at different time points. Given the heterogeneity of developmental programs of neurons, and the very small datasets of neurons studied, it is likely that these studies might have missed general patterns motoneuron dendritic development.

The role of activity in the development of motoneuron dendrites and in the development of spinal motor networks in general is unclear. Since motoneurons receive input from presynaptic neurons distributed throughout the spinal cord, it is not possible to specifically block synaptic input to motoneurons using methods employed in sensory deprivation. Pharmacological experiments that block neuronal activity in general are hard to interpret because the effects seen can be consistent with several different hypotheses or even be a consequence of non-specific actions that are typical of pharmacological blockers. However, in an interesting set of experiments, the dendritic structure of motoneurons in neonatal rats raised in microgravity, on a space shuttle, was compared with littermates raised on the ground [80]. Dendrites of motoneurons that probably innervated proximal and axial musculature in animals that were subjected to microgravity for 16 days were significantly shorter and branched less compared to animals that were raised in normal gravity. These experiments suggest that motoneuron dendritic development can be altered by activity.

Several experiments have studied the role of glutamatergic neurotransmission in motoneuron development. Motoneuron dendritic growth is inhibited in the presence of NMDA-antagonists in early postnatal life [77]. In addition, neonatal, but not adult, motoneurons express high levels of the GluR1 flip subunit of AMPA receptors [81]. When the GluR1 flip subunit is expressed by viral infection in mature motoneurons, it leads to extensive remodeling of dendrites [81]. The authors suggest that the expression of this subunit in neonatal motoneurons is necessary for dendritic

remodeling in early development, although the functional relevance of dendritic remodeling is not known. GluR1 knockout mice show significant locomotor defects and motoneuron dendritic arbors are shorter and have fewer branches [82]. However, since the GluR1 knockout was not specific to motoneurons, the motor impairments and changes in dendritic arbor cannot be specifically attributed to the role of GluR1 in motoneurons. A recent study showed that expression of GluR1 *in vitro* in spinal cord cultures led to a greater number of filopodia as well as higher density of putative excitatory synapses [83]. The authors propose that the early postnatal expression of GluR1 in spinal motoneurons is required for sustained dendrite outgrowth and synaptogenesis.

In summary, we do not understand how connectivity in spinal motor networks is established. Anatomical studies clearly show substantial postnatal motoneuron dendritic growth but it is not clear if this increase in connectivity is arbitrary or constrained by some rules. There is also evidence to suggest that extensive dendritic remodeling occurs during early postnatal development but its functional relevance is unknown. Spinal reflex circuits are an exception to our general lack of understanding of how wiring is established in motor circuits. However, while these circuits are clearly necessary for coordinating limb movement, it is not known if the same wiring rules apply to wiring axial circuits that are necessary for movement across a range of speeds.

Larval zebrafish as a model system to study motor circuit formation

Zebrafish are uniquely poised as a model system to elucidate the mechanisms that determine connectivity in motor circuits. A meaningful understanding of circuit wiring requires not only an experimentally amenable system with access to the nervous

system throughout development, but also a functional understanding of the circuit to put in context the developmental phenomena that are observed. In the following sections I first review the technical advantages of the zebrafish model system to study the wiring of motor systems. I then review recent work that provides a conceptual framework for the organization and function of motor networks within which to study the development of wiring.

Technical advantages of larval zebrafish for studying the development of connectivity

Zebrafish develop rapidly, and by 4 days after fertilization, larval zebrafish are freely swimming [84]. Crucially, from a technical viewpoint, they are transparent throughout development as their motor behavioral repertoire dramatically transitions from spontaneous coiling to basic locomotor patterns similar to axial movements in all vertebrates. Since zebrafish larvae can be embedded in agarose, imaged using confocal microscopy, and then subsequently be returned to their tanks, their transparency provides easy access *in vivo* to the entire motor network as it changes structurally and functionally during development, allowing one to correlate changes in motor circuits to the actual motor behavior [85, 86].

Zebrafish have also emerged as an important genetic model system, and many genetic techniques are available to observe and manipulate different components of the motor network [86, 87]. Work in the last decade has identified several genes that are uniquely expressed in distinct cell types in the zebrafish motor circuit. The promoters of these genes have in turn been used to drive the expression of genes of interest (for example, fluorescent proteins, Gal4 or Cre recombinase) in specific cell types [85-88]. By injecting these genetic constructs at low concentrations in embryos

at the single cell stage, one can stochastically drive the expression of the gene of interest in just one or a few cells. Driving the expression of membrane targeted fluorescent proteins in just a few cells enables visualizing the detailed morphology of single cells including fine structures such as growth cones and filopodia to allow for tracking of changes in morphology as the animal develops [21]. Alternatively, one can use this method to manipulate cellular and molecular properties of individual neurons.

Thus, the transparency of zebrafish throughout the maturation of locomotor behavior in combination with genetic techniques provides an unprecedented ability to observe and manipulate the structure of a vertebrate motor network as motor behavior develops.

An age-related functional topography of spinal neurons provides a conceptual framework to understand motor network development

Locomotion requires the coordination of muscle groups over a range of speeds and strengths. Historically, as reviewed above, work on connectivity in motor networks has largely focused on the dendritic structure of motor neurons in relation to the muscles they innervate. This is relevant to the coordination of muscle gro32ups during movement. In contrast, much less is known about the connectivity that allows animals to produce movements over a broad range of speeds and strengths.

Recent work in the Fetcho lab looked at the relationship between the position of neurons in the spinal cord of larval zebrafish and the swimming speeds at which they are recruited [3]. Remarkably, they found a functional topography in the recruitment of motoneurons and interneurons that are recruited during swimming. Motoneurons and excitatory interneurons near the ventral edge of the spinal cord are recruited at slow swimming speeds and progressively more dorsal cells are recruited

as the swimming speed increases. This paper also showed that this pattern of recruitment correlates with the input resistance of neurons; ventrally located neurons have high input resistance which decreases in dorsally located motoneurons and excitatory interneurons. Inhibitory interneurons follow the opposite pattern of recruitment and input resistance. This finding was especially interesting because it explained the recruitment of multiple cell types in the spinal cord across neurotransmitter and transcription factor phenotypes, thus suggesting a general plan linking the organization of neurons in spinal motor networks in larval zebrafish to swimming speed.

In zebrafish, the most dorsal motoneurons and excitatory interneurons recruited in the most powerful movements are also early born neurons [89-92]. This observation prompted a study to investigate the relationship between the topographic patterns of recruitment, the timing of neuronal differentiation, and the emergence of motor behavior [4]. A careful behavioral analysis showed that large amplitude movements and the interneurons that drive them are the earliest to emerge during development. Small amplitude movements characteristic of slow swimming, and the more ventral interneurons that underlie these, emerge later in development. These findings show that the dorsoventral topography seen for excitatory interneurons in the previous study is, in fact, an age-related organization of neurons that relates the age, the dorsoventral location and the swimming speeds at which they are recruited. The authors also review previous literature in light of this pattern and find several previous studies that suggest that motor development of tetrapods, including humans, has striking parallels with the pattern of motor development seen in larval zebrafish. Whether the underlying neuronal circuitry is also developmentally layered, as seen in zebrafish, remains to be seen.

Thus, in addition to a transcription factor based organization of the spinal cord across vertebrates, there might exist an age related organization of neurons underlying motor behaviors that may be conserved in all vertebrates. This, in turn, provides a framework to relate the age, anatomical organization of axons and dendrites, and the function of neurons involved in locomotion across all vertebrates. Given that the repertoire of movements seen during zebrafish development is similar to the development of locomotor movements in higher vertebrates, understanding how motor circuits are wired in larval zebrafish could provide insights more generally into mechanisms of wiring of motor networks in all vertebrates.

CHAPTER 2

Title: A novel dendritic topography related to motoneuron recruitment in the spinal cord of larval zebrafish

Abstract

Axons and dendrites in many sensory circuits are topographically organized. The topographic organization of vertebrate spinal circuitry underlying locomotion is poorly understood. Here we reveal a novel dendritic organization of motoneuron dendrites in the spinal cord of freely swimming larval zebrafish related to the pattern of recruitment of motoneurons during swimming. We find that dendrites of older motoneurons recruited at faster speeds arborize more dorsally and medially in the neuropil relative to dendrites of younger motoneurons recruited at slower speeds. This topography is present at the time when fish first begin to swim spontaneously and it emerges over a time period when fish are largely sedentary. The pattern is maintained after the onset of spontaneous swimming even as dendritic growth and retraction continues. Since anatomical topography reflects the connectivity of circuits, our results point to an age and speed-related organization of connectivity within vertebrate spinal motor circuits which emerges in the absence of much locomotor activity.

Introduction

Spatial topography is a general feature of organization of axons and dendrites in sensory circuits [1, 93]. In many sensory circuits, a basic topography is present at the time when the animal first starts processing sensory information, and is maintained as axons and dendrites continue to grow after the onset of behavior [94]. In contrast to our understanding of topographic organization and development in sensory circuits, it is not known whether topographic organization exists, or how it develops, in vertebrate spinal motor networks that drive locomotion.

Work on the organization of neuronal circuitry and its development in motor networks has largely focused on motoneuron dendritic organization and development in relation to the muscles they innervate [70, 72, 73]. While there is some evidence for dendritic topography in relation to the muscles they innervate [69, 70, 73], dendrites of motoneurons belonging to the same motor pool or even to different motor pools show substantial intermingling and no obvious topography [68, 72]. However, motoneuron dendritic organization has not been examined in relation to their recruitment at different movement speeds. Similarly, while motoneuron dendritic development has been studied extensively [40, 76, 78, 79], it is not known if and how motoneuron dendrites develop in relation to the maturation of locomotor behavior.

We took advantage of the recent description of an orderly organization of motoneuron somata, related to their recruitment at different swimming speeds [3], to look for patterns of dendritic organization and dendritic development related to soma position as the locomotor behavior of zebrafish develops. Motoneurons near the ventral edge of the cord are recruited at slow swimming speeds and progressively more dorsal cells are recruited as the swimming speed increases. This systematic relationship between the location of motoneuron cell bodies and the pattern of recruitment provides a functional framework to look for patterns in the spatial distribution of dendrites related to motoneuron soma location. The transparency of zebrafish, the quick maturation of locomotor behavior [4, 84, 86] in combination with genetic techniques to visualize the structure of individual neurons and a functional framework to relate these anatomical changes provides a unique opportunity to relate the organization and development of dendrites to the development of locomotor behavior.

Here we first used transient expression of fluorescent proteins to visualize the dendritic structure of motoneurons in zebrafish larvae at a stage when they have been

swimming spontaneously for a few days. We reveal a dorsoventral and mediolateral organization of motoneuron dendrites related to the functional recruitment of motoneurons at different locomotor speeds - dendrites of older motoneurons recruited at faster speeds arborize more dorsally and medially in the neuropil relative to dendrites of younger motoneurons recruited at slower speeds. By tracking the development of individual mGFP expressing motoneurons at different developmental stages, we found that the topography is present at the time when fish first begin to swim spontaneously and it emerges over a time period when fish are largely sedentary. Even though older motoneurons that drive fast movement differentiate before motoneurons that drive slow movement, their dendritic arbors appear to elaborate at the same time suggesting that the topography is not a consequence of temporal layering of dendrites. We also find that only a small fraction of the dendritic structure is pruned after the onset of swimming. Furthermore additional dendritic growth after the onset of spontaneous swimming does not disrupt the initial topography. In summary, there is a dendritic topography related to the recruitment of motoneurons at different locomotor speeds that emerges by the time fish begin to swim, and is maintained even as dendrites grow after the onset of spontaneous swimming. Topography is often an anatomical correlate of specificity in connectivity. Our results point to the possibility of an age and speed-related organization of connectivity, established while the animal is largely sedentary, within vertebrate spinal circuits that underlie the ability to move over a range of speeds.

Results

Dendritic organization of motoneurons in 6 days postfertilization fish, an age at which the fish are freely swimming,

Recent work on the spinal cord of larval zebrafish showed a systematic relationship between the dorsoventral location of a motoneuron and the swimming speed at which it is recruited [3] . The most ventral motoneurons are recruited at the slowest swimming speeds while more dorsal motoneurons are recruited as the swimming speed increases. The discovery of this functional topography provided a functional framework to investigate if there is an anatomical organization of motoneuron dendrites in relation to their recruitment pattern. We first asked if there is any systematic dorsoventral pattern of dendritic distribution in freely swimming larval zebrafish at 6 dpf when fish have been swimming spontaneously for 2 days.

To visualize the entire dendritic arbor of individual motoneurons, we stochastically expressed membrane targeted GFP, under control of the vesicular acetylcholine transporter promoter, by single cell injections of VAchT:Gal4 and UAS:mGFP. The Gal4/UAS system ensured sustained expression of mGFP in motoneurons so as to visualize them easily at 6 dpf. The entire dendritic arbor was imaged by high resolution confocal microscopy in living fish while simultaneously collecting a visible light image of the spinal cord to identify its ventral and dorsal edges. The dendritic arbor was then reconstructed in 3D using BitPlane Imaris filament reconstruction software, and the dorsoventral distribution of dendrites was analyzed with respect to the dorsal and ventral edges of the spinal cord. To compare the dorsoventral distribution of dendrites of motoneurons from different fish we normalized the dorsoventral extent of the spinal cord to 1. The dorsoventral extent of the spinal cord was then divided into 100 equal volumes by horizontal planes and the length of dendritic arbor in each “volume” was calculated. This allowed us to ask if there are systematic patterns of dorsoventral dendritic distribution of motoneurons related to the dorsoventral location of motoneuron somata.

Examples of individually labeled motoneurons whose cell bodies are located at different dorsoventral locations are shown in Figure 2.1A-C. Dendrites of all 67 reconstructed motoneurons imaged in spinal cord segments 9-21 had ipsilateral dendrites that largely extend rostro-caudally. Figure 2.1D-F shows the dorsoventral distribution of reconstructed dendritic arbors of motoneurons shown in Figure 2.1A-C respectively, normalized to the dorsoventral extent of the spinal cord. Figure 2.1G-I represent the dorsoventral distribution of dendrites for motoneurons shown in Figure 2.1A-C as a heat map – the brighter colors signify greater length. Initial examination of the dorsoventral distribution of individual dendritic arbors suggested that dendrites of motoneurons largely arborize in different dorsoventral locations in the spinal cord depending on the dorsoventral location of the motoneuron somata. Figure 2.1J represents the dorsoventral distribution of dendrites of all motoneurons we analyzed, organized from left to right in increasing order of the dorsoventral location of the motoneuron somata. This representation suggested the existence of a dorsoventral topographic organization of dendrites such that dendrites of dorsal motoneurons generally arborize more dorsally than those of ventral motoneurons.

To examine if there is indeed a correlation between dorsoventral distribution of dendritic arbor and the location of somata, we calculated the weighted dorsoventral location of motoneuron dendrites and plotted it as a function of the dorsoventral location of the motoneuron somata as shown in Figure 2.1K. This plot revealed a significant correlation between the weighted dorsoventral locations of the dendritic arbor and the dorsoventral location of motoneuron somata ($n = 67$; $p < 0.0001$). This dendritic topography related to motoneuron position raises the possibility that an

Figure 2.1. **Analysis of the dendritic organization of motoneurons in relation to the dorsoventral location of their somata**. (A-C) Lateral view of mGFP expressing motoneurons located at different dorsoventral locations in 6 dpf fish. (D-F) Dorsoventral distribution of motoneuron dendritic arbors of motoneurons shown in A-C where the 0 plane represents the ventral edge of the spinal cord and 1 represents the dorsal edge. (G-I) Color-coded representation of the normalized dorso-ventral dendritic distribution of motoneurons shown in A-C. The dorsoventral extent of the spinal cord was divided into a hundred equal segments from ventral to dorsal and the dendritic length in each segment was calculated and represented according to the color bar on the right. For the example in A, the heat map shows that most of the dendritic arbor is located mid dorso-ventrally in the spinal cord. (J) Quantification of dendritic distribution of all mGFP expressing motoneurons along the dorsoventral extent of spinal cord. Each column is a quantification of a single motoneuron dendritic arbor as explained in G-I and columns are arranged from left to right in increasing order of dorsoventral cellbody position. The dorsoventral location of the cell body is represented on the column as a white circle. Motoneurons at certain dorsoventral locations are over-represented on this plot. (K) Plot of weighted dorsoventral location of the dendritic arbor versus the dorsoventral location of the neuron. Dendritic arbors of more dorsal motoneurons are more dorsally located than dendritic arbors of ventral motoneurons, with a significant correlation ($n = 67$; $p < 0.0001$) between the DV location of a soma and the location of the dendrites.

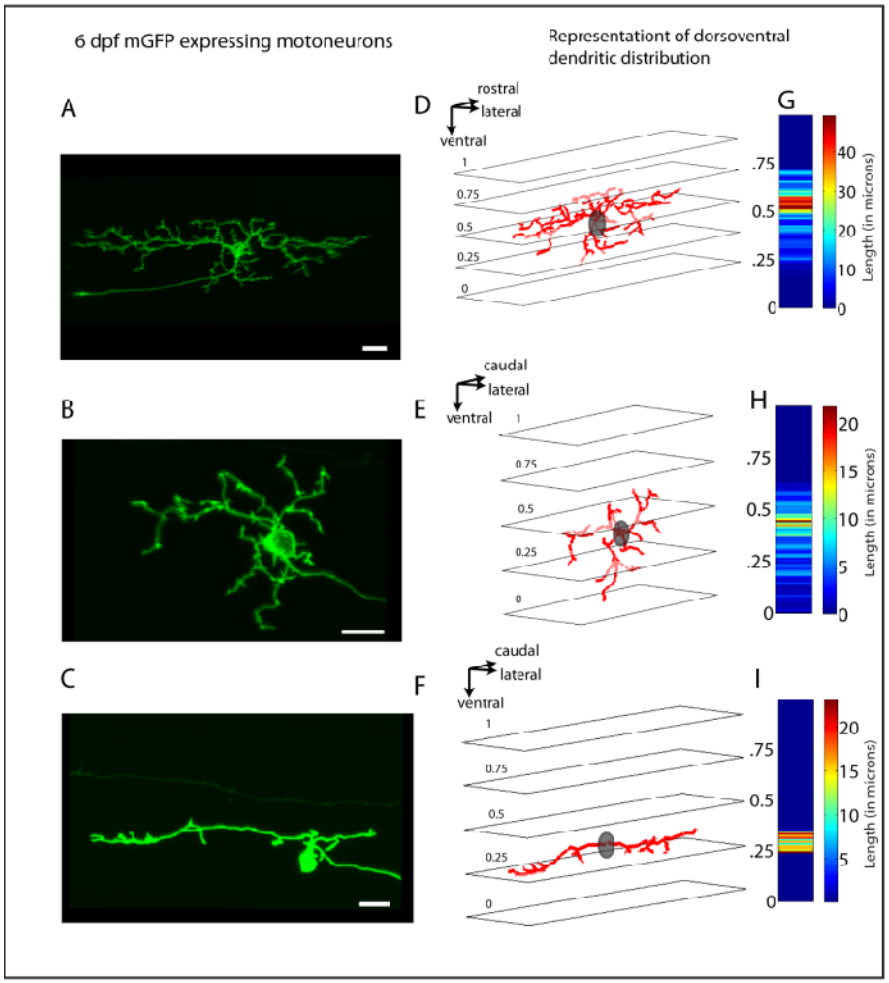
6 dpf mGFP expressing motoneurons
Representationt of dorsoventral dendritic distribution
A
B
C
D
E
F
G
H
I
rostral
lateral
ventral
caudal
lateral
ventral
caudal
lateral
ventral
1
0.75
0.5
0.25
0
.75
0.5
.25
0
40
30
20
10
0
20
15
10
5
0
Length (in microns)

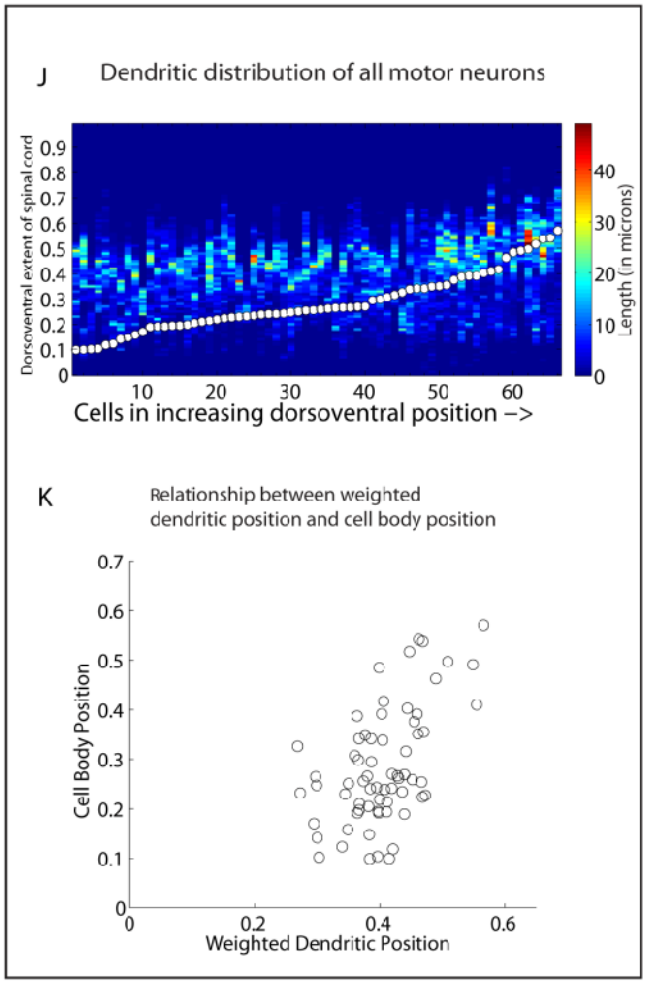
J
Dendritic distribution of all motor neurons
Dorsoventral extent of spinal cord
0.9
0.8
0.7
0.6
0.5
0.4
0.3
0.2
0.1
0
10
20
30
40
50
60
Cells in increasing dorsoventral position –>
40
30
20
10
0
Length (in microns)
K
Relationship between weighted dendritic position and cell body position
Cell Body Position
0.7
0.6
0.5
0.4
0.3
0.2
0.1
0
0
0.2
0.4
0.6
Weighted Dendritic Position

anatomical organization of dendrites could partly underlie the functional topography of motoneuron recruitment.

Mediolateral dendritic organization of motoneurons at 6 days post fertilization, an age at which the fish are swimming freely

Data from the spinal cord and hindbrain suggest that the functional topography of recruitment of motoneurons and interneurons is related to their age such that the oldest neurons are recruited at the fastest speeds and younger neurons are recruited at slower speeds [4, 90]. Moreover, recent examination of the organization of the neuropil of a class of premotor excitatory interneurons suggests an age-related pattern of connectivity might exist in the spinal cord and hindbrain of larval zebrafish (Kinkhabwala *et al* submitted). Premotor interneurons that express the transcription factor Alx (Chx10 in mice) are known to provide excitatory drive to motoneurons [4, 90, 95]. Kinkhabwala *et al* recently showed that the neuropil of Alx interneurons is patterned by age in the spinal cord such that older neuropil lies medial and dorsal to younger neuropil. Since there is evidence that dorsal motoneurons are older than ventral motoneurons [92], the more dorsal location of the dendrites of dorsal motoneurons described in the previous section suggests that their locations parallel the age related location of the axonal processes of premotor interneurons in the dorsoventral extent. We next asked whether the mediolateral organization of motoneuron dendrites in freely swimming 6 dpf larval zebrafish also matched the pattern of distribution of the premotor interneurons, with older axons medial to younger ones.

We used stochastic expression of membrane targeted mCherry protein under control of vesicular acetylcholine transporter (via single-cell stage injections of VAchT:Gal4, UAS;mCherry) in the Alx-GFP [90] transgenic line to randomly label

Figure 2.2. **Analysis of mediolateral distribution of motoneuron dendritic arbor within the Alx neuropil.** (A-C) Lateral, Dorsal and Cross-section views, respectively, of a dorsal motoneuron (in red) labeled with mCherry in an Alx:GFP transgenic fish at 6 dpf. (D) Color-coded representation of the normalized mediolateral dendritic distribution, with reference to the Alx:GFP neuropil, of the motoneuron shown in A-C according to the color bar on the right. (E-G) Lateral, dorsal and cross-section views, respectively, of a ventral motoneuron (in red) labeled with mCherry in an Alx:GFP transgenic fish at 6 dpf. (H) Color-coded representation of the normalized mediolateral dendritic distribution of the motoneuron shown in E-G according to the color bar on the right. (I) Quantification of mediolateral dendritic distribution of all mCherry expressing motoneurons relative to the width of the Alx:GFP neuropil. (J) Plot of weighted mediolateral location of the dendritic arbor versus the dorsoventral location of the motoneuron ($n = 21$; $p < 0.05$).

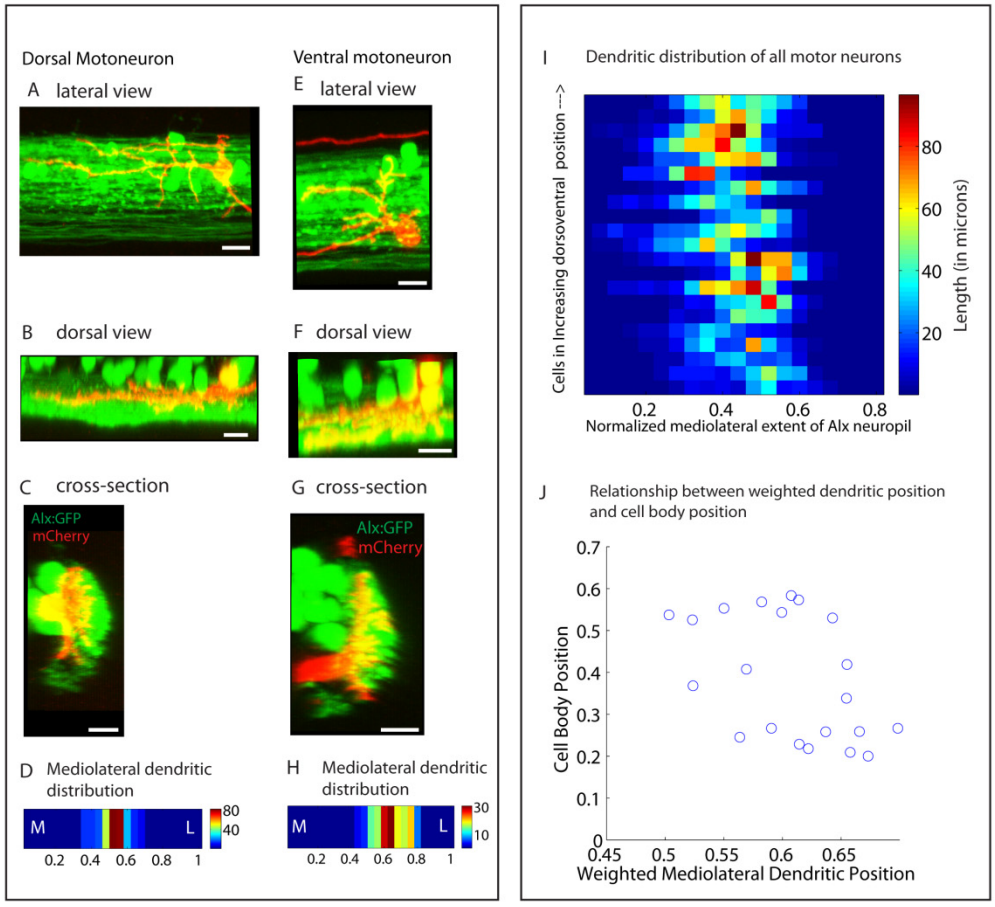
Dorsal Motoneuron
A lateral view
B dorsal view
C cross-section
Alx:GFP
mCherry
D Mediolateral dendritic distribution
M
L
0.2 0.4 0.6 0.8 1
80
40
Ventral motoneuron
E lateral view
F dorsal view
G cross-section
Alx:GFP
mCherry
H Mediolateral dendritic distribution
M
L
0.2 0.4 0.6 0.8 1
30
10
I Dendritic distribution of all motor neurons
Cells in Increasing dorsoventral position --->
0.2 0.4 0.6 0.8
Normalized mediolateral extent of Alx neuropil
80
60
40
20
Length (in microns)
J Relationship between weighted dendritic position and cell body position
Cell Body Position
0.7
0.6
0.5
0.4
0.3
0.2
0.1
0
0.45 0.5 0.55 0.6 0.65
Weighted Mediolateral Dendritic Position

isolated motoneurons in red, and looked at their mediolateral dendritic distribution relative to the Alx-GFP neuropil. Figure 2.2A shows a lateral view of a dorsal motoneuron expressing mCherry in the Alx-GFP transgenic line. Figure 2.2B and 2C are dorsal and cross-sectional views of the same motoneuron and suggest that the dendritic arbor largely arborizes medially in the Alx-GFP neuropil. In contrast, the dendritic arbor of a ventral motoneuron (lateral view in Figure 2.2E) arborizes more laterally in the Alx-GFP neuropil as shown in Figure 2.2F and 2G. Initial visual examination of several motoneurons in this way suggested that dendrites of more dorsal, older motoneurons arborize more medially and dendrites of ventral, younger motoneurons tend to arborize more laterally in the Alx-GFP neuropil.

To compare the mediolateral distribution of motoneuron dendrites across fish, we normalized the mediolateral extent of the Alx-GFP neuropil to 1 such that 0 represents the most medial edge of the Alx-GFP neuropil and 1 was the lateral limit. This mediolateral volume was then divided into 25 equal volumes and the length of the reconstructed dendritic arbor in each mediolateral volume was calculated. For the two motoneurons shown in Figure 2.2A-C and 2E-G, their quantified mediolateral dendritic distributions are shown in Figure 2.2D and 2H respectively. This quantification confirmed that the dendritic arbor of the ventral motoneuron was distributed more laterally than the dendritic arbor of the dorsal motoneuron. Figure 2.2I represents the mediolateral distribution of 22 motoneurons studied in this way, and this distribution suggests that despite considerable overlap between dendritic arbors, dendrites of older, dorsal motoneurons arborize more medially relative to dendrites of ventral motoneurons. Our conservative criteria (see Methods) for the mediolateral extent of the Alx-GFP neuropil explains why the dendrites appear to be primarily located between 0.4 and 0.8 of the mediolateral extent of the neuropil.

To examine if there was a correlation between mediolateral distribution of dendritic arbor and the location of somata, we calculated the weighted mediolateral location of motoneuron dendrites and plotted it as a function of the dorsoventral location of the motoneuron somata as shown in Figure 2.2J. This plot revealed a significant correlation

between the weighted mediolateral locations of the dendritic arbor and the dorsoventral location of motoneuron somata ($n = 21$; $p < 0.05$). Thus, our data indicate that dendrites of dorsal motoneurons are distributed more medially while dendrites of ventral motoneurons are distributed more laterally. This mediolateral dendritic topography related to motoneuron position is consistent with the idea of an age-related patterning of connectivity as previously suggested by an analysis of the Alx-GFP neuropil.

Taken together, our data reveal the dorsoventral and mediolateral location of the dendrites of a motoneuron vary systematically with the location of its soma, which also reflects its age and the speed at which they are recruited. These data raise the possibility of an age-related specificity in connectivity between premotor interneurons and motoneurons that may contribute to the functional patterns of recruitment of motoneurons at different swimming speeds.

Dendritic distribution of a class of inhibitory interneurons recruited during swimming

It can be argued that the motoneuron dendritic organization we observe is simply a consequence of dendrites emerging from motoneuron somata and elaborating close to the soma. If this were the case, one would expect that dendrites of any spinal interneuron also elaborate from their soma. Moreover, if the somas are dorsoventrally organized, the dendrites would also be dorsoventrally organized. We examined if this was the case by looking at the dendritic distribution of a class of inhibitory interneurons called Commissural Bifurcating Longitudinal (CoBL) neurons in relation

to the location of their somata. CoBLs are recruited topographically during swimming but their soma distribution and pattern of recruitment is inverted compared to motoneurons [3]. The most dorsal CoBLs are located near the dorsal edge of the spinal cord and are recruited at the slowest swimming speeds. The most ventral CoBLs located mid dorsoventrally in the spinal cord are recruited at the fastest swimming speeds.

Since CoBLs are inhibitory interneurons, we used stochastic expression of membrane targeted GFP protein under control of glycine transporter promoter (via single-cell stage injections of GlyT2:Gal4, UAS:mGFP) in wild-type zebrafish to randomly label isolated CoBLs. Figure 2.3A-C show individual CoBLs located at different dorsoventral locations in the spinal cord. While a soma may have a few small dendritic branches arising from it, most of the dendritic arbor does not emerge from the soma. Figure 2.3D-F represents the reconstructed dendritic arbor of the CoBLs shown in Figure 2.3A-C respectively and Figure 2.3G-I show a quantification of the dorsoventral dendritic distribution of their dendritic arbors. Figure 2.3J shows the dorsoventral dendritic distribution of all 40 CoBLs we imaged. Each column represents a single CoBL. Visual examination of this distribution did not suggest any obvious dorsoventral organization of dendrites related to CoBL soma position, unlike the general dendritic organization seen for motoneurons (Figure 2.3K). A plot of the weighted dorsoventral dendritic position versus the dorsoventral location of CoBL cell bodies reveals a much weaker, just insignificant relationship (Figure 2.3L,M blue circles; $n = 40$, $p = 0.053$), as opposed to the strong correlation seen for motoneurons (Figure 2.3M black circles; $n = 67$, $p < 0.0001$).

Our analysis of the dendritic distribution of CoBL interneurons suggests that the dendritic organization we observe for motoneurons is not simply a consequence of dendrites elaborating close to their somata.

Figure 2. 3. Analysis of the dendritic organization of CoBLs in relation to dorsoventral location of their somata. (A-C) Lateral view of mGFP expressing CoBL interneurons located at different dorsoventral locations in 6 dpf fish. (D-F) Dorsoventral distribution of CoBL dendritic arbors in A-C where plane 0 represents the ventral edge of the spinal cord and 1 represents the dorsal edge. (G-I) Color-coded representation of the normalized dorso-ventral dendritic distribution of motoneurons shown in A-C. The dorsoventral extent of the spinal cord was divided into a hundred equal segments from ventral to dorsal and the dendritic length in each segment was calculated and represented according to the color bar on the right. For the example in A, the heat map shows that most of the dendritic arbor is located mid dorso-ventrally in the spinal cord. (J) Quantification of dendritic distribution of all mGFP expressing CoBLs along the normalized dorsoventral axis of the spinal cord. Each column is a quantification of the dorsoventral distribution of the dendritic arbor of an individual CoBL as explained in G-I and columns are arranged from left to right in increasing order of dorsoventral cellbody position. The normalized dorsoventral location of the cell body is represented on the column as a white circle. (L) Plot of weighted mean dorsoventral location of the dendritic arbor versus the dorsoventral location for CoBLs ($n = 40$; $p = 0.053$) . (M). Plot of total dendritic length versus the dorsoventral location of the motoneuron.

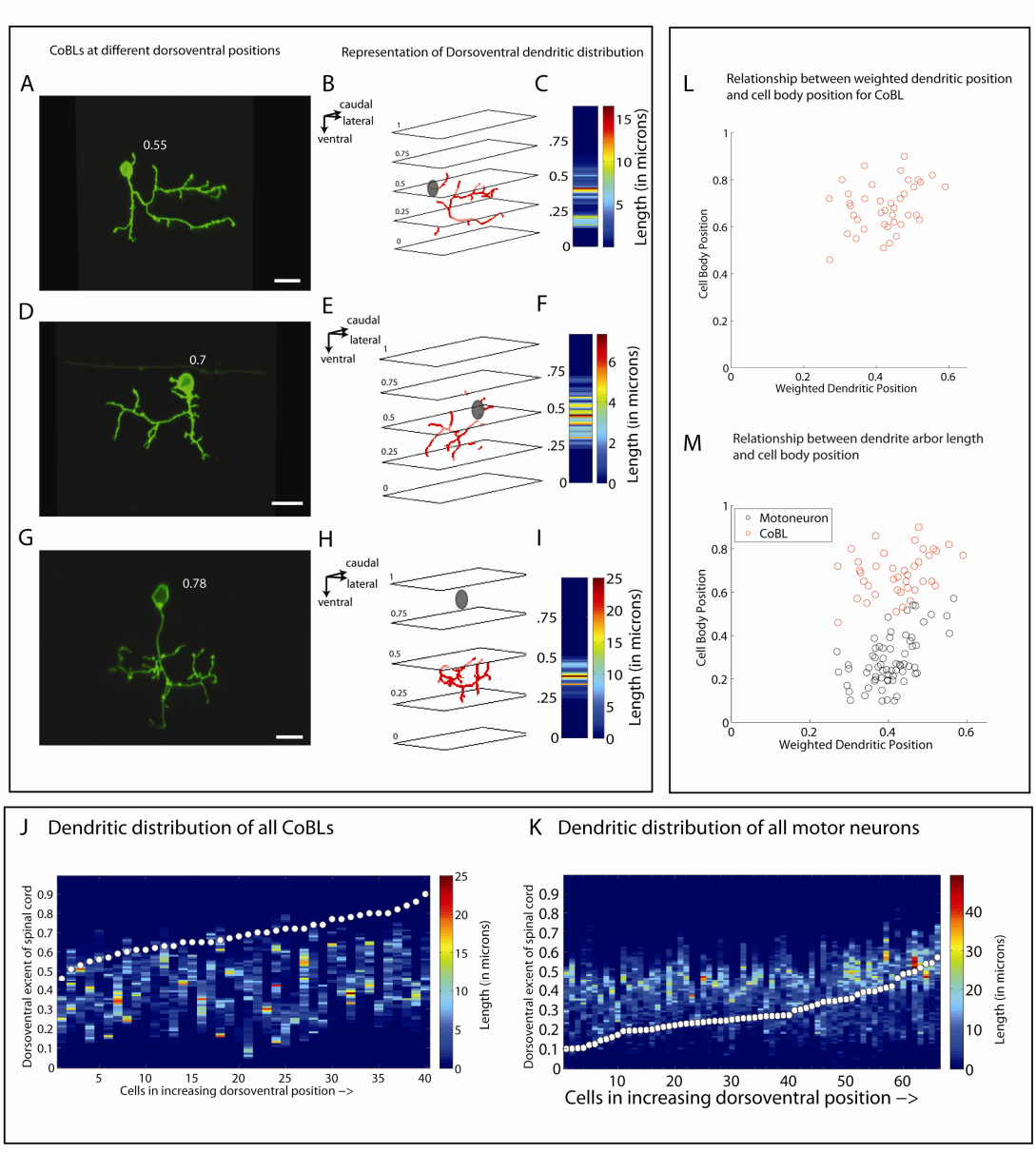
CoBLs at different dorsoventral positions
Representation of Dorsoventral dendritic distribution
A
B
C
0.55
caudal
lateral
ventral
Length (in microns)
D
E
F
0.7
G
H
I
0.78
L
Relationship between weighted dendritic position and cell body position for CoBL
Cell Body Position
Weighted Dendritic Position
M
Relationship between dendrite arbor length and cell body position
Motoneuron
CoBL
J
Dendritic distribution of all CoBLs
Dorsoventral extent of spinal cord
Cells in increasing dorsoventral position –>
K
Dendritic distribution of all motor neurons

Dendritic structure of motoneurons in embryos

So far we have shown that, in the spinal cord of freely swimming larval zebrafish, motoneuron dendrites are organized mediolaterally and dorsoventrally in relationship to their soma position and patterns of recruitment and that this pattern of dendritic organization is probably not simply a consequence of dorsoventral cell body organization. In the next series of experiments, we asked when this organization develops relative to the development of locomotor behavior.

Previous work has showed that the motor behavior of zebrafish changes from spontaneous coiling at 20 hpf, to being largely sedentary (though they will swim away with strong body bends to touch stimuli) between 20 hpf and 4 dpf, to swimming around spontaneously after 4 dpf [84]. We investigated the dendritic structure of motoneurons at different time points during the behavioral maturation of zebrafish locomotion to understand if changes in dendritic organization correlate with the maturation of locomotor behavior. We first looked at the dendritic structure of motoneurons at 2 dpf in embryonic zebrafish when they are largely sedentary. Randomly labeled individual motoneurons expressing mGFP were imaged at 2 dpf. Figure 2.4A-L shows examples of motoneurons in 2 dpf fish. Most motoneurons do not have extensive dendrites at this stage. Instead they are characterized by several fine small dendritic branches that could be exploratory filopodial structures that are characteristic of developing neurons.

Our data hints at two interesting phenomena. First, the fact that most motoneurons do not have dendrites at 2 dpf, well after spontaneous coiling has occurred, suggests that spontaneous activity might not play a role in fine tuning connections on to dendrites. Second, since some of the most dorsal motoneurons differentiate at 14-16 hpf and still do not appear to have dendrites at 48 hpf (2dpf), our data suggests that the time of dendritic outgrowth does not correspond to when the

Figure 2. 4 Dendritic structure of motoneurons at 2 dpf. (A-L) Representative images of motoneuron dendritic structure at 2 dpf. Arrows point to motoneuron axons. The dorsoventral-orientation for all neurons is as shown in 4A. The Anterio-Posterior axis is shown in the bottom left corner of each panel.

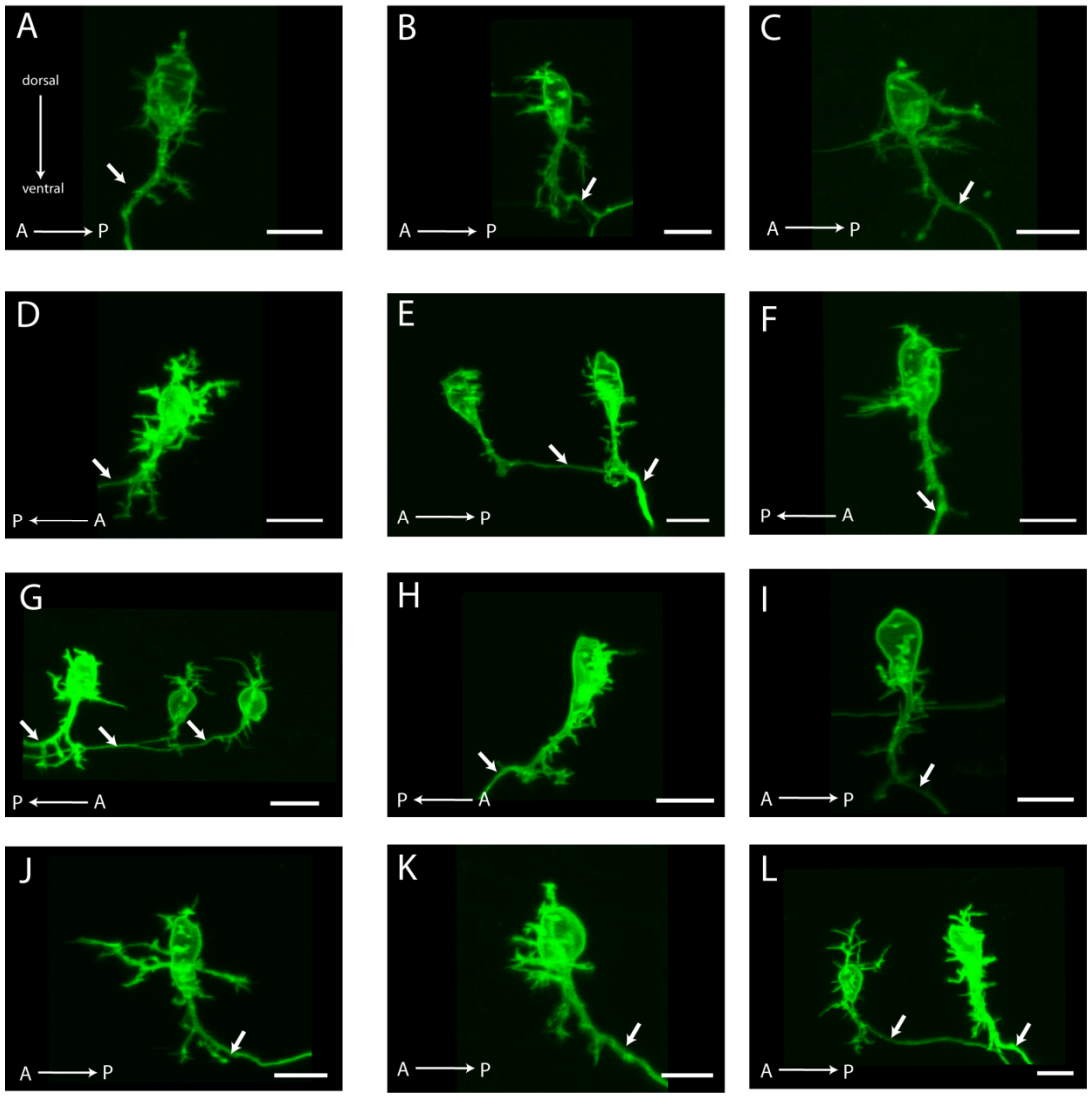
A
dorsal
ventral
A P
B
A P
C
A P
D
P A
E
A P
F
P A
G
P A
H
P A
I
A P
J
A P
K
A P
L
A P

neuron is born. This suggests that specific age related branching patterns might not simply reflect when the neurons elaborate dendrites relative to one another.

Comparison of dorsoventral dendritic distribution and dendritic arbor length between 4 dpf and 6 dpf.

The motor behavior of zebrafish changes dramatically between 2 dpf and 4 dpf [4] and new classes of premotor excitatory interneurons emerge during this time [4]. This prompted us to examine the dendritic structure and dorsoventral distribution of motoneuron dendrites at a time when zebrafish just begin to swim spontaneously at 4 dpf. In order to do this, we imaged the dendritic arbor of individually labeled motoneurons at 4 dpf soon after fish begin swimming spontaneously.

Most motoneurons at different dorsoventral positions have substantial dendritic arbors at 4 dpf as shown in representative images of mGFP expressing motoneurons (Figure 2.5A-C). Moreover, the dendritic arbors appear to elaborate at dorsoventral locations that correlate with the location of the motoneuron soma as shown by the dendritic arbor representations in Figure 2.5D-F and the dorsoventral quantification of dendritic length as shown in Figure 2.5G-I. We imaged dendritic arbors of 53 motoneurons to determine if a dorsoventral dendritic organization was present at 4 dpf. Figure 2.5J shows the dorsoventral distribution of all 53 motoneuron dendrites imaged at 4 dpf. A general dorsoventral topographic organization of motoneuron dendrites is evident at this stage. A plot of the weighted dorsoventral dendritic location versus the dorsoventral location of motoneuron somata shows that the dorsoventral dendritic distribution systematically varies with the dorsoventral location of motoneuron somata at 4 dpf ($n = 53$; R-squared = 0.43; $p < 0.0001$).

These data reveal that a dorsoventral dendritic topography is present at the time when the fish begins swimming freely at 4 dpf, at a time when the swim bladder

Figure 2.5. Relationship between dendritic arbor distribution and location of motoneuronal somata at 4 dpf versus 6 dpf. (A-C). Lateral view of individual mGFP expressing motoneurons located at different dorsoventral positions at 4 dpf. (D-F) Dorsoventral distribution of reconstructed dendritic arbors of motoneurons shown in A-C. (G-I) Color-coded representation of the normalized dorso-ventral dendritic distribution of motoneurons shown in A-C. (J) Quantification of dendritic distribution of all mGFP expressing motoneurons in normalized dorsoventral extent of spinal cord. Each column is a quantification of the dorsoventral distribution of the dendritic arbor of an individual motoneuron as explained in G-I and columns are arranged from left to right in increasing order of dorsoventral cell body position. The normalized dorsoventral location of the cell body is represented on the column as a white circle. (K) Plot of weighted mean dorsoventral location of the dendritic arbor versus the dorsoventral location of a neuron. ($n = 53$; $p < 0.0001$) (L) Plot of dendritic length versus dorsoventral location of motoneuron somata at 4 dpf. (M) Plot of dendritic length versus dorsoventral location of somata at 6 dpf. (N) Overlay of L and M. (O-Q) Lateral view of motoneurons shown at 6 dpf (same neurons as in A-C at 4 dpf). (R-T) Dorsoventral distribution of reconstructed dendritic arbors of motoneurons in O-Q. (U-W) Color-coded representation of the normalized dorsoventral dendritic distribution of motoneurons shown in O-Q. (X) Representation of dendritic distribution of mGFP expressing motoneurons at 6 dpf. (W) Plot of weighted dorsoventral location of the dendritic arbor versus the dorsoventral location of a neuron ($n = 53$; $p < 0.0001$)

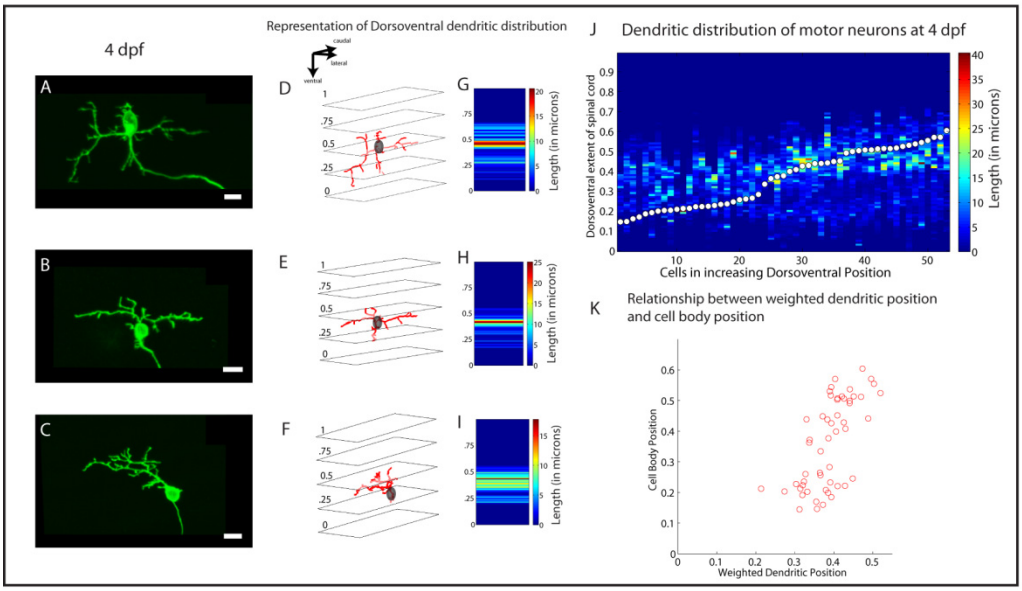
4 dpf
Representation of Dorsoventral dendritic distribution
J Dendritic distribution of motor neurons at 4 dpf
A
B
C
D
E
F
G
H
I
Length (in microns)
Dorsoventral extent of spinal cord
Cells in increasing Dorsoventral Position
K Relationship between weighted dendritic position and cell body position
Cell Body Position
Weighted Dendritic Position

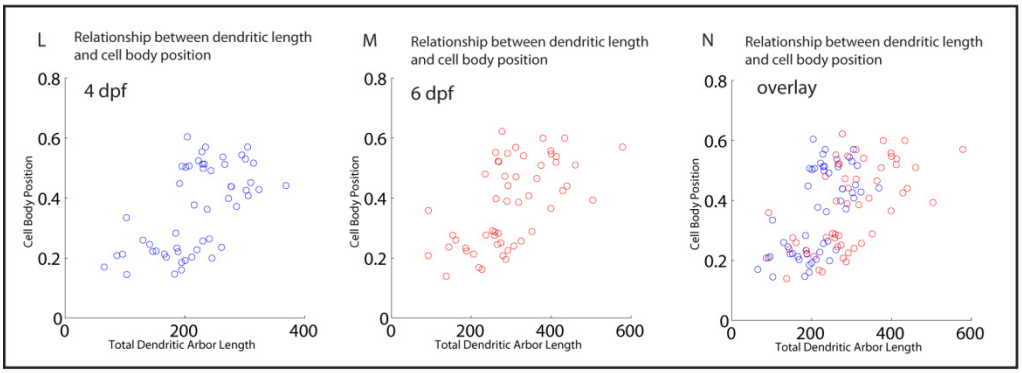
L Relationship between dendritic length and cell body position
4 dpf
M Relationship between dendritic length and cell body position
6 dpf
N Relationship between dendritic length and cell body position
overlay
Cell Body Position
Total Dendritic Arbor Length

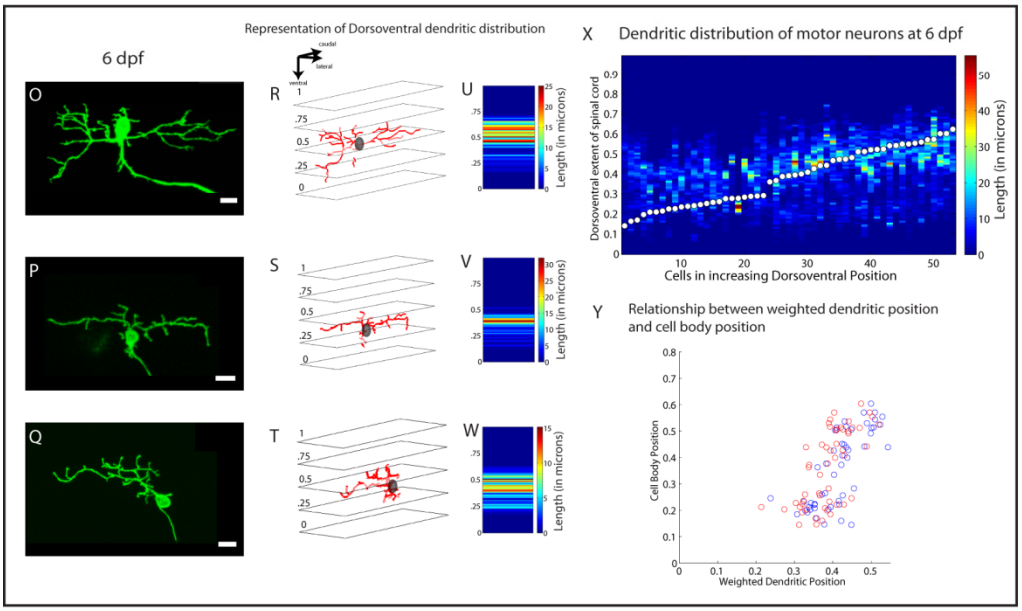
6 dpf
Representation of Dorsoventral dendritic distribution
X Dendritic distribution of motor neurons at 6 dpf
O
P
Q
R
S
T
U
V
W
Length (in microns)
Dorsoventral extent of spinal cord
Cells in increasing Dorsoventral Position
Y Relationship between weighted dendritic position and cell body position
Cell Body Position
Weighted Dendritic Position

inflates and the fish are swimming up in the water column. Taken together with the data that most motoneurons do not have extensive dendrites at 2 dpf (Figure 2.4), our data suggests that a dorsoventral motoneuron dendritic topography emerges between 2 dpf and 4 dpf accompanied by differentiation of new premotor excitatory interneuron [4]. These data also suggests that the initial dorsoventral topography emerges at a time when fish are largely sedentary.

Change in dendritic length and topography after the onset of spontaneous swimming

Several early studies of sensory circuits suggested that the topographic organization of neuronal circuits seen in adults emerges from the pruning of imprecise and exuberant axonal and dendritic structures present early in development. More recent work suggests that initial topography is quite precise early in development and is maintained in spite of the substantial growth of axons and dendrites after the onset of behavior [94]. This motivated us to investigate if motoneuron dendrites grow after the onset of swimming and if this growth changes the dorsoventral topography seen at the onset of spontaneous swimming at 4 dpf. To do this we imaged those motoneurons studied at 4 dpf (analyzed in the previous section) again at 6 dpf, after larvae have been swimming spontaneously for 2 days, and asked how their length and dorsoventral distribution changes.

We first analyzed if dendritic arbors grow in size between 4 dpf and 6 dpf for the set of motoneurons shown in Figure 2.5K. Figure 2.5L is a plot of dendritic length versus cell body position at 4 dpf and Figure 2.5M is the plot for the same motoneurons at 6 dpf. As is evident from Figure 2.5N, the dendritic arbors are significantly longer at 6 dpf compared to 4 dpf ($n = 53$; $p < 0.0001$ paired t-test) showing that significant dendritic growth continues after the onset of spontaneous swimming.

We then asked if this increase in dendritic length alters the dorsoventral topography seen at 4 dpf. To do this, we analyzed the dorsoventral distribution of motoneuron dendrites at 6 dpf for motoneurons that had been imaged previously at 4 dpf. Initial examination of motoneuron dendritic structure that had been imaged at 4 dpf (Figure 2.5A-C) and then imaged again at 6 dpf (Figure 2.5O-Q) suggested that the general dorsoventral organization seen at 4 dpf is not dramatically altered at 6 dpf. As seen in the the dorsoventral distribution of reconstructed dendritic arbors (compare Figure 2.5D-F with Figure 2.5R-T), with the exception of the more dorsal motoneuron (compare 5A and 5O), the dendritic arbors of motoneurons do not substantially shift their general dorsoventral location. The dorsoventral distribution of dendritic arbors of these motoneurons is quantified in Figure 2.5U-W and shows that only the dendritic arbor of the more dorsal motoneuron shifts more dorsally. We next examined, at 6 dpf, the dorsoventral distribution of all 53 motoneurons that had been imaged before at 4 dpf (Figure 2.5X). This representation suggested that the dorsoventral topography present at 4 dpf is maintained at 6 dpf in spite of dendritic growth. A plot of the weighted dorsoventral dendritic location versus the dorsoventral location of motoneuron somata shows significant correlation between dorsoventral dendritic distribution and the dorsoventral location of motoneuron somata at 6 dpf ($n = 53$; R-squared = 0.51; $p < 0.0001$;).

These data show that the dendrites of motoneurons continue to grow significantly after the onset of spontaneous swimming. They also show that the dendritic topography observed at 4 dpf is maintained in the face of additional dendritic growth between 4 dpf and 6 dpf.

Quantification of dendritic growth and retraction between 4 dpf and 6 dpf

Several studies in sensory circuits suggested that substantial dendritic pruning occurs after the onset of function [39]. While our analysis of dendritic length clearly

showed that motoneuron dendrites grow after the onset of swimming, this analysis did not rule out the possibility of substantial dendritic retraction that was masked by even greater dendritic growth. Initial visual comparison of dendritic arbors between 4 dpf and 6 dpf suggested that not much dendritic retraction appears to take place. To confirm if this was in fact the case, we chose to quantify the amount of dendritic growth and retraction between the two time points.

Using custom software (see Materials and Methods) we superimposed dendritic arbors from the two time points in 3D. Our program reliably and accurately aligned 40 out of the 53 motoneurons analyzed in the previous section. This alignment allowed us to confidently quantify the amount of dendritic growth and retraction that took place between 4 dpf and 6 dpf.

Figure 2.6A shows a dorsal motoneuron at 4 dpf and Figure 2.6B shows the structure of the same motoneuron at 6 dpf. Figure 2.6C shows an image of the superimposed dendritic structures between 4 dpf and 6 dpf. Figure6D-F and Figure 2.6G-I show images of more ventrally located motoneurons. Figure 2.6K is quantification of the amount of dendritic growth and retraction of all 40 motoneurons and Figure 2.6L is a quantification of the net dendritic change between 4 dpf and 6 dpf. Some, but not extensive, dendritic retraction does occur after the onset of spontaneous swimming. We also find that the amount of retraction is significantly correlated with the dorsoventral location of somata (Figure 2.6M; $n = 40$; $p < 0.05$).

Most of the change in dendritic structure between 4 dpf and 6 dpf can be attributed to dendritic growth (Figure 2.6K) because the length of added processes was much greater than the length of retractions. The amount of dendritic addition also correlated significantly with the dorsoventral location of motoneuron cell body (Figure 2.5O; $n = 40$; $p < 0.0001$).

Figure 2.6. Analysis of dendritic growth and retraction between 4 dpf and 6 dpf. (A-I). Representative images of motoneurons at 4 dpf and 6 dpf and at different dorsoventral locations. The overlaid image reveals how much the dendritic structure has changed between the two time points. (K). Quantification of dendritic growth and retraction between 4 dpf and 6 dpf for 40 motoneurons organized from bottom to top in increasing order of dorsoventral soma location. (L). Net dendritic change in motoneurons shown in (K). (M). Plot of the amount of dendritic retraction versus soma position ($n = 40$; $p < 0.05$). (N). Plot of dendritic growth versus soma position ($n = 40$; $p < 0.0001$). (O). Overlaid plot of growth and retraction versus soma position.

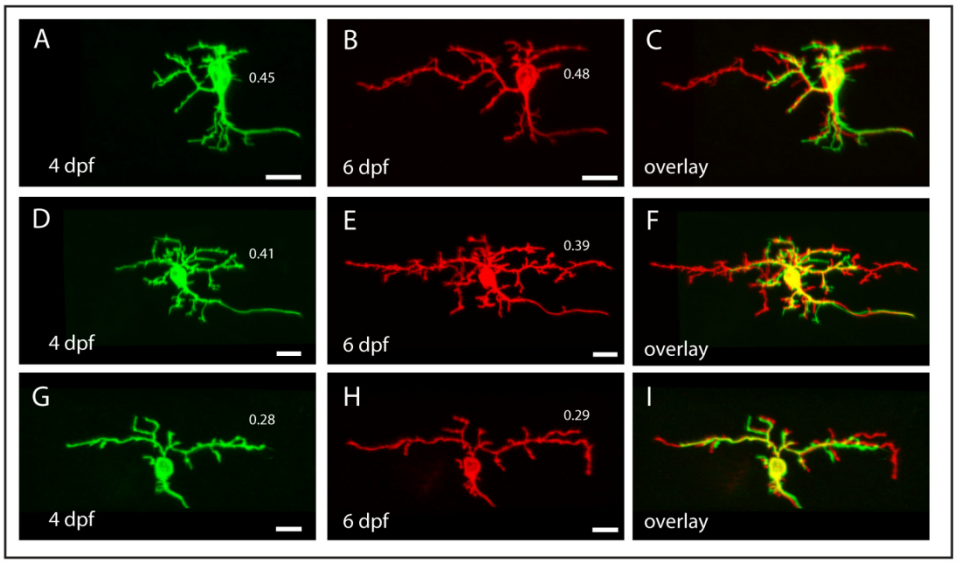
A
0.45
4 dpf
B
0.48
6 dpf
C
overlay
D
0.41
4 dpf
E
0.39
6 dpf
F
overlay
G
0.28
4 dpf
H
0.29
6 dpf
I
overlay

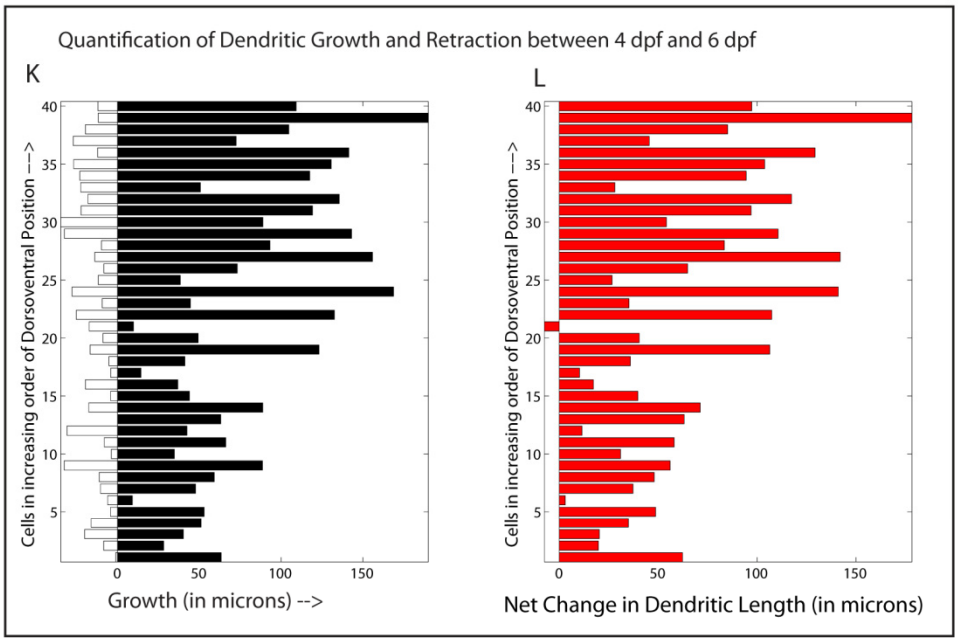
Quantification of Dendritic Growth and Retraction between 4 dpf and 6 dpf
K
L
Cells in increasing order of Dorsoventral Position --->
Growth (in microns) -->
Net Change in Dendritic Length (in microns)

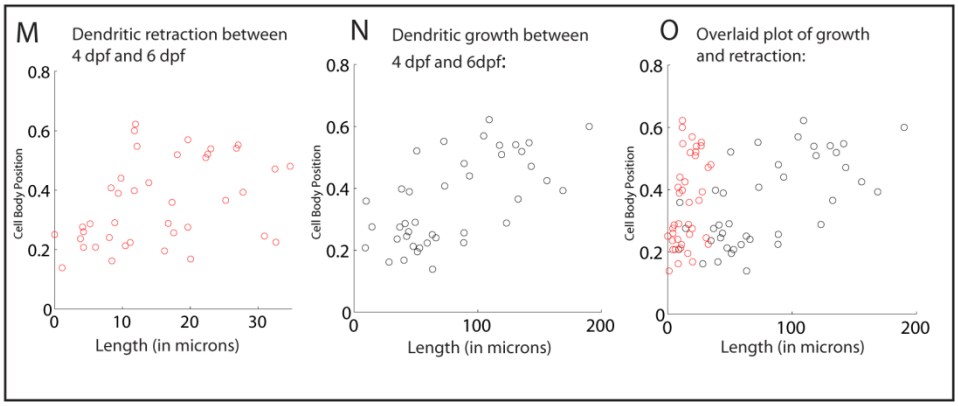
M
Dendritic retraction between 4 dpf and 6 dpf
N
Dendritic growth between 4 dpf and 6dpf:
O
Overlaid plot of growth and retraction:
Cell Body Position
Length (in microns)

Since dendritic pruning is thought to signify the elimination of inappropriate connectivity, the absence of much dendritic retraction suggests that the initial topography of motoneuron dendrites that emerges by 4 dpf, in the absence of locomotor activity, may be quite precise. Our data also suggests that the amount of dendritic growth and retraction vary along the dorsoventral gradient of soma position suggesting that changes in dendritic structure may be influenced by the recruitment pattern of motoneurons. It should be noted that the relationship between cell body location and the amount of retraction is not significant when the retraction is normalized for the length of the dendritic arbor at 4 dpf.

Dorsoventral distribution of dendritic growth and retraction

We next asked if there was a systematic pattern in the dorsoventral distribution of dendritic growth and retraction between 4 dpf and 6 dpf.

Examination of 3 superimposed motoneuron dendritic structures from 6 dpf and 4 dpf indicated that the dorsoventral location of dendritic growth correlated with the dorsoventral location of motoneuron somata as shown by representative images of motoneurons located at different dorsoventral locations (Figure 2.7A-C; 7E-F; 7I-K). Since the amount of dendritic retraction is small compared to the amount of growth, a dorsoventral pattern of dendritic retraction does not stand out by visual examination (Figure 2.7A-C; 7E-F; 7I-K). For the examples shown in Figure 2.7A-K, the correlation between motoneuron soma location and the dorsoventral distribution of dendritic growth is clearer when we quantified the growth along the dorsoventral axis (Figure 2.7D,H,L; left panels). However, dendritic retraction did not appear to occur preferentially in a dorsoventral region (Figure 2.7D,H,L; right panels). We then examined patterns of dorsoventral dendritic growth and retraction for all 40 motoneurons, imaged at 4 dpf and then at 6 dpf, whose dendritic structures could be

Figure 2.7. Analysis of dorsoventral distribution of dendritic growth and retraction between 4 dpf and 6 dpf. (A-B). Representative example of a dorsal motoneuron at 4 dpf (A) and the same motoneuron at 6 dpf (B). (C) Overlaid image to quantify the dorsoventral location of dendritic addition and retraction. (D) Color coded map of the dorsoventral distribution of dendritic growth and retraction. (E-L). Representative examples of dorsoventral patterns of growth and retraction for more ventrally located motoneurons. (M). Dorsoventral distribution of dendritic growth for all 40 motoneurons. Each column represents a single neuron and rows are organized from left to right in increasing order of dorsoventral soma position. White circle overlaid represents normalized dorsoventral soma position (N) Dorsoventral distribution of dendritic retraction for all 40 motoneurons. (O). Dorsoventral distribution of net dendritic change for all 40 motoneurons. (P) Plot of weighted dorsoventral dendritic growth between 4 dpf and 6dpf versus normalized dorsoventral soma position. ($n = 40$; $p < 0.05$) (Q) Plot of weighted dorsoventral dendritic retraction versus normalized dorsoventral soma position ($n = 40$; $p = 0.5$). (R) Overlaid plot of weighted dendritic growth and retraction in relation to soma position.

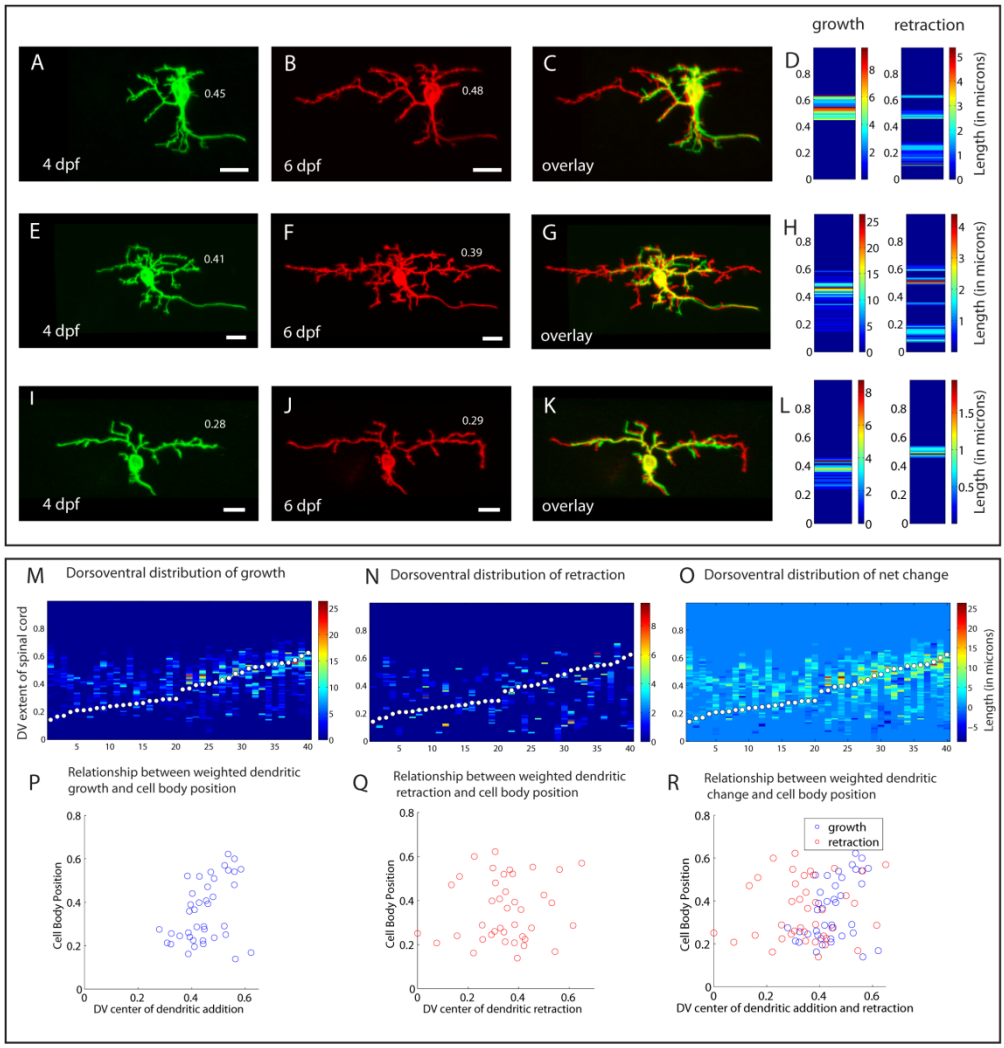
growth
retraction
A
0.45
4 dpf
B
0.48
6 dpf
C
overlay
D
E
0.41
4 dpf
F
0.39
6 dpf
G
overlay
H
I
0.28
4 dpf
J
0.29
6 dpf
K
overlay
L
Length (in microns)
M Dorsoventral distribution of growth
N Dorsoventral distribution of retraction
O Dorsoventral distribution of net change
DV extent of spinal cord
P Relationship between weighted dendritic growth and cell body position
Q Relationship between weighted dendritic retraction and cell body position
R Relationship between weighted dendritic change and cell body position
Cell Body Position
DV center of dendritic addition
DV center of dendritic retraction
DV center of dendritic addition and retraction
growth
retraction

aligned reliably. Visual examination suggests that dorsoventral location of dendritic growth correlates with motoneuron soma position especially for the more dorsally located motoneurons (Figure 2.7M) while no pattern appears to exist for dendritic retraction (Figure 2.7N). We then examined the dorsoventral distribution of net dendritic change (by subtracting the distributions in 7N from the distributions in 7M). As shown in Figure 2.7O, this representation does not suggest any dorsoventral pattern of net dendritic elimination (darker blue shades) relative to where dendritic growth occurs

dorsoventrally. We then determined the weighted dorsoventral location of dendritic growth and dendritic retraction to see if these correlated with the dorsoventral location of motoneuron somata. The weighted dorsoventral dendritic growth is significantly correlated with motoneuron soma position (Figure 2.7P; $n = 40$; $p < 0.05$) whereas there is no relationship between dorsoventral dendritic retraction and soma position (Figure 2.7Q; $n = 40$; $p = 0.5$). Figure 2.7R shows the overlaid patterns of dorsoventral dendritic growth and retraction. Though we could not analyze this statistically, dendritic retraction appears to take place more ventrally relative to dendritic growth for more dorsal motoneurons. Taken together, these data suggest that dendritic growth, and hence the potential addition of new synapses, is systematically related to motoneuron soma location, and this could contribute to maintaining dendritic topography even as dendrites grow after fish begin swimming freely.

Discussion

While the topographic organization, and development, of axons and dendrites underlying sensory function is understood in some detail [93], whether there is any topography in spinal motor circuits of vertebrates is not clear. Though there is some

evidence for dendritic organization in vertebrate motoneurons [69, 70, 73], other studies have not found any obvious relation between dendritic organization and motoneuron soma position or the muscles these motoneurons innervate [68, 72, 73]. However, motoneuron dendritic organization in relation to their patterns of recruitment during locomotion at different speeds has not been studied. The spinal circuits of most vertebrates do not lend themselves to an analysis of motoneuron dendritic organization in relation to locomotor function. In this paper we took advantage of a recently discovered organization of motoneuron somata in relation to locomotor speed in larval zebrafish [3], and asked how the organization of motoneuron dendrites relates to soma position. The rapid maturation of locomotor behavior in zebrafish [84, 86] and their transparency also allowed us to ask when this organization develops in relation to the development of locomotor behavior.

We discovered a novel dendritic topography related to motoneuron soma position and the speed at which they are recruited in freely swimming larval zebrafish – dendrites of dorsal, older motoneurons that drive fast swimming arborize more dorsally and medially in the neuropil relative to dendrites of ventral, younger motoneurons recruited at slower speeds.. This topography is present at the time when fish start swimming spontaneously and is only modified qualitatively after the onset of spontaneous swimming. Finally our results show that relatively little dendritic pruning occurs after the onset of spontaneous swimming and the amount of dendritic growth correlates with the dorsoventral position of motoneuron somata. Taken together, these data point to an age and speed-related organization of dendrites of vertebrate spinal motor circuits that underlie the ability to move over a range, and suggest that this organization emerges in the absence of much locomotor activity.

Dendritic topography of motoneurons: Implications for the organization of connectivity in spinal motor circuits

The topographic organization of axons and dendrites has been explored extensively in sensory circuits [93] and more recently in invertebrate motor networks [63, 64, 66, 96] and is thought to have two advantages for neuronal function and organization of neuronal connectivity. First, topography is thought to confer specificity in the connectivity of circuits and helps determine the activation of appropriate neurons. Second, topographic organization is thought to be a mechanism for wiring minimization in circuits – axons and dendrites are metabolically expensive to maintain and topographic organization maximizes connectivity while minimizing the cost of wiring [97-99]. Our discovery of dorsoventral and mediolateral topography of motoneuron dendrites has implications for the organization of connectivity related to the pattern of recruitment of motoneurons as well as for the optimal organization of wiring underlying motor pattern generation.

Based on recent work [3] we know that motoneuron somata are topographically organized in the spinal cord of zebrafish in relation to the swimming speed at which they are recruited; the most ventrally located motoneurons are recruited at the slowest swimming speeds while progressively more dorsal motoneurons get recruited as fish swim faster. This pattern of recruitment is thought to be a consequence of a dorsoventral gradient of excitability that maps on to the dorsoventral pattern of recruitment so that the most ventral motoneurons recruited at the slowest speeds are the most excitable while more dorsal motoneurons are recruited at faster speeds because they are less excitable. The dendritic topography we describe may act in concert with the dorsoventral gradient of excitability to determine the recruitment pattern seen in motoneurons. The patterns of dendritic distribution of

motoneurons may ensure that motoneurons receive appropriate descending input to be recruited only at specific speeds.

There is functional data to suggest that there is specificity in connectivity between premotor excitatory interneurons and motoneurons. Ablating MCoD interneurons in larval zebrafish specifically perturbs slow swimming [3] whereas ablating CiD interneurons specifically perturbs swimming at faster speeds . These data suggest that MCoD interneurons innervate ventral motoneurons that are active during slow swimming while CiD interneurons innervate more dorsal motoneurons that drive fast swimming. If so, we would expect that MCoD axons would be in close proximity to dendrites of ventral secondary motoneurons while CiD axons would branch closer to dendrites of dorsal motoneurons.

There is some evidence for the topographic organization of presynaptic input for at least one class of interneurons that provide excitatory drive to motoneurons. Excitatory interneurons in the hindbrain and spinal cord (CiDs) that express the transcription factor *Alx* (*Chx10* in mice) provide excitatory drive to motoneurons during swimming [90, 95, 100]. Recent work suggests a functional organization in the processes of Alx neurons - neuropil of older Alx cells recruited in fast swimming is medial and dorsal to younger neuropil (Kinkhabwala *et al* submitted). The organization of motoneuron dendrites we describe mirrors this organization of excitatory presynaptic input. Dendrites of older, dorsal motoneurons arborize more medially and dorsally relative to dendrites of younger, ventral motoneurons.

The implication is that the motoneuron dendritic organization we observe in freely swimming larval zebrafish might be important for the appropriate functional recruitment of motoneurons. The organization of premotor axons and motoneuron dendrites is also consistent with the idea of an age related wiring of neural circuits underlying the ability to move at a range of speeds such that older neurons connect

with each other to drive fast locomotor behavior while progressively younger neurons connect with each other and drive swimming at slower speeds. The predictions of connectivity based on the topographic pattern we observe are testable using anatomical techniques such as Brainbow [101] and new optogenetic techniques such as channelrhodopsin [102].

Emergence of motoneuron dendritic topography during development: Implications for the development of connectivity in spinal motor circuits

Motoneuron dendritic development has been studied in some detail in different vertebrates, but it is still not clear if and how motoneuron dendritic development is influenced by motor activity. Zebrafish motor behavioral repertoire transitions from spontaneous coiling (at 20 hpf) to fast swimming (at 2 dpf) to basic locomotor patterns (at 4 dpf) similar to the development of axial movements in all vertebrates [4]. By observing the dendritic structure of motoneurons at 2 dpf , 4 dpf and 6 dpf, we were able to correlate changes in dendritic structure and organization to the development of locomotor behavior.

We first looked at motoneuron dendritic structure at 2 dpf (48 hpf), well after the period of spontaneous coiling which occurs around 20 hpf, and found that most motoneurons do not have much dendritic structure at this time point. Spontaneous network activity is known to occur in many developing motor networks though its specific role in setting up connectivity is not clear. One possibility is that the spontaneous activity could play a role in refining synaptic connectivity onto dendrites according to Hebbian mechanisms. Our finding that most motoneurons do not have dendrites even at 2 dpf (48 hpf) shows that spontaneous coiling movements that occur at 20 hpf is not directly involved in fine tuning connectivity onto motoneuron dendrites. However, it is possible that early spontaneous activity is required for establishing connectivity on somata and processes that give rise to the axon. It is also

possible that early spontaneous activity initiates genetic programs that eventually influence dendritic topography.

When we looked at motoneuron dendritic structure soon after larvae start swimming freely (4 dpf), we found that a dorsoventral dendritic topography in relation to motoneuron position and recruitment is already present. Prior to 4 dpf, fish are largely sedentary. These data indicate that acquiring the initial dendritic topography does not require the activity associated with free swimming. Given that most motoneurons do not have dendrites at 2 dpf, our data also suggests that initial dendritic topography emerges between 2 dpf and 4 dpf even though the oldest motoneurons are already present by 15-16 hpf. This raises the possibility that dendritic topography does not emerge simply because dendrites of older, dorsal motoneurons elaborate before younger, more ventral motoneurons. However, based on our choice of time points, we cannot definitely rule out that there is no age related order in the development of dendrites between 2 dpf and 4 dpf.

A key question in the development of nervous systems is if and how dendritic organization changes after the onset of functional activity. Our comparison of the dendritic structure between 4 dpf and 6 dpf suggests that the activity associated with spontaneous swimming does not significantly affect dendritic topography even as dendrites continue to grow. Our finding that relatively little dendritic retraction takes place after the onset of spontaneous swimming is similar to recent studies in sensory systems of vertebrates that show that “appropriate” dendritic structure can be established without much dendritic pruning. Intriguingly, we also find that dendrites of more older, dorsal motoneurons grow more than dendrites of younger, ventral motoneurons between 4 dpf and 6 dpf even when normalized for their lengths at 4 dpf. This systematic variation in the amount of dendritic growth in relation to the dorsoventral location of motoneuron somata suggests that different motor circuit

components do not follow a universal growth program. Instead their specific functional patterns of recruitment might influence the extent and pattern of connectivity they receive during development.

Our observation that dendritic topography is present at the onset of spontaneous swimming and changes only qualitatively after the onset of swimming (between 4 dpf and 6 dpf) is reminiscent of the development of topography in many sensory systems wherein a basic topography is present at the onset of sensory function and is maintained in the face of neuronal growth and continued synaptogenesis that occurs after an animal is born [94]. Work in sensory circuits has showed that initial topography is set up by genetic cues while maintaining it subsequently requires neuronal activity. It is tempting to speculate that this might be the case in the topography of motoneuron dendrites in vertebrates as well. These parallels also suggest that the rules determining the wiring of motor circuits and sensory circuits might not be as dramatically different as thought previously.

Our results suggest that the topography of neuronal circuitry underlying the ability to move at different speeds is organized according to the age and recruitment pattern of neurons. Moreover we find that the initial dendritic organization emerges in the absence of much locomotor activity, and dendritic growth and retraction after fish begin swimming freely do not alter this topography significantly. Given the universality of the size principle of motoneuron recruitment, the conservation of cell types that drive locomotor behavior in many different vertebrates and parallels in the development of motor behavior with other vertebrates [4], we think that this topography and its developmental pattern of assembly might be a general principle of organizing and assembling connectivity in spinal neuronal circuits underlying locomotion across all vertebrates.

Materials And Methods

Fish care

Experiments were performed on 2 to 6 day old zebrafish (*Danio rerio*) obtained from a laboratory stock of wild type adults. Embryos were raised at 28.5^{o}C in the same system as adults (Aquatic Ecosystems, Inc.,Apopka,FL). At these ages, larval fish are still nourished by the remnants of their yolk sac. All procedures conform to the National Institutes of Health guidelines regarding animal experimentation and were approved by Cornell University's Institutional Animal Care and Use committee.

Transient Expression of Fluorescent Reporter in Individual Motoneurons

DNA injected at low concentrations (20-30 ng/ul) into fertilized eggs at the single cell stage resulted in stochastic expression of fluorescent protein in isolated motoneurons. Embryos were screened for expression of fluorescence at 48-80 hours post fertilization (hpf) and embryos where individually labeled motoneurons could be seen unambiguously were selected for imaging. All injections were done as previously described. In order to increase reporter expression levels, the Gal4-VP16/14XUAS system was utilized [103]. A bacterial artificial chromosome containing regulatory elements for Vesicular Acetylcholine Transporter (VAchT) was modified by homologous recombination to create a VAchT:Gal4 driver to drive expression specifically in motoneurons. To drive the expression of membrane targeted GFP, a 14X*UAS*:mGFP reporter construct was coinjected with VAchT:Gal4. The 14X*UAS*:mGFP construct was derived from 14XUAS [103]and *brn3c:mGFP* [104]. To look at the mediolateral distribution of dendrites, a 14X UAS:mMCherry reporter construct was coinjected with VAchT:Gal4 in the Alx:GFP transgenic line at the single cell stage.

For tracking motoneuron dendritic structure during development, images of dendritic structure of the same motoneuron were collected at 4 dpf and 6 dpf using the "catch and release" protocol. Initially fish screened for mGFP expressing motoneurons

were anesthetized, embedded in agarose and imaged (as described below) at 4 dpf soon after they began swimming. After each imaging session, the agarose was gently pried apart with forceps until the embedded fish was released into the overlying solution. The larvae were then allowed to swim around freely in zebrafish tanks maintained at 28.5^0C for 2 days and the same motoneuron was imaged again at 6 dpf.

In vivo Confocal Microscopy

Larvae were anesthetized in a 0.02% solution of MS-222. Once larvae were immobilized (2-3 minutes), they were embedded in low melting-point agarose, covered in 10% Hank's solution. Fish were oriented such that motoneurons were imaged from the lateral view. Hank's solution was maintained at 28.5^oC for the duration of imaging. Labeled cells were imaged using a confocal microscope (Zeiss LSM 510, Carl Zeiss). An image of the entire dendritic arbor was collected simultaneously with the DIC image of the spinal cord. This DIC image was collected to determine the dorsoventral distribution of dendrites and to determine the location of the neuron in the spinal cord relative to the dorsal and ventral edge of the cord.

Quantification of dorsoventral dendritic distribution

Custom Matlab scripts were written to analyze the dorsoventral distribution of dendrites. The reconstructed dendritic arbor was superimposed on the DIC z-stack of the spinal cord. The DIC image of the spinal cord was used to identify the ventral and dorsal edges of the spinal cord. The dorsoventral extent of the spinal cord was normalized so that the ventral edge was 0 and the dorsal edge was 1. The dorsoventral volume was then divided into a 100 equal dorsoventral sections and the length of the reconstructed dendritic arbor in each dorsoventral volume was calculated.

To calculate the weighted dorsoventral position of dendrites, the fraction of dendritic arbor relative to the total dendritic length, was calculated for each dorsoventral volume. The fractional length was multiplied by the average of the

normalized dorsoventral limits of the volume and this value for all dorsoventral locations was summed to give the weighted dorsoventral location of the dendritic arbor or filopodial extensions. Motoneuron location was determined by averaging three measurements from the bottom of spinal cord to the middle of the cell body using either Zeiss software. This value was then normalized to an average of three measurements of the total dorso-ventral extent of spinal cord.

Quantification of mediolateral dendritic distribution

Custom Matlab scripts were written to analyze the mediolateral distribution of dendrites. The mediolateral extent of the Alx:GFP neuropil at 6 dpf was visually determined in Imaris. This mediolateral range was superimposed in 3D on the reconstructed dendritic arbor. The mediolateral extent of the spinal cord was normalized so that the medial limit was 0 and the lateral limit was 1. The mediolateral volume was then divided into a 25 equal mediolateral sections and the length of the reconstructed dendritic arbor in each mediolateral volume was calculated.

To calculate the weighted mediolateral position of dendrites, the fraction of dendritic arbor relative to the total dendritic length, was calculated for each mediolateral volume. The fractional length was multiplied by the average of the normalized mediolateral limits of the volume and this value for all mediolateral locations was summed to give the weighted mediolateral location of the dendritic arbor. Motoneuron location was determined as described in the previous section.

Analysis of dendritic growth and retraction

Custom Matlab scripts that incorporated programs from the SPM Matlab toolbox (http://www.fil.ion.ucl.ac.uk/spm/software/spm2/) were used to align dendritic structures from 4 dpf and 6 dpf in 3D. Some z-stacks were manually adjusted using the "Channel Shift" function in Imaris to ensure that images were well aligned. These aligned images were then used to visually guide the 3D reconstruction of dendritic

growth and retraction using the Filament function of Imaris (Bitplane, Inc.). These reconstructions were then overlaid on the DIC image collected at 6 dpf to calculate the dorsoventral distribution of dendritic growth and retraction as described above.

CHAPTER 3

Title: Dendritic dynamics of motoneurons in the spinal cord of larval zebrafish vary systematically with location and excitability.

ABSTRACT:

Dendritic arbors of developing neurons constantly extend and retract filopodia and this exploratory behavior sub-serves synapse formation and dendritic growth in developing circuits. Here we use *in vivo* imaging in the spinal cord of larval zebrafish (*Danio rerio)* to reveal a systematic relationship between the location of a spinal motoneuron and the dynamics of its dendritic arbor. The youngest, ventral motoneurons are least dynamic whereas increasingly older and more dorsal motoneurons are more dynamic. This pattern of dynamics correlates with dendritic growth; dendrites of dorsal motoneurons also grow more than those of ventral motoneurons. This pattern of dendritic dynamics and dendritic growth could be explained at least partly by the dorso-ventral gradient in the excitability of motoneurons, because ventral motoneurons have higher input resistances than dorsal ones and so could be more excitable. We tested this possibility genetically by expressing Kir2. to suppress excitability of individual motoneurons. This led to a dramatic increase in the dynamics of ventral motoneurons, which became more dynamic than more dorsal ones. Our results suggest that a naturally occurring dorsoventral gradient of excitability may contribute to the variation in dendritic dynamics and could be a mechanism for regulating connectivity and dendritic growth in developing motor circuits.

Introduction

Dendritic arbors of developing neurons are highly dynamic [42, 49, 105]. Rapid time lapse imaging of developing dendrites in different parts of the brain has revealed filopodial structures that extend and retract from primary dendritic branches

on the time scale of minutes [42]. Dendritic filopodia are considered to be exploratory structures seeking to form connections with presynaptic neurons, leading to new synapses and dendritic growth [49, 50, 106]. While filopodial structures are abundant on the dendrites of developing neurons, they reduce substantially as neurons grow older – imaging studies of older neurons reveal that that they are less dynamic than younger neurons [41, 45, 49, 50, 106]. This has led to the proposal that dendritic dynamics decreases once a neuron receives sufficient synaptic input . [45, 107]. Consistent with this idea, perturbing excitatory synapse formation post-synaptically results in more dynamic dendritic arbors in optic tectal neurons that receive visual input[108]. However, neural circuits have several different cell types which have different functional roles and might vary in the amount of synaptic input they receive. This raises the possibility that dendritic dynamics underlying the formation of new synapses during development might vary according to the specific functional role of the neuron in the network.

Historically, studies on dendritic dynamics have been done without a clear functional role for the neurons being studied or a detailed understanding of their activity patterns. Most studies of dendritic dynamics have been done in *in vitro* preparations of neurons which cannot mimic dendritic dynamics in a functioning network. *In vivo* studies of tectal neurons have revealed how neurotransmission modulates dendritic growth and dynamics [36, 49]. These studies have not, however, examined the dendritic dynamics of neurons in relation to their cellular properties or specific functional role in the circuit. Until recently, there was no experimentally accessible neuronal circuit that could be imaged *in vivo* and showed a systematic variation in cellular properties and functional recruitment patterns.

The spinal motor system of zebrafish now offers this opportunity. Recent work shows that spinal neurons in larval zebrafish vary systematically in their input

resistance and the speed at which they are recruited during swimming and this variation maps onto their dorsoventral location in the spinal cord [3]. Motoneurons and excitatory interneurons located at the ventral edge of the spinal cord are recruited at the slowest swimming speeds and progressively more dorsal neurons are recruited at faster speeds. This pattern of recruitment and dorso-ventral location of neurons correlates with a gradient of input resistance; the most ventral motoneurons have the highest input resistances, with input resistance decreasing systematically in increasingly more dorsal neurons.

We studied the dendritic dynamics of spinal motoneurons innervating axial musculature in larval zebrafish to understand if dendritic dynamics of developing neurons is influenced by intrinsic cellular excitability. The ability to use transient mosaic expression of noninvasive reporters such as GFP and high-resolution in vivo confocal microscopy to image dendritic dynamics of spinal motoneurons in larval zebrafish made it an ideal system to understand the relationship between naturally occurring variation in cellular excitability and dendritic dynamics. We found that, at 4 days post fertilization, when larval zebrafish begin to swim around spontaneously, there is a relationship between the extent of filopodial extension of spinal motoneurons and their dorsoventral location in the spinal cord. The filopodial length extended by dendritic arbors of ventral motoneurons was less than that of dorsal motoneurons, even when corrected for the smaller overall dendritic length of the neurons. This pattern of dynamics was correlated with dendritic growth because dendrites of more dorsal motoneurons grew more than dendrites of ventral motoneurons. Since the dorsoventral location of neurons correlates systematically with their excitability, we tested the hypothesis that the dendritic dynamics of developing spinal motoneurons was influenced by their intrinsic excitability. We found that genetically decreasing the excitability of individual motoneurons inverts the

relationship between filopodial extension and the dorsoventral location of motoneurons, so that ventral motoneurons after the perturbation extend more filopodia than dorsal motoneurons. These data suggest that, at least in vertebrate spinal motor networks, in contrast to sensory systems, developing dendritic arbors of younger neurons are less dynamic than dendritic arbors of older motoneurons. Instead, the dendritic dynamics of motoneurons are influenced by the intrinsic excitability and the recruitment pattern of motoneurons, which might be a mechanism to tie in developmental phenomena that establish connectivity with the functional role of neurons.

Results

Distribution of putative synaptic sites on dendrites of developing motoneurons

Dendritic arbors of developing neurons are characterized by fine filopodial processes, most of which are retracted within a short time [42, 46, 47]. It is known that because filopodia are exploratory, they often do not bear functional, mature synapses. We first wanted to determine, using light microscopy, if dendritic arbors of motoneurons in larval zebrafish contained filopodia-like structures. We hypothesized that if we simultaneously visualized synapses and dendritic structure, we would see small branches on the primary dendritic arbor that would usually not contain synapses. To visualize synapses, we used a GFP-tagged version of PSD-95 (SAP-90), a scaffolding protein known to localize to the postsynaptic density (PSD) of excitatory synapses. Several previous studies show that PSD95 is a reliable marker of excitatory synapses [50]. To visualize fine dendritic structure, we chose to use a version of membrane targeted red fluorescent protein (mCherry). We used the Gal4-UAS system to specifically drive the expression of PSD95:EGFP and mCherry in motoneurons using a motoneuron specific driver (Vesicular Acetylcholine Transporter) for Gal4

expression. Plasmids were injected into embryos at the single cell stage at low concentrations which resulted in stochastic labeling of individual motoneurons.

Figure 3.1A-D shows punctuate expression of PSD95:GFP in individual motoneurons whose dendrites are labeled with mCherry. These motoneurons were imaged in larval zebrafish at 4 dpf soon after they began swimming spontaneously. Several small branches are evident on all motoneurons we imaged (n = 20) that did not bear any obvious PSD95 puncta. The absence of PSD95:GFP associated puncta on several small, fine branches is consistent with the idea that dendrites of motoneurons are in fact extending filopodia-like structures in larval zebrafish at 4 dpf.

Filopodial dynamics of developing motoneurons

To more closely examine the dynamics of filopodial structures, we did rapid time lapse imaging of the dendritic structure of individual motoneurons *in vivo* in larval zebrafish soon after they began swimming spontaneously at 4 dpf.

Individual motoneurons were visualized by using the zebrafish Vesicular acetylcholine promoter to drive the expression of a membrane targeted green fluorescent protein (mGFP). Using membrane targeted fluorescent protein allows visualizing fine neuronal structures even at low laser intensities with a high signal to noise ratio. The entire dendritic arbor of individually labeled motoneurons was imaged every 5 minutes for 30 minutes in immobilized fish. We studied the dynamics in immobilized, but not anesthetized fish so as to minimally disrupt the functional network activity underlying swimming behavior.

Initial examination of time lapse movies suggested that the older, dorsal motoneurons (Figure 3.2E-H) extended more filopodia than younger ventral motoneurons (Figure 3.2A-D). We examined this more closely in a quantitative way by looking at the relationship between neuronal location and the total number of filopodial extensions during the imaging period. A plot of cell body position versus

Figure 3.1. Simultaneous visualization of dendritic structure and putative synapses. (A-D) Representative motoneuron dendrites and putative glutamatergic postsynaptic sites visualized by expressing membrane tagged mCherry and PSD95-EGFP. Arrows point to filopodia-like structures that do not bear PSD95-EGFP puncta.

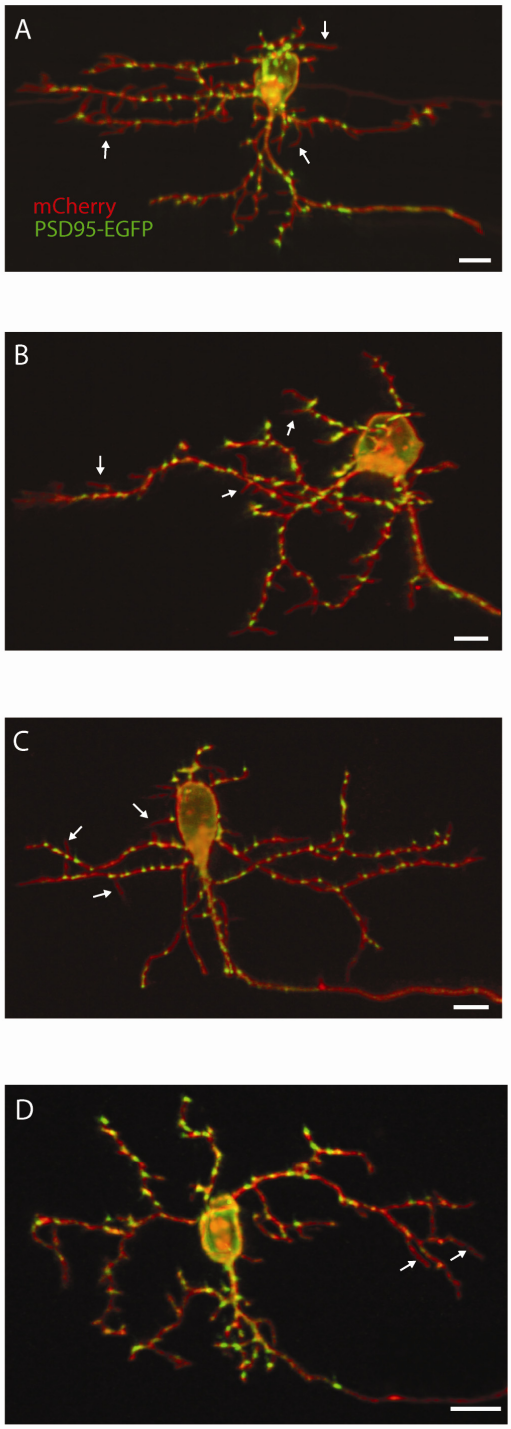
A
mCherry
PSD95-EGFP
B
C
D

Figure 3.2. Rapid time-lapse imaging of the dendritic structure of mGFP expressing motoneurons located at different dorsoventral locations. (A,B) Images of a ventral motoneuron at the first two consecutive time points (0 min and 5 min). (C) overlaid image of B and A.Arrows point to filopodial extensions. (D) Reconstruction (in white) of dendritic extensions over a 30 minute period. (E,F) Images of a dorsal motoneuron at the first two consecutive time points (0 min and 5 min). (G) overlaid image of F and E. Arrows point to filopodial extensions; (H) Reconstruction (in white) of filopodial extensions over a 30 minute period. (I) Plot of cell body position versus dendritic arbor length that remained constant over the entire imaging period ($n = 34$; $p = 0.0087$). Locations are normalized with respect to the dorsal (one) and ventral (zero) edges of spinal cord in all figures. (J) Plot of cell body position versus total number of filopodia extended in the 30 minute imaging period ($n = 34$; $p < 0.0001$). (K) Plot of position versus the summed length of all filopodial extensions over the entire imaging period ($n = 34$; $p < 0.0001$). (L) Plot of position of versus normalized filopodial dynamics ($n = 34$; $p = 0.0012$) (calculated by dividing the sum of all filopodial extensions for a cell with the dendritic arbor length of the cell).

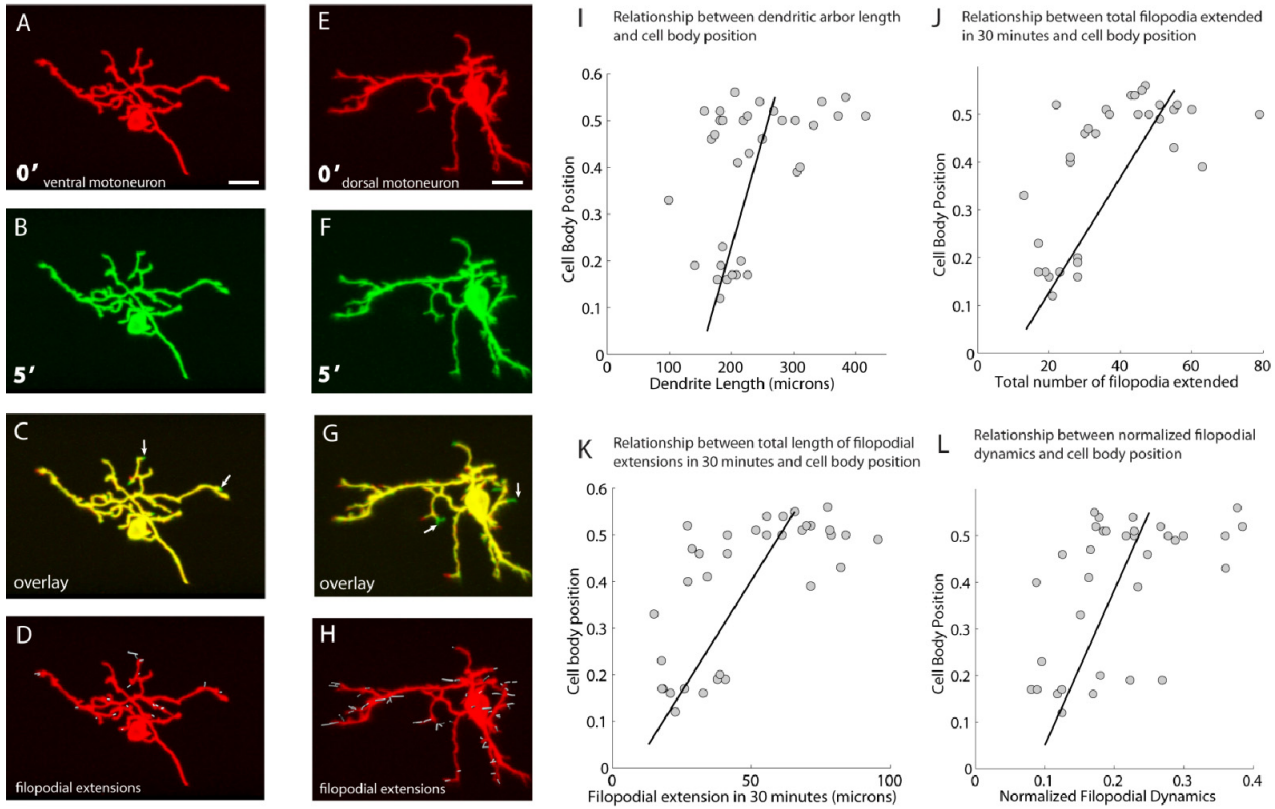
A
0′ ventral motoneuron
B
5′
C
overlay
D
filopodial extensions
E
0′ dorsal motoneuron
F
5′
G
overlay
H
filopodial extensions
I
Relationship between dendritic arbor length and cell body position
Cell Body Position
Dendrite Length (microns)
J
Relationship between total filopodia extended in 30 minutes and cell body position
Cell Body Position
Total number of filopodia extended
K
Relationship between total length of filopodial extensions in 30 minutes and cell body position
Cell body position
Filopodial extension in 30 minutes (microns)
L
Relationship between normalized filopodial dynamics and cell body position
Cell Body Position
Normalized Filopodial Dynamics

the number of filopodial extensions (Figure 3.2J) revealed a significant correlation ($n = 34$; $p < 0.0001$). Similarly, a plot of the position of motoneurons along the dorso-ventral axis of the cord against the summed length of all filopodial extensions (Figure 3.2K) revealed a significant correlation ($n = 34$; $p < 0.0001$). These data suggest that total filopodial length extended by ventral motoneurons was less than that of dorsal motoneurons. This could be a consequence of dorsally located motoneurons having longer dendrites that contain more filopodia . A plot of motoneuron position against the dendritic arbor length of the neurons did reveal that dorsally located motoneurons have longer dendrites than ventrally located motoneurons (Figure 3.2I; $n = 34$; $p = 0.0087$). However, even after the total filopodial extension was normalized for dendritic arbor length (Figure 3.2L) the total filopodial extension was still significantly greater for dorsal motoneurons than ventral motoneurons ($n = 34$; $p = 0.0012$) showing that increased filopodial extension in more dorsal motoneurons is not simply because they have more dendrite to give rise to filopodia. Collectively, these data lead to the perhaps counterintuitive conclusion that the dendritic arbors of the youngest neurons are the least dynamic ones.

Filopodial Dynamics of Kir2.1 expressing motoneurons

Based upon earlier work, the position of a neuron correlates with its input resistance and recruitment, with the more ventral cells having higher input resistances and being recruited more often during swimming than dorsal cells [3]. We explored whether the potential differences in excitability might contribute to the differences in dendritic dynamics by genetically suppressing the activity of individual motoneurons and examining the relationship between the dorsoventral position of the perturbed motoneurons and their dendritic dynamics.

The activity of individual neurons was suppressed by using the human inward rectifier K^+ channel Kir2.1. A previous study used calcium imaging to show that

Kir2.1 expressing cells in the spinal cord of larval zebrafish were significantly less active than controls that expressed a mutant non-conducting version of the channel [109], thus showing that expression of Kir2.1 channel is an effective way to suppress the excitability of individual neurons. To visualize the dynamics of Kir2.1 expressing neurons, we used the viral 2a technique to simultaneously express the Kir2.1 channel and mGFP [110, 111]. As a control, we also used a non conducting version of Kir2.1 (mutKir2.1) and expressed it with mGFP in motoneurons, and these cells were analyzed blind to the experimental condition.

Previous work has suggested that Kir2.1 expression results in shorter dendritic arbors [112]. We first analyzed the dendritic arbor length of motoneurons expression Kir2.1-viral2a-mGFP in 4 dpf fish. A plot of motoneuron dendritic length versus cell body position showed that older, more dorsal motoneurons have longer dendrites compared to younger, ventral motoneurons ($n = 16$; $p < 0.0001$; Figure 3.3I). This relationship is not significantly different from motoneurons expressing mGFP (Wilcoxon test; $p = 0.2$) or mutKir2.1-viral2a-mGFP (Wilcoxon text; $p = 0.62$). These data suggest that, at least at 4 dpf, Kir2.1 expression does not affect motoneuron dendritic length.

We next analyzed if the amount of filopodial extension is influenced by Kir2.1 expression. Visual examination of dendritic dynamics suggested that, unlike mGFP expressing motoneurons, the number of filopodia extended by ventral motoneurons expressing Kir2.1 (Figure 3.3A-D) was comparable to the number of filopodia extended by dorsal motoneurons expressing Kir2.1 (Figure 3.3E-H). Quantification of filopodial number as a function of dorsoventral position of Kir2.1 expressing motoneurons revealed that indeed the number of filopodia extended did not correlate with

Figure 3.3. Rapid time-lapse imaging of dendritic structure of Kir2.1-viral2a-mGFP expressing motoneurons. (A,B) Images of a ventral motoneuron at the first two consecutive time points (0 min and 5 min). (C) overlaid image of B and A. Arrows point to filopodial extensions; (D) Reconstruction (in white) of dendritic extensions over a 30 minute period. (E,F) Images of a dorsal motoneuron at the first two consecutive time points (0 min and 5 min). (G) overlaid image of F and E. Arrows point to filopodial extensions; (H) Reconstruction (in white) of filopodial extensions over a 30 minute period. (I) Plot of cell body position versus dendritic arbor length that remained constant over the entire imaging period for motoneurons expressing Kir2.1-viral2a-mGFP (red circles; $n = 16$; $p < 0.0001$)), mGFP (gray circles; $n = 34$) or mutantKir2.1-viral2a-mGFP (blue circles; $n = 7$). Locations are normalized with respect to the dorsal (one) and ventral (zero) edges of spinal cord in all figures. (J) Plot of cell body position versus total number of filopodia extended in the 30 minute imaging period. (K) Plot of position versus sum of all filopodial extensions over the entire imaging period. (L) Plot of position of versus normalized filopodial dynamics (calculated by dividing the sum of all filopodial extensions for a cell with the dendritic arbor length of the cell)

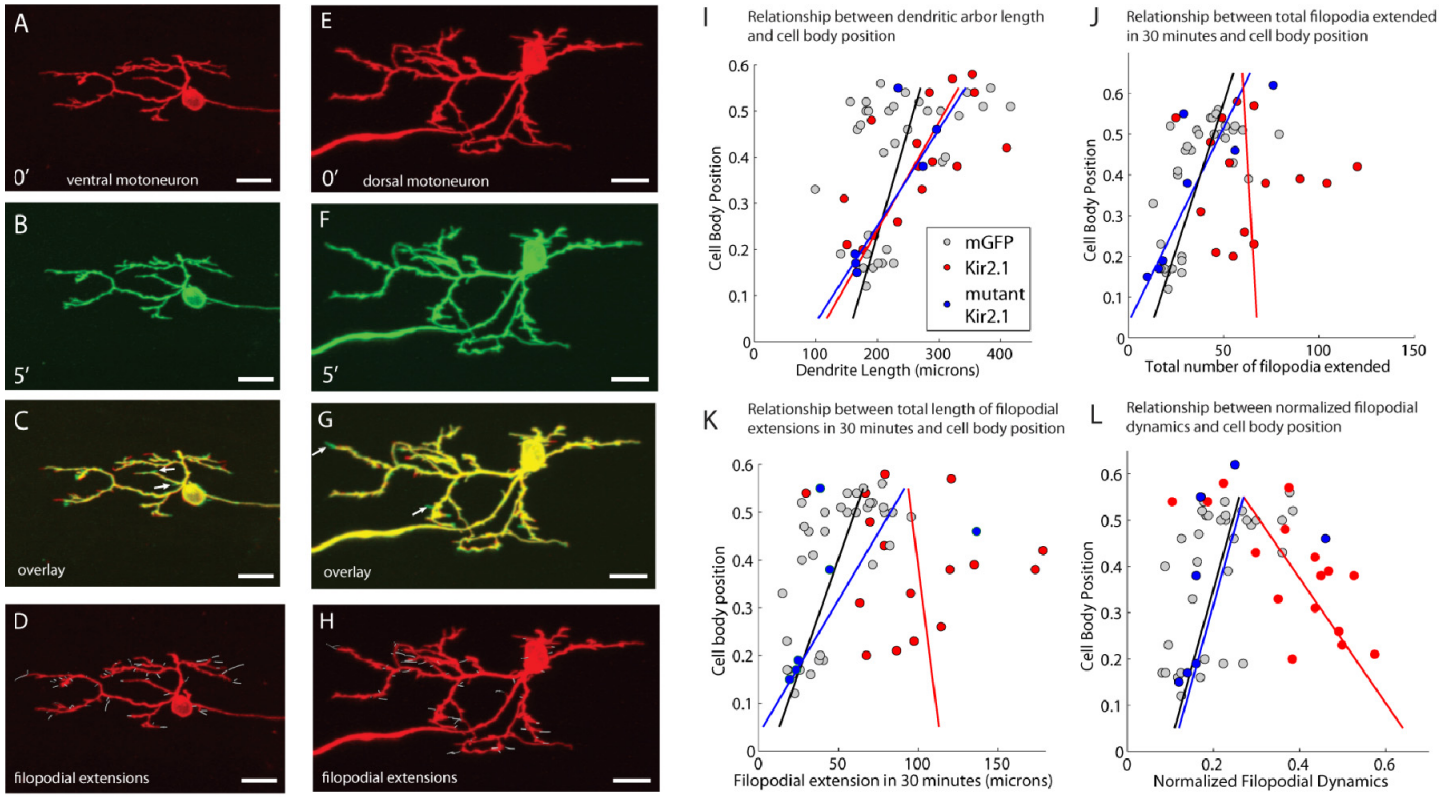
A
0′
ventral motoneuron
E
0′
dorsal motoneuron
B
5′
F
5′
C
overlay
G
overlay
D
filopodial extensions
H
filopodial extensions
I
Relationship between dendritic arbor length and cell body position
Cell Body Position
Dendrite Length (microns)
mGFP
Kir2.1
mutant Kir2.1
J
Relationship between total filopodia extended in 30 minutes and cell body position
Cell Body Position
Total number of filopodia extended
K
Relationship between total length of filopodial extensions in 30 minutes and cell body position
Cell body position
Filopodial extension in 30 minutes (microns)
L
Relationship between normalized filopodial dynamics and cell body position
Cell Body Position
Normalized Filopodial Dynamics

dorsoventral position of the motoneuron somata (Figure 3.3I; n = 16; p = 0.8171). This absence of relationship between filopodia number and cell body position for Kir2.1 expressing motoneurons is significantly different from mGFP (Wilcoxon test; $p < 0.0001$) or mutKir2.1 (Wilcoxon text; $p < 0.05$) expressing motoneurons. Similarly, analysis of the total filopodial length extended during the imaging period by Kir2.1 expressing motoneurons motoneurons revealed no significant relationship between the total length of filopodia extended and the dorsoventral location of the motoneuron in the perturbed motoneurons (Figure 3.3K; n = 16; p = 0.7187) which was significantly different from mGFP (Wilcoxon test; $p < 0.0001$) expressing motoneurons and just insignificant for mutKir2.1 expressing motoneurons (Wilcoxon test; p = 0.053). Normalizing the total filopodial extension for the length of the dendritic arbor revealed an inverse relationship between the extent of filopodial extension and the dorsoventral location of Kir2.1 expressing motoneurons (n = 16; p = 0.0017) which was significantly different from mGFP (Wilcoxon test; $p < 0.0001$) or mutKir2.1 (Wilcoxon test; $p < 0.05$) expressing motoneurons.

Our data reveal that for motoneurons expressing Kir2.1, the more younger, ventral neurons were the more dynamic ones – just the opposite of the normal relationship. Genetically suppressing the electrical activity of motoneurons thus inverted the relationship between normalized filopodial extension and dorsoventral location seen in normal mGFP expressing motoneurons. Taken together, our data suggest that the dorsoventral gradient of dendritic dynamics for normal mGFP expressing motoneurons can at least partially be attributed to differences in the excitability of motoneurons. Since the gradient of excitability may contribute to different patterns of recruitment during swimming, our data raises the possibility that it is the recruitment of motoneurons, and not simply the age that determines how dynamic and exploratory their dendritic arbors are.

Analysis of filopodial retractions and net dendritic growth

Previous work has showed that most filopodia extended by developing dendrites are transient and retracted on the time scale of minutes with filopodial extension roughly balanced by filopodial retraction in the short term. Initial visual examination of the dendritic structure of mGFP or Kir2.1-viral2a-mGFP expressing motoneurons suggested that there was no obvious change in the total dendritic arbor length over the 30 minute imaging period (Figure 3.4A-F; Figure 3.5A-F). Most of the extended filopodia appear to be retracted within the imaging period. However, detailed analysis of mGFP expressing neurons suggested that while filopodial extensions were balanced by retractions for ventral motoneurons, more dorsal motoneurons appeared to grow in the imaging period (Figure 3.4G-I). This is apparent from the significant correlation seen when net dendritic change is plotted as a function of dorsoventral position of motoneuron somata (Figure 3.4J; $n = 34$, $p = 0.011$). The correlation is even more significant when dendritic growth is normalized for the length of the dendritic arbor (Figure 3.4K; $n = 34$; $p = 0.009$). These data show that dendritic arbors of more dorsal motoneurons grew more than the dendritic arbors of ventral motoneurons raising the possibility that dendrites of less excitable, dorsal motoneurons grow more than dendrites of more excitable motoneurons at 4 dpf when fish just begin to swim.

This observation prompted us to analyze the relationship between dendritic growth and soma position for Kir2.1-viral2a-mGFP expressing motoneurons (Figure 3.5G-I). A plot of soma position versus net dendritic change (Figure 3.5J; $n = 16$, $p = 0.3$) and normalized dendritic change (Figure 3.5K; $n = 16$; $p = 0.45$) did not reveal a significant correlation. These data show that the relationship between dendritic growth and soma position seen for mGFP expressing motoneurons was not simply a consequence of the dorsoventral location of motoneuron somata and may instead be influenced by the excitability of the motoneuron and the amount of filopodia extended.

Figure 3.4. Analysis of filopodial extension, retraction and net dendritic change in mGFP expressing motoneurons. (A,B) Image of a mGFP expressing motoneuron at the first, A, and last, B, time points (0 min and 25 min). (C) overlaid image of B and A. (D-F) Reconstruction of all filopodial extensions (in red) and retractions (in green) over the entire imaging period for the cell shown in A-C. (G) Quantification of filopodial extensions between consecutive time points for all mGFP expressing motoneurons. Each row represents a single cell and the rows are stacked from bottom to top in increasing order of dorsoventral position of the cell. Each column represents the total length of filopodial extension between two consecutive time points. The color scales according to the colorbar on the right. (H) Quantification of filopodial retraction between successive time points for all mGFP expressing motoneurons according to the scheme in G. (I) Sum of total filopodial extension (black), total filopodial retraction (white), and net change (red) in dendritic arbor for each motoneuron represented in G and H. (J) Plot of cell body position versus net dendritic growth. (K) Plot of cell body position versus dendritic growth normalized for the length of the dendritic arbor that remained constant during the imaging period.

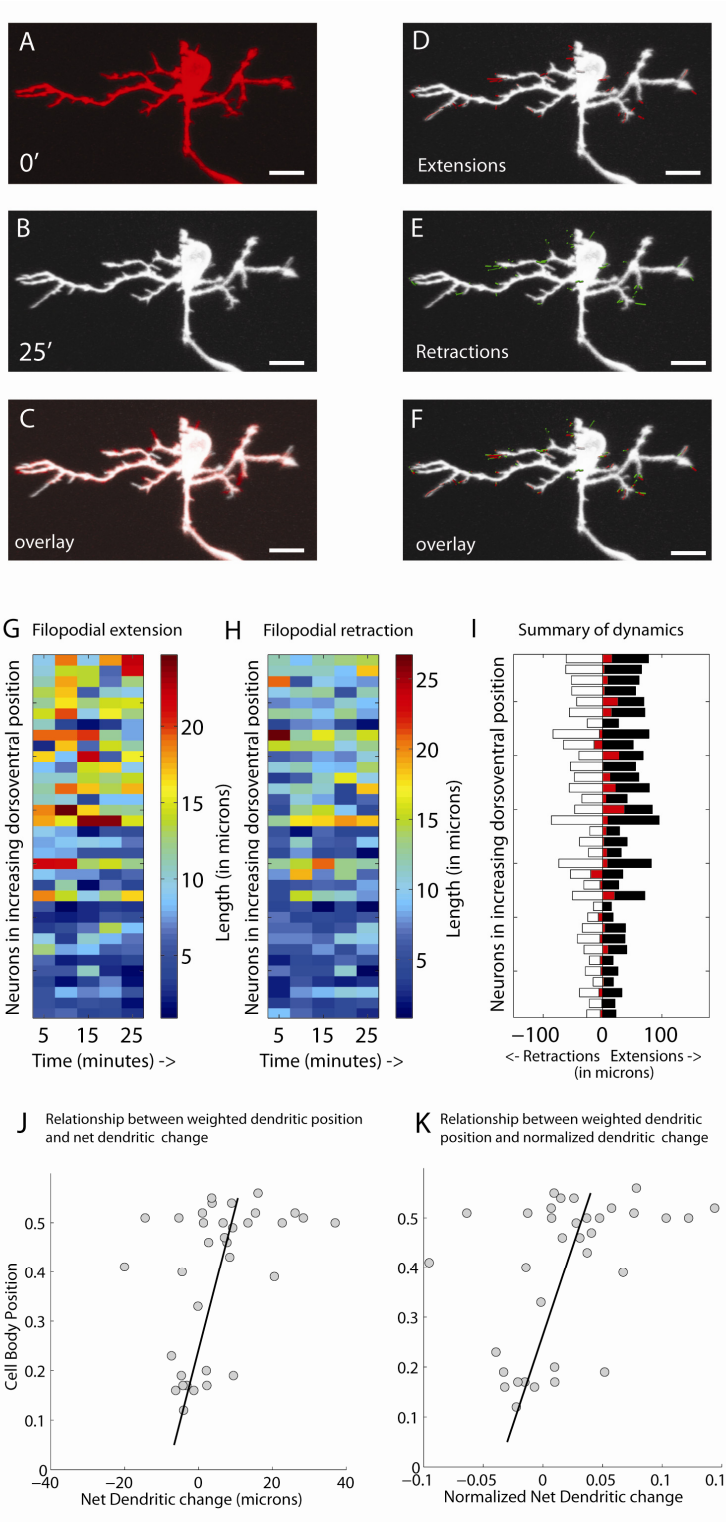
A
0′
B
25′
C
overlay
D
Extensions
E
Retractions
F
overlay
G Filopodial extension
H Filopodial retraction
I Summary of dynamics
Neurons in increasing dorsoventral position
Length (in microns)
5
10
15
20
25
Time (minutes) ->
<- Retractions Extensions ->
(in microns)
−100
0
100
J Relationship between weighted dendritic position and net dendritic change
K Relationship between weighted dendritic position and normalized dendritic change
Cell Body Position
Net Dendritic change (microns)
Normalized Net Dendritic change

Figure 3.5. Analysis of filopodial extension, retraction and net dendritic change in motoneurons expressing Kir2.1-viral2a-mGFP. (A,B) Image of a Kir2.1-viral2a-mGFP expressing motoneuron at the first, A, and last, B, time points (0 min and 25 min). (C) overlaid image of B and A. (D-F) Reconstruction of all filopodial extensions (in red) and retractions (in green) over the entire imaging period for the cell shown in A-C. (G) Quantification of filopodial extensions between consecutive time points for all Kir2.1-viral2a-mGFP expressing motoneurons. Each row represents a single cell and the rows are stacked from bottom to top in increasing order of dorsoventral position of the cell. Each column represents the total length of filopodial extension between two consecutive time points. The color scales according to the colorbar on the right. (H) Quantification of filopodial retraction between successive time points for all mGFP expressing motoneurons according to the scheme in G. (I) Sum of total filopodial extension (black), total filopodial retraction (white), and net change (red) in dendritic arbor for each motoneuron represented in G and H. (J) Plot of cell body position versus net dendritic growth for motoneurons expressing Kir2.1-viral2a-mGFP (red circles; n = 16), mGFP (gray circles; n =34). (K) Plot of cell body position versus dendritic growth normalized for the length of the dendritic arbor that remained constant during the imaging period.

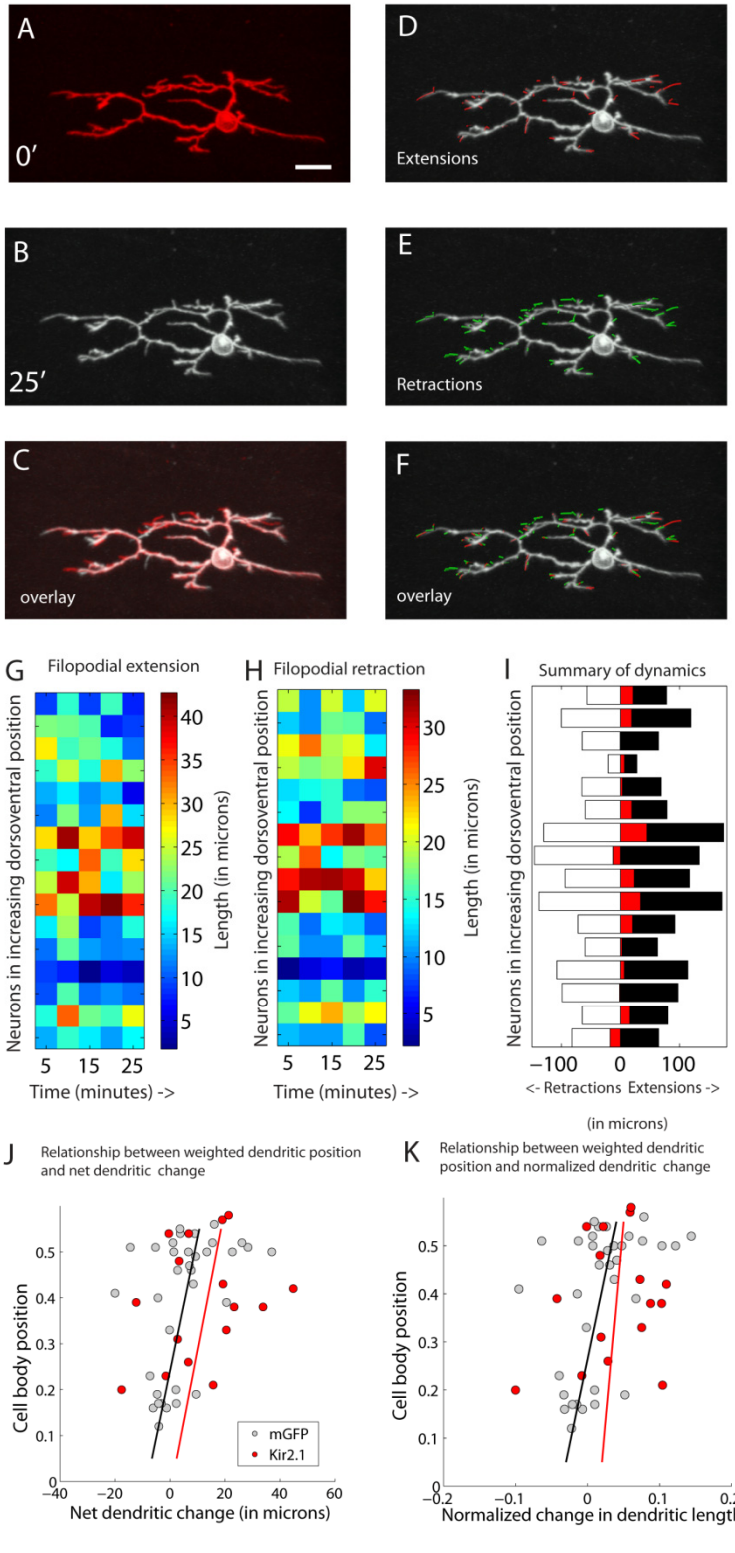
A
0′
B
25′
C
overlay
D
Extensions
E
Retractions
F
overlay
G
Filopodial extension
Neurons in increasing dorsoventral position
Length (in microns)
Time (minutes) ->
H
Filopodial retraction
Neurons in increasing dorsoventral position
Length (in microns)
Time (minutes) ->
I
Summary of dynamics
Neurons in increasing dorsoventral position
<- Retractions Extensions ->
(in microns)
J
Relationship between weighted dendritic position and net dendritic change
Cell body position
Net dendritic change (in microns)
mGFP
Kir2.1
K
Relationship between weighted dendritic position and normalized dendritic change
Cell body position
Normalized change in dendritic length

We next analyzed if net dendritic growth is correlated with the amount of filopodia extended. There is a significant correlation between total filopodial extension and net dendritic change for both mGFP (plot not shown; $n = 34$; $p < 0.0001$) and Kir2.1-t2a-mGFP (plot not shown; $n = 16$; $p < 0.05$) expressing motoneurons suggesting that filopodial extensions subserve a general program for dendritic growth.

Collectively, these data suggest that increased filopodial extension sub-serves a general program for dendritic growth and dendrites of less excitable, older motoneurons grow more than dendrites of ventral motoneurons. The systematic variation between excitability, dendritic dynamics and cell body position may be a mechanism for regulating dendritic growth according to functional recruitment pattern of motoneurons.

Analysis of dendritic and filopodial distribution

The previous sections focused on the relationship between dorsoventral location of motoneuron somata and the structural plasticity of their dendritic arbors and revealed that there is a gradient of filopodial extension and dendritic growth related to soma position and this gradient might be influenced by the gradient of input resistance of the motoneurons. Previous work has showed that disruption of activity patterns can lead to changes in the topographic organization of axons and dendrites [113, 114]. This prompted us to ask if perturbing the excitability of motoneurons shifts the dorsoventral distribution of their dendritic arbors and filopodial extensions.

Examples of dendritic arbors of mGFP expressing dorsal and ventral motoneurons are shown in Fig. 3.6A-C and Fig. 3.6D-F respectively. The reconstructed dendritic arbor of the dorsal motoneuron (Figure 3.6A) is shown in Figure 3.6B relative to the normalized dorsoventral extent of the spinal cord and the actual dorsoventral dendritic distribution is shown in Figure 3.6C. As is evident from

Figure 3.6. **Analysis of dorsoventral dendritic and filopodial distribution of mGFP expressing motoneurons.** (A) Image of a mGFP expressing dorsal motoneuron. (B) Representation of dorsoventral distribution of reconstructed dendritic arbor of motoneuron in A in a normalized dorsoventral representation of spinal cord where 0 represents the ventral edge of the spinal cord and 1 represents the dorsal edge of the spinal cord. (C) color-coded map of dorsoventral dendritic distribution according to color bar on the right. Briefly, the dorsoventral extent of the spinal cord was divided into hundred equal segments from ventral to dorsal and the dendritic length in each segment was calculated and represented according to the color bar on the right. For the example in A, the heat map shows that most of the dendritic arbor is located mid dorso-ventrally in the spinal cord. (D) Image of a mGFP expressing ventral motoneuron. (E,F) 3-D Representation and quantification of dorsoventral dendritic distribution of neuron in D as explained above. (G) Quantification of dendritic distribution in normalized dorsoventral extent of spinal cord of all mGFP expressing motoneurons. Each column is a quantification of a single motoneuron dendritic arbor as explained in C and columns are arranged from left to right in increasing order of dorsoventral cellbody position (white circle overlaid on the column). (H) Quantification of filopodial distribution in normalized dorsoventral extent of spinal cord of all mGFP expressing motoneurons. (I) Plot of cell body position versus weighted dorsoventral dendritic position for all cells shown in G. (J) Plot of cell body position versus weighted dorsoventral filopodial location.

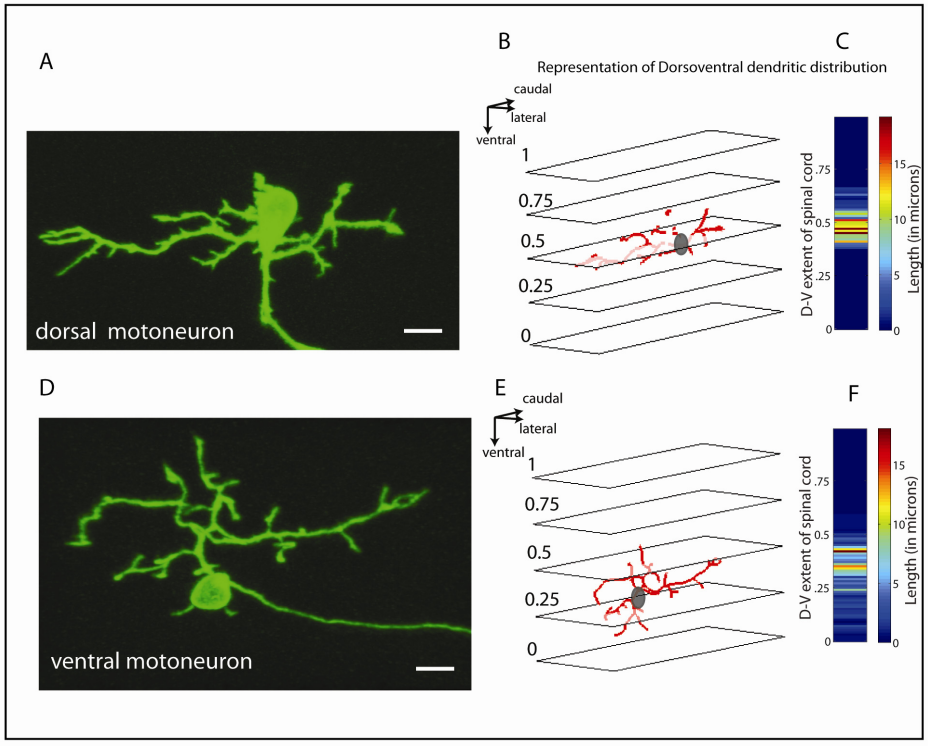
A
B
C
Representation of Dorsoventral dendritic distribution
caudal
lateral
ventral
1
0.75
0.5
0.25
0
dorsal motoneuron
D-V extent of spinal cord
Length (in microns)
D
E
F
ventral motoneuron

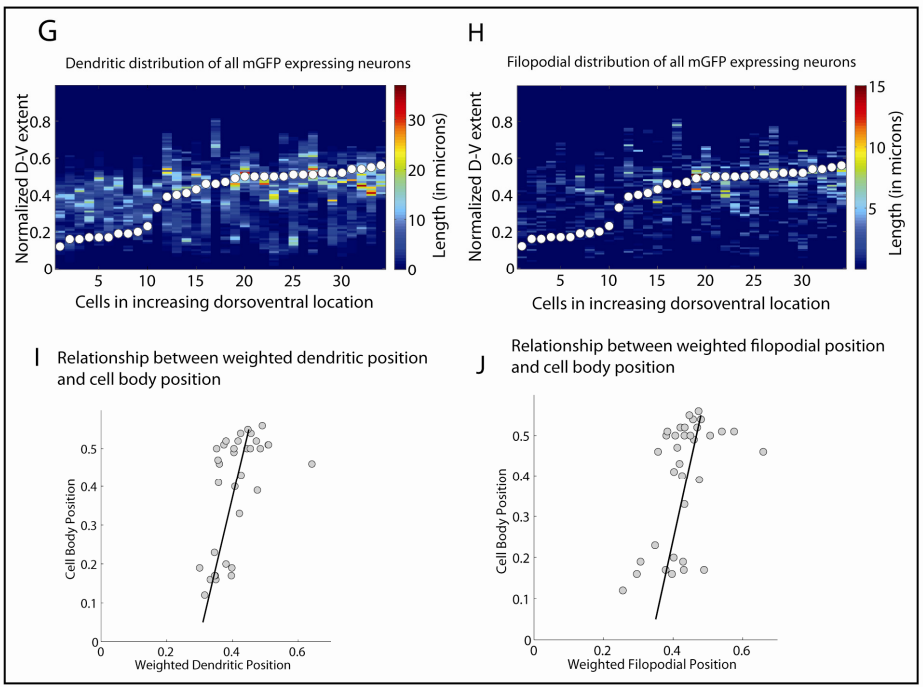
G
Dendritic distribution of all mGFP expressing neurons
Normalized D-V extent
Length (in microns)
Cells in increasing dorsoventral location
H
Filopodial distribution of all mGFP expressing neurons
I
Relationship between weighted dendritic position and cell body position
Cell Body Position
Weighted Dendritic Position
J
Relationship between weighted filopodial position and cell body position
Weighted Filopodial Position

Figure 3.6C, the bulk of the dendritic arbor of this motoneuron is located mid dorso-ventrally in the spinal cord. Comparing Figure 3.6F to3. 6C reveals that the dendritic arbor of the more ventral motoneuron is distributed ventrally relative to the dendritic arbor of the dorsal motoneuron.

We analyzed the dendritic distribution of all 34 motoneurons that were analyzed for dendritic dynamics. Figure 3.6G shows the dorsoventral distribution of dendritic arbors of all 34 mGFP expressing motoneurons. This plot suggests that while there is overlap between the dendritic arbors of motoneurons located at different dorsoventral locations, generally dendrites of dorsal motoneurons arborize more dorsally than those of ventral motoneurons. To determine if this was the case, we calculated the weighted dorsoventral location of the dendritic arbor of each neuron and plotted it versus the dorsoventral location of motoneuron somata (Figure 3.6I). This plot revealed a significant correlation between the weighted dorsoventral location of the dendritic and the dorso-ventral location of motoneuron somata ($n = 34$; $p = 0.0002$).

Analysis of total filopodia extended over the 30 minute period revealed a significant correlation between the weighted dorsoventral distribution of filopodial extensions and the dorsoventral location of somata (Figure 3.6H, Figure 3.6J; $n = 34$; $p = 0.002$). This is not entirely surprising since filopodial extensions are likely to reflect the distribution of the dendritic arbor. It is however interesting to note that the dorsoventral distribution of filopodial extensions of ventral motoneurons is over a greater dorsoventral region than that of the dendritic arbors itself (Figure 3.6I and 3.6J). The dorsoventral distribution of filopodial extensions in Figure 3.6H also suggests that there may be overlap between filopodial extensions from ventral motoneurons and dorsal motoneurons.

We then analyzed if Kir2.1 expression affected the dorsoventral distribution of dendrites and filopodia. Examples of the dendritic distribution of dorsal and ventral Kir2.1-viral2a-mGFP expressing motoneurons are shown in Figure 3.7A-F. Visual examination of dorsoventral dendritic distribution did not suggest any dramatic differences in dendritic distribution compared to mGFP expressing motoneurons. Figure 3.7G shows the dorsoventral distribution of dendritic arbors of all 16 Kir2.1-viral2a-mGFP expressing motoneurons and suggests that a general dorsoventral topography of dendritic distribution is preserved in Kir2.1-viral2a-mGFP expressing motoneurons at 4 dpf. Similarly, the dorsoventral distribution of filopodia mirrors the dorsoventral distribution of dendrites as shown in Figure 3.7H. A plot of the weighted dendritic position as a function of the soma position of Kir2.1 expressing motoneurons revealed a significant correlation (Figure 3.7I; $n = 16$; $p = 0.0002$) and this relationship was not significantly different from motoneurons expressing only mGFP. Similarly, the weighted filopodial distribution also showed a significant correlation with the dorsoventral position of the soma (Figure 3.7J; $n = 16$; $p = 0.002$) suggesting that even though the amount of filopodial extension is greater in ventral Kir2.1 expressing motoneurons, their dorsoventral distribution is not significantly different from mGFP expressing motoneurons. This raises the possibility that, at any given dorsoventral location, the amount of filopodia extended by a Kir2.1-viral2a-mGFP expressing motoneuron is greater than an mGFP motoneuron at a comparable dorsoventral position.

Taken together these data suggest that, at 4 days post fertilization, when larvae just begin swimming around spontaneously, Kir2.1-viral2a-mGFP expression does not significantly change the dorsoventral distribution of dendrites and filopodial extensions seen in mGFP expressing motoneurons. This suggests that the initial

Figure 3.7. **Analysis of dorsoventral dendritic and filopodial distribution of Kir2.1-viral2a-mGFP expressing motoneurons.** (A) Image of a Kir2.1-viral2a-mGFP expressing dorsal motoneuron. (B) Representation of dorsoventral distribution of reconstructed dendritic arbor of motoneuron in A in a normalized dorsoventral representation of spinal cord where 0 represents the ventral edge of the spinal cord and 1 represents the dorsal edge of the spinal cord. (C) color-coded map of dorsoventral dendritic distribution according to color bar on the right. Briefly, the dorsoventral extent of the spinal cord was divided into hundred equal segments from ventral to dorsal and the dendritic length in each segment was calculated and represented according to the color bar on the right. For the example in A, the heat map shows that most of the dendritic arbor is located mid dorso-ventrally in the spinal cord. (D) Image of a mGFP expressing ventral motoneuron. (E,F) 3-D Representation and quantification of dorsoventral dendritic distribution of neuron in D as explained above. (G) Quantification of dendritic distribution in normalized dorsoventral extent of spinal cord of all mGFP expressing motoneurons. Each column is a quantification of a single motoneuron dendritic arbor as explained in C and columns are arranged from left to right in increasing order of dorsoventral cellbody position (white circle overlaid on the column). (H) Quantification of filopodial distribution in normalized dorsoventral extent of spinal cord of all mGFP expressing motoneurons. (I) Plot of cell body position versus weighted dorsoventral dendritic position for motoneurons expressing Kir2.1-viral2a-mGFP (red circles; n = 16) or mGFP (gray circles; n = 34). (J) Plot of cell body position versus weighted dorsoventral filopodial location.

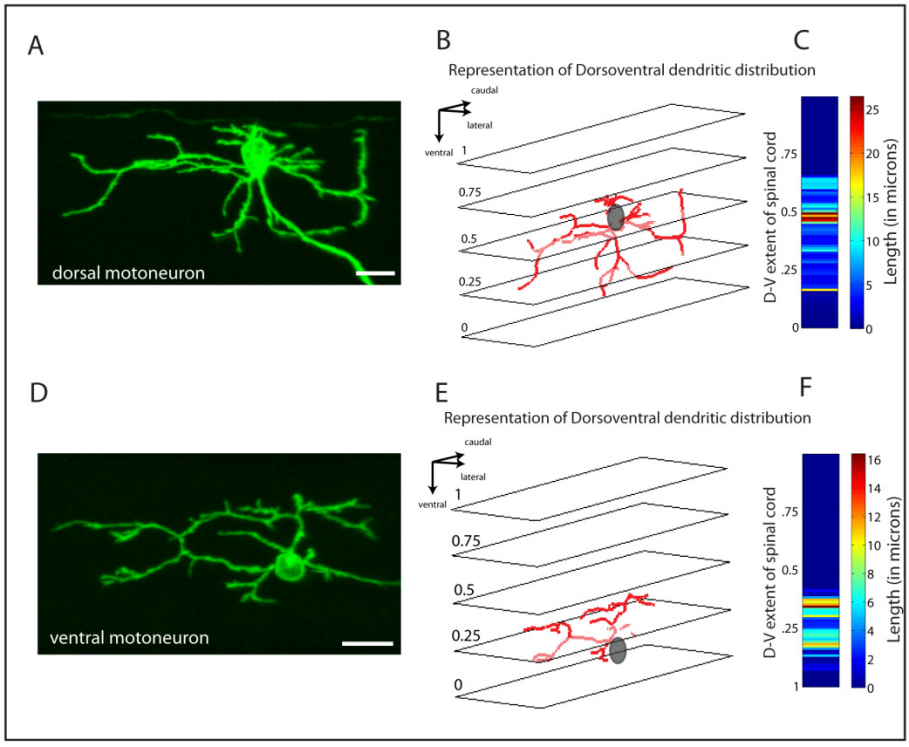
A
B
C
Representation of Dorsoventral dendritic distribution
dorsal motoneuron
caudal
lateral
ventral
1
0.75
0.5
0.25
0
D-V extent of spinal cord
.75
0.5
.25
Length (in microns)
25
20
15
10
5
D
E
F
Representation of Dorsoventral dendritic distribution
ventral motoneuron
16
14
12
10
8
6
4
2
1

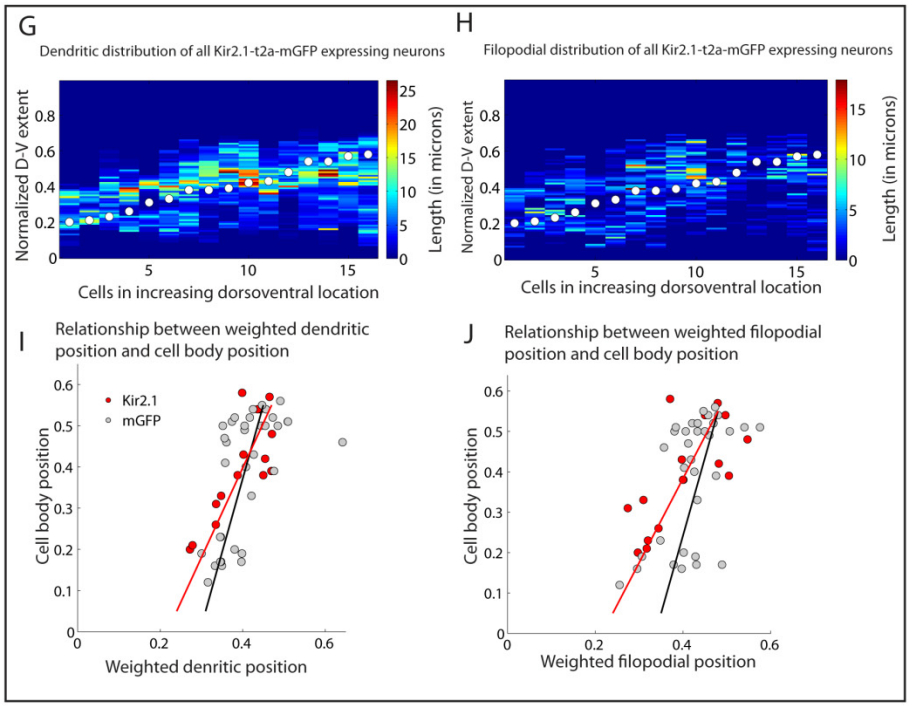
G
Dendritic distribution of all Kir2.1-t2a-mGFP expressing neurons
H
Filopodial distribution of all Kir2.1-t2a-mGFP expressing neurons
Normalized D-V extent
0.8
0.6
0.4
0.2
0
Length (in microns)
25
20
15
10
5
0
5
10
15
Cells in increasing dorsoventral location
I
Relationship between weighted dendritic position and cell body position
J
Relationship between weighted filopodial position and cell body position
Kir2.1
mGFP
Cell body position
0.6
0.5
0.4
0.3
0.2
0.1
0
0.2
0.4
0.6
Weighted denritic position
Weighted filopodial position

dorsoventral topography of motoneuron dendrites and filopodial extensions which emerges when fish are largely sedentary (see Chapter 2) is not affected by the excitability of motoneurons. However, it is possible that prolonged disruption of activity patterns after fish begin to swim spontaneously will lead to disrupt the dorsoventral distribution of motoneuron dendrites and may lead to inappropriate recruitment of motoneurons during motor behavior.

Discussion

Dendrites of developing neurons extend and retract branches on the time scale of minutes [42, 105]. This highly dynamic dendritic structure is an exploratory mechanism for establishing new synapses and concomitantly increasing dendritic length in developing neural circuits [50]. Dendritic arbors become less dynamic as circuits mature [21, 45, 107, 115]. The exact factors that control the extent of dendritic dynamics are poorly understood. The amount of dendritic dynamics varies in different cell types in different circuits and is thought to be modulated by activity and molecular cues [42, 49, 108]. Neural circuits are made up of different cell types with different physiological properties, raising the possibility that variations in intrinsic physiological properties, and the consequent variation in activity patterns of neurons, can also modulate the extent of dendritic dynamics during development. These variations could be very important in setting up patterns of connectivity in functionally heterogeneous populations of neurons during development. We took advantage of a naturally occurring topographic organization of motoneurons by age, input resistance, and functional roles in different swimming speeds to ask if variations in excitability and different patterns of recruitment influence the dendritic dynamics of motoneurons in the spinal cord of larval zebrafish *in vivo* at an age when they begin to swim freely.

We found a novel relationship between the amount of dendritic dynamics and the topographic organization of motoneuron recruitment – dendrites of ventral motoneurons recruited during slow swimming are less dynamic than dendrites of more dorsal motoneurons recruited at faster speeds. This pattern of dendritic dynamics correlates with the amount of dendritic growth measured over the imaging period such that dendritic arbors of more dynamic dorsal motoneurons grew more than the dendritic arbors of less dynamic ventral motoneuron arbors. Since the pattern of motoneuron recruitment correlates with the excitability of motoneurons, we tested if the variation in motoneuron excitability contributes to the variation in dendritic dynamics and dendritic growth. Genetically suppressing the excitability of motoneurons dramatically altered the pattern of dendritic dynamics - dendrites of more ventrally located motoneurons become much more dynamic when their excitability is decreased . Changing the excitability also resulted in disrupting the patterns of dendritic growth such that there was no longer a dorsoventral gradient of dendritic growth. These data suggest that, at least in vertebrate spinal motor networks, the dendritic dynamics of motoneurons are influenced by the intrinsic excitability and the recruitment pattern of motoneurons. This might be a mechanism to tie in developmental phenomena that establish connectivity with the functional role of neurons.

The pattern of dendritic dynamics we see is contrary to what would be expected from the birth order of motoneurons. Previous work has suggested that younger neurons are more dynamic than older neurons in the optic tectum of Xenopus [45] . Though we do not know the time of differentiation of motoneurons in our experiments, previous work showed that the most dorsal motoneurons are the earliest born and younger neurons are located more ventrally [92]. This indicates that dendritic arbors of ventral, younger motoneurons are less dynamic than older, dorsal

motoneurons at the time when larval zebrafish begin swimming spontaneously raising the possibility that the functional pattern of neuronal recruitment is a more important determinant of the extent of dendritic dynamics than simply the age of the neuron.

This unexpected pattern of dendritic dynamics may be explained by the fact that neurons behave homeostatically and adjust the amount of excitatory input they receive to maintain their firing rate within a dynamic range [116-118]. Based on recent work, we know that the youngest, most excitable ventral motoneurons are recruited at the slowest swimming speeds and progressively older, less excitable dorsal motoneurons are recruited only at faster swimming speeds [3]. The implication of this pattern of recruitment is that the range of swimming speeds over which motoneurons are active narrows with increasing dorsoventral position and the most dorsal motoneurons are least active while the most ventral motoneurons are activated much more often. Since more ventral motoneurons are activated much more often as fish spend most of their time swimming around slowly, it is likely that younger, ventral motoneurons fire closer to their firing range. Hence they do not "need" more excitatory input and consequently are less dynamic. Genetically reducing the excitability of ventral motoneurons resulted in a dramatic increase in dendritic dynamics. This could arguably be because the genetically perturbed ventral motoneurons are recruited much less often than their wild-type counterparts and fire less than their dynamic firing range. This, in turn, leads to an increase in dendritic dynamics to search for more excitatory input. Mechanistically, the history of activation could be linked to the amount of dendritic dynamics via signaling pathways that link global calcium increases (when the neuron fires) to transcriptional pathways that regulate dendritic outgrowth [119-123].

We find that the amount of filopodial dynamics correlates with the amount of dendritic growth during our 30 minute imaging window such that dendritic arbors of

more dorsal motoneurons grow more than the dendritic arbors of ventral motoneurons. In Chapter 2, longer term imaging of motoneuron dendritic arbors over a 2 day period, after fish begin swimming, showed that the dendritic arbors of dorsal motoneurons grow more than those of ventral motoneurons even when normalized for their original length. The size of a dendritic arbor is one mechanism to control the amount of synaptic input a neuron receives. Recent work showed that dendrites act as homeostatic devices to compensate for natural variability in the location of presynaptic input [67] or the strength of excitatory input by increasing or decreasing their dendritic size [124] . Our work suggests that naturally occurring systematic variability in intrinsic excitability may be one way to control the amount of excitatory input motoneurons receive to account for variations in recruitment patterns during locomotion. It should be noted that dendritic growth is a consequence of net stabilization of filopodia. From a Hebbian "wire together fire together" perspective of dendritic growth, one might expect that dendrites of more excitable ventral motoneurons would be stabilized more easily than those of dorsal motoneurons. It is not clear why dendritic arbors of motoneurons that are less excitable grow more. It is possible that reduced excitability of motoneurons triggers the expression of synaptic adhesion molecules that may play a role in synapse stabilization and dendritic growth.

In addition to influencing dendritic growth, another consequence of this variation in dendritic growth could be to maintain appropriate dendritic topography related to the appropriate functional recruitment of motoneurons. In Chapter 2, we showed that a dorsoventral dendritic topography of motoneuron dendrites is present at a time when fish first begin to swim (at 4 dpf) and this topography is maintained even as dendrites continue to grow after fish begin swimming. This dorsoventral dendritic topography suggests that an age-related organization contributes to the appropriate recruitment of motoneurons during swimming - older interneurons that participate in

fast movements connect to motoneurons that drive fast movement and younger interneurons that participate in slower movements connect to younger motoneurons that drive slow movement. Based on recent work we also know that excitatory interneurons that drive slow movement are turned off at faster swimming speeds [4]. If Hebbian mechanisms determine synapse stabilization, ventral motoneurons that are more excitable are more likely to "win" in competition for input from faster interneurons. This could lead to inappropriate connectivity and hence inappropriate recruitment of motoneurons such that motoneurons that drive slow swimming are recruited instead of motoneurons required for faster movements when the fish needs to swim faster. How is appropriate topography maintained even as dendrites grow? The difference in dendritic dynamics for neurons recruited at different locomotor speeds may reduce their competition between younger motoneurons and older motoneurons. Since the dendritic arbors of ventral motoneurons are less dynamic, it effectively reduces the amount of competition from more ventral motoneurons, and dorsal motoneurons are more likely to establish connections with premotor excitatory interneurons that drive fast swimming. Hence, a simple consequence of this difference in dendritic dynamics could be to maintain appropriate dendritic topography underlying motoneuron recruitment as dendrites grow during development. This hypothesis can be tested experimentally by looking at the connectivity pattern of ventral motoneurons whose excitability has been suppressed genetically. We would predict that these ventral motoneurons would make more connections with premotor interneurons that drive faster swimming than ventral motoneurons that do not express Kir2.1. Techniques such as channelrhodosin and genetic tracing that help assess connectivity within circuits will allow us to test this prediction.

The relationship between age, excitability, functional recruitment, dendritic dynamics and dendritic growth has general implications for controlling wiring in

motor circuits in vertebrates where general mechanisms that determine wiring are largely unknown. Recent work shows that the relationship between age, excitability and functional recruitment is true not just for motoneurons but for other cell types of motor circuits in the spinal cord [4, 90] and hindbrain (Kinkhabwala, Riley et al. in preparation, Koyama et al. in preparation) of larval zebrafish. Older, less excitable neurons are recruited during fast movements while younger more excitable neurons are recruited during slower movements. If the relationship we see between excitability, dendritic dynamics and dendritic growth in motoneurons is true of other neurons in motor circuits, excitability could contribute to establishing appropriate connectivity between neurons according to their functional role and time of differentiation in many cell types throughout the hindbrain and spinal cord of vertebrates.

Materials And Methods

Fish care

All experiments were performed on 4 day old zebrafish (*Danio rerio*) obtained from a laboratory stock of wild type adults. Embryos were raised at 28.5^{o}C in the same system as adults (Aquatic Ecosystems, Inc.,Apopka,FL) until they became freely swimming (4 days) and then experiments were performed at physiologically relevant temperature (28.5^{o}C). At these ages, larval fish are still nourished by the remnants of their yolk sac. All procedures conform to the National Institutes of Health guidelines regarding animal experimentation and were approved by Cornell University's Institutional Animal Care and Use committee.

Transient Expression of Fluorescent Reporter in Individual Motoneurons

DNA injected at low concentrations (20-30 ng/ul) into fertilized eggs at the single cell stage resulted in stochastic expression of fluorescent protein in isolated motoneurons. Embryos were screened for expression of fluorescence at 72-80 hours post fertilization

(hpf) and embryos where individually labeled motoneurons could be seen unambiguously were selected for imaging. All injections were done as previously described. In order to increase reporter expression levels, the Gal4-VP16/14XUAS system was utilized [103]. A Bacterial Artificial Chromosome containing regulatory elements for Vesicular Acetylcholine Transporter (VAchT) was modified by homologous recombination to create a VAchT:Gal4 driver to drive expression specifically in motoneurons. To drive the expression of membrane targeted GFP, a 14X*UAS*:mGFP reporter construct was coinjected with VAchT:Gal4. The 14X*UAS*:mGFP construct was derived from 14XUAS [103]and *brn3c:mGFP* [104]. To drive the expression of Kir2.1 and membrane targeted GFP in the same neuron, we used the viral2a approach to co-express the two proteins. A 14X*UAS*Kir2.1-viral2a-mGFP construct was created using the Tol2 cloning approach [125]. A non-conducting version of Kir2.1, mut.Kir2.1, was constructed similarly to make the 14X*UAS*mutKir2.1-viral2a-mGFP construct. Details of the cloning are available on request.

In vivo Confocal Microscopy

Larvae were anesthetized in a 0.02% solution of MS-222 and then paralyzed by immersion in 1mg/ml alpha bungarotoxin (Sigma Co.) in 10% Hank's solution. Once larvae were immobilized (2-3 minutes), they were embedded in low melting-point agarose, covered in 10% Hank's solution. Fish were oriented such that motoneurons were imaged from the lateral view. Hank's solution was maintained at 28.5^{o}C for the duration of imaging. Labeled cells were imaged using a inverted confocal microscope (Zeiss LSM 510, Carl Zeiss) with a Zeiss C-Apochromat 40X water lens. Green fluorescence was excited using 488 nm laser light and emission was typically collected with band pass emission filters (505-530 nm or 505-550 nm). For dendritic dynamics experiments, the entire dendritic arbor was imaged every 5 min for 30 min

total. A subsequent image was collected where the dendritic structure was imaged simultaneously with a DIC image of the spinal cord. This was done to determine the dorsoventral location of the neuron in the spinal cord.

Image processing and quantification of changes in dendritic structure

3D image rendering and analyses of dendrite dynamics were performed using Imaris (Bitplane, Inc.). Any drift during imaging was corrected by using the SPM Matlab toolbox and custom Matlab scripts that aligned the 3 dimensional z-stacks at each time point using the z-stack at the first time point as the reference. Some z-stacks were manually adjusted using the "Channel Shift" function in Imaris to ensure that the images were perfectly aligned. All aligned z-stacks were then smoothed by median filtering to aid in dendritic reconstruction. The images were checked manually to ensure that no obvious artifacts were introduced due to smoothing.

For reconstructing filopodial extensions and retractions, 3D renderings of z-stacks from two consecutive time points were overlaid and pseudocolored red and green and non-overlapping parts of the dendritic structure were drawn in 3D in Imaris (Filament function) and classified as extensions or retractions between those two points. This was then done for all time points and the total extension and retraction were thus quantified between all consecutive time points. The reconstructed dendritic arbor was the dendritic arbor that was conserved over the entire imaging period. Briefly, the dendritic arbor was reconstructed in 3D in Imaris (Filament function) using the first the z-stack from the first timepoint as the reference. This reconstruction was then overlaid on a 3D rendering of the z-stack from the last time point and edited so that it represented the dendritic arbor that was conserved between the first and the last time point.

Quantification of dorsoventral dendritic and filopodial distribution

Custom Matlab scripts were written to analyze the dorsoventral distribution of dendrites and filopodia. The reconstructed dendritic arbor and filopodial extensions were superimposed on the DIC z stack of the spinal cord. The DIC image of the spinal cord was used to identify the ventral and dorsal edges of the spinal cord. The dorsoventral extent of the spinal cord was normalized so that the ventral edge was 0 and the dorsal edge was 1. The dorsoventral volume was then divided into a 100 equal dorsoventral sections and the length of the reconstructed dendritic arbor in each dorsoventral volume was calculated.

To calculate the weighted dorsoventral position of dendrites and filopodia, the fraction of dendritic arbor or filopodia relative to the total dendritic length or total filopodial extension respectively, was calculated for each dorsoventral volume. The fractional length was multiplied by the average of the normalized dorsoventral limits of the volume and this value for all dorsoventral locations was summed to give the weighted dorsoventral location of the dendritic arbor or filopodial extensions. Motoneuron location was determined by averaging three measurements from the bottom of spinal cord to the middle of the cell body using Zeiss software. This value was then normalized to an average of three measurements of the total dorso-ventral extent of spinal cord.

CHAPTER 4

SUMMARY AND CONCLUSIONS

Axons and dendrites in many sensory circuits are topographically organized [12, 93]. In contrast, we do not know whether systematic patterns of axonal and dendritic organization exist in vertebrate spinal motor networks. Recent work showed that motoneuron somata are topographically organized in the spinal cord of larval zebrafish in relation to the swimming speed at which they are recruited.[3]. The most ventrally located motoneurons are recruited at the slowest swimming speeds, while progressively more dorsal motoneurons are recruited as fish swim faster. I took advantage of this neuronal organization to look for patterns of dendritic organization and development in relation to the location, and thus, recruitment pattern of motoneurons. The transparency of zebrafish throughout the maturation of locomotor behavior in combination with genetic techniques makes it a favorable model system to discover patterns of dendritic organization and development in relation to the patterns of recruitment of neurons during locomotor behavior.

I first looked at the dendritic organization of motoneurons in freely swimming fish and tracked when this organization emerges in relation to the maturation of locomotor behavior (Chapter 2). I used transient expression of fluorescent proteins to visualize the dendritic structure of motoneurons in zebrafish larvae at a stage when they have been swimming spontaneously for a few days. My work revealed a dorsoventral and mediolateral organization of motoneuron dendrites related to the functional recruitment of motoneurons at different locomotor speeds - dendrites of older motoneurons recruited at faster speeds arborize more dorsally and medially in the neuropil relative to dendrites of younger motoneurons recruited at slower speeds. By tracking the development of individual mGFP expressing motoneurons at different developmental stages, I found that the topography is present at the time when fish first

begin to swim spontaneously and it emerges over a time period when fish are largely sedentary. Furthermore additional dendritic growth after the onset of spontaneous swimming does not disrupt the initial topography. In summary, there is a dendritic topography related to the recruitment of motoneurons at different locomotor speeds that emerges by the time fish begin to swim, and is maintained even as dendrites grow after the onset of spontaneous swimming.

I then went on to study the structural dynamics of dendritic arbors of individual motoneurons in larval zebrafish soon after they begin swimming (Chapter 3). Dendritic arbors of developing neurons constantly extend and retract filopodia and this exploratory behavior sub-serves synapse formation and dendritic growth in developing circuits. I found a systematic relationship between the location of a spinal motoneuron and the dynamics of its dendritic arbor – youngest, ventral motoneurons are least dynamic whereas increasingly older and more dorsal motoneurons are more dynamic. This is contrary to the idea that dendrites of younger neurons are more dynamic than dendrites of older neurons because younger ones are growing more. I then asked if this pattern of dendritic dynamics is related to the systematic variation of excitability of motoneurons described recently. I tested this possibility genetically by expressing Kir2.1 to suppress excitability of individual motoneurons. This led to a dramatic increase in the dynamics of ventral motoneurons, which became more dynamic than more dorsal ones. Our results suggest that a naturally occurring dorsoventral gradient of excitability (and probably the associated activity levels in the neurons) may contribute to the variation in dendritic dynamics.

Taken together, my work reveals systematic patterns of motoneuron dendritic organization and development in relation to the development of locomotor behavior and the patterns of recruitment of motoneurons described recently. These findings have implications for the organization of connectivity and how it might be established

during development in vertebrate spinal motor networks. Even though motoneuron dendritic organization and development have been studied in some detail in other species, no obvious patterns in relation to their functional recruitment have been reported previously. Technical limitations and the lack of a functional framework might have preempted the discovery of these patterns in other vertebrates.

Our data allow us now to make some predictions about general patterns of dendritic organization and development in vertebrate spinal motor network that have implications, as discussed below, for how connectivity is organized in vertebrate spinal motor networks and how it is established during development. Since topography is an anatomical correlate of specificity in connectivity, our results point to the possibility of an age and speed-related organization of circuitry within vertebrate neural circuits that underlie the ability to move over a range of speeds. Previous work in mammalian circuits has looked at differences in the dendritic organization of motoneuron pools in relation to the muscles they innervate [68-70, 72, 73], but not in relation to the strength or speed of movements. We predict that an age and function related separation of dendritic territories might exist within motoneurons of individual motor pools in mammals allowing motoneurons to be recruited at different strengths of movement.

Our data also show that a basic motoneuron dendritic topography emerges over a time period when fish are largely sedentary and an increase in motoneuron dendrite length after fish start swimming does not substantially alter this topography. Recent analysis of the development of motor behavior in zebrafish showed that fast motor behavior emerges before slow motor behavior and this sequence of development is mirrored in the development of neuronal circuitry that drives this behavior. This pattern of maturation of locomotor behavior bears strong similarities to the development of locomotor behavior in other vertebrates including humans. Based on

these similarities in the development of locomotor behavior, we predict an age related dendritic topography of motoneurons related to function would be present by the time when animals first begin to move and this topography would not be dramatically altered subsequently in spite of the substantial postnatal motoneuron dendritic growth that is known to occur in vertebrates.

Our observation that dendritic topography is present at the onset of function is similar to the development of topography in sensory circuits such as ocular dominance columns where topography is present at the onset of function, but its maintenance requires neuronal activity. Similarly, it is possible that dendritic growth and the concomitant addition of synapses are guided by patterns of motor activity to maintain the topography that is present when fish first start swimming. In fact, we observe that the amount of motoneuron dendritic dynamics varies systematically with the recruitment pattern of motoneurons when fish first begin to swim spontaneous. Perturbing the excitability of motoneurons, and presumably their recruitment pattern, dramatically changes the amount of dendritic dynamics. Thus, activity based variation in dendritic dynamics might contribute to maintaining the dendritic topography that is present at the onset of locomotion even as additional dendritic growth occurs.

The patterns of dendritic organization and development we describe are linked to the age, excitability and recruitment of motoneurons. It is known that the patterns of recruitment of premotor interneurons that are involved in rhythmic motor behavior in the spinal cord and perhaps even in the hindbrain of larval zebrafish are also correlated with their age and excitability - older, less excitable neurons generally participate in faster movements and younger, more excitable behaviors participate in slower movements. Thus, it is possible that the age and function-related patterns of dendritic organization and growth suggested by our data for motoneurons might be applicable to

interneurons as well, and thus provide a general principle of organization for the circuitry underlying vertebrate locomotion.

REFERENCES

1. Sanes, J.R. and M. Yamagata, *Formation of lamina-specific synaptic connections.* Current opinion in neurobiology, 1999. **9**(1): p. 79-87.
2. Sanes, J.R. and M. Yamagata, *Many paths to synaptic specificity.* Annual Review of Cell and Developmental Biology, 2009. **25**: p. 161-195.
3. McLean, D.L., et al., *A topographic map of recruitment in spinal cord.* Nature, 2007. **446**(7131): p. 71-75.
4. McLean, D.L. and J.R. Fetcho, *Spinal interneurons differentiate sequentially from those driving the fastest swimming movements in larval zebrafish to those driving the slowest ones.* The Journal of neuroscience : the official journal of the Society for Neuroscience, 2009. **29**(43): p. 13566-13577.
5. Sperry, R.W., *Nature of functional recovery following regeneration of the oculomotor nerve in amphibians.* Anat Rec, 1947. **97**(3): p. 293-316.
6. Hubel, D.H. and T.N. Wiesel, *Receptive fields of single neurones in the cat's striate cortex.* J Physiol, 1959. **148**: p. 574-91.
7. Wiesel, T.N. and D.H. Hubel, *Effects of Visual Deprivation on Morphology and Physiology of Cells in the Cats Lateral Geniculate Body.* J Neurophysiol, 1963. **26**: p. 978-93.
8. Hubel, D.H. and T.N. Wiesel, *Anatomical demonstration of columns in the monkey striate cortex.* Nature, 1969. **221**(5182): p. 747-50.
9. Hubel, D.H., T.N. Wiesel, and S. LeVay, *Plasticity of ocular dominance columns in monkey striate cortex.* Philos Trans R Soc Lond B Biol Sci, 1977. **278**(961): p. 377-409.

10. LeVay, S., T.N. Wiesel, and D.H. Hubel, *The development of ocular dominance columns in normal and visually deprived monkeys.* J Comp Neurol, 1980. **191**(1): p. 1-51.
11. Luo, L. and D.D. O'Leary, *Axon retraction and degeneration in development and disease.* Annu Rev Neurosci, 2005. **28**: p. 127-56.
12. Crowley, J.C. and L.C. Katz, *Ocular dominance development revisited.* Current opinion in neurobiology, 2002. **12**(1): p. 104-109.
13. Ruthazer, E.S., *You're perfect, now change--redefining the role of developmental plasticity.* Neuron, 2005. **45**(6): p. 825-828.
14. Nelson, R., E.V. Famiglietti, Jr., and H. Kolb, *Intracellular staining reveals different levels of stratification for on- and off-center ganglion cells in cat retina.* J Neurophysiol, 1978. **41**(2): p. 472-83.
15. Greenough, W.T. and F.L. Chang, *Dendritic pattern formation involves both oriented regression and oriented growth in the barrels of mouse somatosensory cortex.* Brain Res, 1988. **471**(1): p. 148-52.
16. Katz, L.C., C.D. Gilbert, and T.N. Wiesel, *Local circuits and ocular dominance columns in monkey striate cortex.* J Neurosci, 1989. **9**(4): p. 1389-99.
17. Malun, D. and P.C. Brunjes, *Development of olfactory glomeruli: temporal and spatial interactions between olfactory receptor axons and mitral cells in opossums and rats.* The Journal of comparative neurology, 1996. **368**(1): p. 1-16.
18. Bodnarenko, S.R. and L.M. Chalupa, *Stratification of ON and OFF ganglion cell dendrites depends on glutamate-mediated afferent activity in the developing retina.* Nature, 1993. **364**(6433): p. 144-146.

19. Bodnarenko, S.R., G. Jeyarasasingam, and L.M. Chalupa, *Development and regulation of dendritic stratification in retinal ganglion cells by glutamate-mediated afferent activity.* The Journal of neuroscience : the official journal of the Society for Neuroscience, 1995. **15**(11): p. 7037-7045.

20. Komiyama, T. and L. Luo, *Intrinsic control of precise dendritic targeting by an ensemble of transcription factors.* Current biology : CB, 2007. **17**(3): p. 278-285.

21. Mumm, J.S., et al., *In vivo imaging reveals dendritic targeting of laminated afferents by zebrafish retinal ganglion cells.* Neuron, 2006. **52**(4): p. 609-621.

22. Coombs, J.L., D. Van Der List, and L.M. Chalupa, *Morphological properties of mouse retinal ganglion cells during postnatal development.* J Comp Neurol, 2007. **503**(6): p. 803-14.

23. Kim, I.J., et al., *Laminar restriction of retinal ganglion cell dendrites and axons: subtype-specific developmental patterns revealed with transgenic markers.* J Neurosci. **30**(4): p. 1452-62.

24. Lee, T. and L. Luo, *Mosaic analysis with a repressible cell marker (MARCM) for Drosophila neural development.* Trends Neurosci, 2001. **24**(5): p. 251-4.

25. Jefferis, G.S., et al., *Target neuron prespecification in the olfactory map of Drosophila.* Nature, 2001. **414**(6860): p. 204-8.

26. Jefferis, G.S., et al., *Developmental origin of wiring specificity in the olfactory system of Drosophila.* Development, 2004. **131**(1): p. 117-30.

27. Komiyama, T., et al., *Graded expression of semaphorin-1a cell-autonomously directs dendritic targeting of olfactory projection neurons.* Cell, 2007. **128**(2): p. 399-410.

28. Hong, W., et al., *Leucine-rich repeat transmembrane proteins instruct discrete dendrite targeting in an olfactory map.* Nat Neurosci, 2009. **12**(12): p. 1542-50.

29. Yamagata, M. and J.R. Sanes, *Dscam and Sidekick proteins direct lamina-specific synaptic connections in vertebrate retina.* Nature, 2008. **451**(7177): p. 465-469.

30. Woolsey, T.A. and H. Van der Loos, *The structural organization of layer IV in the somatosensory region (SI) of mouse cerebral cortex. The description of a cortical field composed of discrete cytoarchitectonic units.* Brain Res, 1970. **17**(2): p. 205-42.

31. Harris, R.M. and T.A. Woolsey, *Morphology of golgi-impregnated neurons in mouse cortical barrels following vibrissae damage at different post-natal ages.* Brain Res, 1979. **161**(1): p. 143-9.

32. Harris, R.M. and T.A. Woolsey, *Dendritic plasticity in mouse barrel cortex following postnatal vibrissa follicle damage.* J Comp Neurol, 1981. **196**(3): p. 357-76.

33. Law, M.I. and M. Constantine-Paton, *Anatomy and physiology of experimentally produced striped tecta.* J Neurosci, 1981. **1**(7): p. 741-59.

34. Constantine-Paton, M. and M.I. Law, *Eye-specific termination bands in tecta of three-eyed frogs.* Science, 1978. **202**(4368): p. 639-41.

35. Katz, L.C. and M. Constantine-Paton, *Relationships between segregated afferents and postsynaptic neurones in the optic tectum of three-eyed frogs.* J Neurosci, 1988. **8**(9): p. 3160-80.

36. Sin, W.C., et al., *Dendrite growth increased by visual activity requires NMDA receptor and Rho GTPases.* Nature, 2002. **419**(6906): p. 475-480.

37. Verhage, M., et al., *Synaptic assembly of the brain in the absence of neurotransmitter secretion.* Science, 2000. **287**(5454): p. 864-9.

38. Kerschensteiner, D., et al., *Neurotransmission selectively regulates synapse formation in parallel circuits in vivo.* Nature, 2009. **460**(7258): p. 1016-1020.

39. McAllister, A.K., *Cellular and molecular mechanisms of dendrite growth.* Cereb Cortex, 2000. **10**(10): p. 963-73.

40. Vaughn, J.E., R.P. Barber, and T.J. Sims, *Dendritic development and preferential growth into synaptogenic fields: a quantitative study of Golgi-impregnated spinal motor neurons.* Synapse, 1988. **2**(1): p. 69-78.

41. Dailey, M.E. and S.J. Smith, *The dynamics of dendritic structure in developing hippocampal slices.* J Neurosci, 1996. **16**(9): p. 2983-94.

42. Wong, W.T. and R.O. Wong, *Rapid dendritic movements during synapse formation and rearrangement.* Curr Opin Neurobiol, 2000. **10**(1): p. 118-24.

43. Dunaevsky, A., et al., *Developmental regulation of spine motility in the mammalian central nervous system.* Proc Natl Acad Sci U S A, 1999. **96**(23): p. 13438-43.

44. Dailey, M.E., et al., *Mossy fiber growth and synaptogenesis in rat hippocampal slices in vitro.* J Neurosci, 1994. **14**(3 Pt 1): p. 1060-78.

45. Wu, G.Y., et al., *Dendritic dynamics in vivo change during neuronal maturation.* J Neurosci, 1999. **19**(11): p. 4472-83.

46. Jontes, J.D. and S.J. Smith, *Filopodia, spines, and the generation of synaptic diversity.* Neuron, 2000. **27**(1): p. 11-4.

47. Jontes, J.D., J. Buchanan, and S.J. Smith, *Growth cone and dendrite dynamics in zebrafish embryos: early events in synaptogenesis imaged in vivo.* Nat Neurosci, 2000. **3**(3): p. 231-7.

48. Lohmann, C. and T. Bonhoeffer, *A role for local calcium signaling in rapid synaptic partner selection by dendritic filopodia.* Neuron, 2008. **59**(2): p. 253-260.

49. Cline, H. and K. Haas, *The regulation of dendritic arbor development and plasticity by glutamatergic synaptic input: a review of the synaptotrophic hypothesis.* J Physiol, 2008. **586**(6): p. 1509-17.

50. Niell, C.M., M.P. Meyer, and S.J. Smith, *In vivo imaging of synapse formation on a growing dendritic arbor.* Nat Neurosci, 2004. **7**(3): p. 254-60.

51. Maletic-Savatic, M., R. Malinow, and K. Svoboda, *Rapid dendritic morphogenesis in CA1 hippocampal dendrites induced by synaptic activity.* Science, 1999. **283**(5409): p. 1923-7.

52. Rajan, I. and H.T. Cline, *Glutamate receptor activity is required for normal development of tectal cell dendrites in vivo.* J Neurosci, 1998. **18**(19): p. 7836-46.

53. Rajan, I., S. Witte, and H.T. Cline, *NMDA receptor activity stabilizes presynaptic retinotectal axons and postsynaptic optic tectal cell dendrites in vivo.* J Neurobiol, 1999. **38**(3): p. 357-68.

54. Portera-Cailliau, C., D.T. Pan, and R. Yuste, *Activity-regulated dynamic behavior of early dendritic protrusions: evidence for different types of dendritic filopodia.* J Neurosci, 2003. **23**(18): p. 7129-42.

55. Shen, W., et al., *Type A GABA-receptor-dependent synaptic transmission sculpts dendritic arbor structure in Xenopus tadpoles in vivo.* J Neurosci, 2009. **29**(15): p. 5032-43.

56. Luikart, B.W., et al., *Neurotrophin-dependent dendritic filopodial motility: a convergence on PI3K signaling.* J Neurosci, 2008. **28**(27): p. 7006-12.

57. Kayser, M.S., M.J. Nolt, and M.B. Dalva, *EphB receptors couple dendritic filopodia motility to synapse formation.* Neuron, 2008. **59**(1): p. 56-69.

58. Lohmann, C., K.L. Myhr, and R.O. Wong, *Transmitter-evoked local calcium release stabilizes developing dendrites.* Nature, 2002. **418**(6894): p. 177-181.

59. Lohmann, C., A. Finski, and T. Bonhoeffer, *Local calcium transients regulate the spontaneous motility of dendritic filopodia.* Nature neuroscience, 2005. **8**(3): p. 305-312.

60. Wierenga, C.J., N. Becker, and T. Bonhoeffer, *GABAergic synapses are formed without the involvement of dendritic protrusions.* Nat Neurosci, 2008. **11**(9): p. 1044-52.

61. Garner, C.C., C.L. Waites, and N.E. Ziv, *Synapse development: still looking for the forest, still lost in the trees.* Cell Tissue Res, 2006. **326**(2): p. 249-62.

62. Ziv, N.E. and C.C. Garner, *Principles of glutamatergic synapse formation: seeing the forest for the trees.* Curr Opin Neurobiol, 2001. **11**(5): p. 536-43.

63. Baek, M. and R.S. Mann, *Lineage and birth date specify motor neuron targeting and dendritic architecture in adult Drosophila.* J Neurosci, 2009. **29**(21): p. 6904-16.

64. Brierley, D.J., et al., *Dendritic targeting in the leg neuropil of Drosophila: the role of midline signalling molecules in generating a myotopic map.* PLoS Biol, 2009. **7**(9): p. e1000199.

65. Landgraf, M., et al., *Embryonic origins of a motor system: motor dendrites form a myotopic map in Drosophila.* PLoS biology, 2003. **1**(2): p. E41.

66. Mauss, A., et al., *Midline signalling systems direct the formation of a neural map by dendritic targeting in the Drosophila motor system.* PLoS biology, 2009. **7**(9): p. e1000200.

67. Tripodi, M., et al., *Structural homeostasis: compensatory adjustments of dendritic arbor geometry in response to variations of synaptic input.* PLoS biology, 2008. **6**(10): p. e260.

68. Cullheim, S., et al., *Three-dimensional architecture of dendritic trees in type-identified alpha-motoneurons.* J Comp Neurol, 1987. **255**(1): p. 82-96.

69. Ruigrok, T.J., A. Crowe, and H.J. ten Donkelaar, *Dendrite distribution of identified motoneurons in the lumbar spinal cord of the turtle Pseudemys scripta elegans.* J Comp Neurol, 1985. **238**(3): p. 275-85.

70. Okado, N., et al., *Distribution patterns of dendrites in motor neuron pools of lumbosacral spinal cord of the chicken.* Anat Embryol (Berl), 1990. **182**(2): p. 113-21.

71. Lichtman, J.W. and E. Frank, *Physiological evidence for specificity of synaptic connections between individual sensory and motor neurons in the brachial spinal cord of the bullfrog.* J Neurosci, 1984. **4**(7): p. 1745-53.

72. Lichtman, J.W., S. Jhaveri, and E. Frank, *Anatomical basis of specific connections between sensory axons and motor neurons in the brachial spinal cord of the bullfrog.* J Neurosci, 1984. **4**(7): p. 1754-63.

73. Vrieseling, E. and S. Arber, *Target-induced transcriptional control of dendritic patterning and connectivity in motor neurons by the ETS gene Pea3.* Cell, 2006. **127**(7): p. 1439-52.

74. Livet, J., et al., *ETS gene Pea3 controls the central position and terminal arborization of specific motor neuron pools.* Neuron, 2002. **35**(5): p. 877-92.

75. Pecho-Vrieseling, E., et al., *Specificity of sensory-motor connections encoded by Sema3e-Plxnd1 recognition.* Nature, 2009. **459**(7248): p. 842-6.

76. Scheibel, M.E. and A.B. Scheibel, *Developmental relationship between spinal motoneuron dendrite bundles and patterned activity in the hind limb of cats.* Exp Neurol, 1970. **29**(2): p. 328-35.

77. Kalb, R.G., *Regulation of motor neuron dendrite growth by NMDA receptor activation.* Development, 1994. **120**(11): p. 3063-71.

78. Li, Y., et al., *Developmental changes in spinal motoneuron dendrites in neonatal mice.* J Comp Neurol, 2005. **483**(3): p. 304-17.

79. Ulfhake, B., S. Cullheim, and P. Franson, *Postnatal development of cat hind limb motoneurons. I: Changes in length, branching structure, and spatial distribution of dendrites of cat triceps surae motoneurons.* J Comp Neurol, 1988. **278**(1): p. 69-87.

80. Inglis, F.M., K.E. Zuckerman, and R.G. Kalb, *Experience-dependent development of spinal motor neurons.* Neuron, 2000. **26**(2): p. 299-305.

81. Inglis, F.M., et al., *The AMPA receptor subunit GluR1 regulates dendritic architecture of motor neurons.* J Neurosci, 2002. **22**(18): p. 8042-51.

82. Zhang, L., et al., *Role of GluR1 in activity-dependent motor system development.* J Neurosci, 2008. **28**(40): p. 9953-68.

83. Prithviraj, R., et al., *Differential regulation of dendrite complexity by AMPA receptor subunits GluR1 and GluR2 in motor neurons.* Dev Neurobiol, 2008. **68**(2): p. 247-64.

84. Brustein, E., et al., *Steps during the development of the zebrafish locomotor network.* J Physiol Paris, 2003. **97**(1): p. 77-86.

85. Fetcho, J.R. and D.H. Bhatt, *Genes and photons: new avenues into the neuronal basis of behavior.* Curr Opin Neurobiol, 2004. **14**(6): p. 707-14.

86. McLean, D.L. and J.R. Fetcho, *Using imaging and genetics in zebrafish to study developing spinal circuits in vivo.* Developmental neurobiology, 2008. **68**(6): p. 817-834.

87. Higashijima, S., *Transgenic zebrafish expressing fluorescent proteins in central nervous system neurons.* Dev Growth Differ, 2008. **50**(6): p. 407-13.

88. Asakawa, K. and K. Kawakami, *The Tol2-mediated Gal4-UAS method for gene and enhancer trapping in zebrafish.* Methods, 2009. **49**(3): p. 275-81.

89. Beattie, C.E., et al., *Temporal separation in the specification of primary and secondary motoneurons in zebrafish.* Dev Biol, 1997. **187**(2): p. 171-82.

90. Kimura, Y., Y. Okamura, and S. Higashijima, *alx, a zebrafish homolog of Chx10, marks ipsilateral descending excitatory interneurons that participate in the regulation of spinal locomotor circuits.* J Neurosci, 2006. **26**(21): p. 5684-97.

91. Liu, D.W. and M. Westerfield, *Function of identified motoneurones and co-ordination of primary and secondary motor systems during zebra fish swimming.* J Physiol, 1988. **403**: p. 73-89.

92. Myers, P.Z., J.S. Eisen, and M. Westerfield, *Development and axonal outgrowth of identified motoneurons in the zebrafish.* J Neurosci, 1986. **6**(8): p. 2278-89.

93. Luo, L. and J.G. Flanagan, *Development of continuous and discrete neural maps.* Neuron, 2007. **56**(2): p. 284-300.

94. Ruthazer, E.S., *You're perfect, now change--redefining the role of developmental plasticity.* Neuron, 2005. **45**(6): p. 825-8.

95. Bhatt, D.H., et al., *Grading movement strength by changes in firing intensity versus recruitment of spinal interneurons.* Neuron, 2007. **53**(1): p. 91-102.

96. Kim, M.D., Y. Wen, and Y.N. Jan, *Patterning and organization of motor neuron dendrites in the Drosophila larva.* Dev Biol, 2009. **336**(2): p. 213-21.

97. Chklovskii, D.B. and A.A. Koulakov, *Maps in the brain: what can we learn from them?* Annu Rev Neurosci, 2004. **27**: p. 369-92.

98. Stepanyants, A. and D.B. Chklovskii, *Neurogeometry and potential synaptic connectivity.* Trends Neurosci, 2005. **28**(7): p. 387-94.

99. Wen, Q. and D.B. Chklovskii, *A cost-benefit analysis of neuronal morphology.* J Neurophysiol, 2008. **99**(5): p. 2320-8.

100. McLean, D.L., et al., *Continuous shifts in the active set of spinal interneurons during changes in locomotor speed.* Nature neuroscience, 2008. **11**(12): p. 1419-1429.

101. Livet, J., et al., *Transgenic strategies for combinatorial expression of fluorescent proteins in the nervous system.* Nature, 2007. **450**(7166): p. 56-62.

102. Zhang, F., et al., *Circuit-breakers: optical technologies for probing neural signals and systems.* Nat Rev Neurosci, 2007. **8**(8): p. 577-81.

103. Koster, R.W. and S.E. Fraser, *Tracing transgene expression in living zebrafish embryos.* Dev Biol, 2001. **233**(2): p. 329-46.

104. Muto, A., et al., *Forward genetic analysis of visual behavior in zebrafish.* PLoS Genet, 2005. **1**(5): p. e66.

105. Wong, W.T., et al., *Rapid dendritic remodeling in the developing retina: dependence on neurotransmission and reciprocal regulation by Rac and Rho.* J Neurosci, 2000. **20**(13): p. 5024-36.

106. Heiman, M.G. and S. Shaham, *Twigs into branches: how a filopodium becomes a dendrite.* Current opinion in neurobiology, 2009.

107. Wu, G.Y. and H.T. Cline, *Stabilization of dendritic arbor structure in vivo by CaMKII.* Science, 1998. **279**(5348): p. 222-6.

108. Haas, K., J. Li, and H.T. Cline, *AMPA receptors regulate experience-dependent dendritic arbor growth in vivo.* Proc Natl Acad Sci U S A, 2006. **103**(32): p. 12127-31.

109. Hua, J.Y., et al., *Regulation of axon growth in vivo by activity-based competition.* Nature, 2005. **434**(7036): p. 1022-1026.

110. Provost, E., J. Rhee, and S.D. Leach, *Viral 2A peptides allow expression of multiple proteins from a single ORF in transgenic zebrafish embryos.* Genesis, 2007. **45**(10): p. 625-9.

111. Tang, W., et al., *Faithful expression of multiple proteins via 2A-peptide self-processing: a versatile and reliable method for manipulating brain circuits.* J Neurosci, 2009. **29**(27): p. 8621-9.

112. Cancedda, L., et al., *Excitatory GABA action is essential for morphological maturation of cortical neurons in vivo.* J Neurosci, 2007. **27**(19): p. 5224-35.

113. Yu, C.R., et al., *Spontaneous neural activity is required for the establishment and maintenance of the olfactory sensory map.* Neuron, 2004. **42**(4): p. 553-66.

114. Smear, M.C., et al., *Vesicular glutamate transport at a central synapse limits the acuity of visual perception in zebrafish.* Neuron, 2007. **53**(1): p. 65-77.

115. Lendvai, B., et al., *Experience-dependent plasticity of dendritic spines in the developing rat barrel cortex in vivo.* Nature, 2000. **404**(6780): p. 876-81.

116. Turrigiano, G.G., *The self-tuning neuron: synaptic scaling of excitatory synapses.* Cell, 2008. **135**(3): p. 422-35.

117. Burrone, J. and V.N. Murthy, *Synaptic gain control and homeostasis.* Curr Opin Neurobiol, 2003. **13**(5): p. 560-7.

118. Burrone, J., M. O'Byrne, and V.N. Murthy, *Multiple forms of synaptic plasticity triggered by selective suppression of activity in individual neurons.* Nature, 2002. **420**(6914): p. 414-8.

119. Konur, S. and A. Ghosh, *Calcium signaling and the control of dendritic development.* Neuron, 2005. **46**(3): p. 401-5.

120. Wu, J.I., et al., *Regulation of dendritic development by neuron-specific chromatin remodeling complexes.* Neuron, 2007. **56**(1): p. 94-108.

121. Lohmann, C. and R.O. Wong, *Regulation of dendritic growth and plasticity by local and global calcium dynamics.* Cell calcium, 2005. **37**(5): p. 403-409.

122. Schwartz, N., A. Schohl, and E.S. Ruthazer, *Neural activity regulates synaptic properties and dendritic structure in vivo through calcineurin/NFAT signaling.* Neuron, 2009. **62**(5): p. 655-69.

123. Redmond, L. and A. Ghosh, *Regulation of dendritic development by calcium signaling.* Cell Calcium, 2005. **37**(5): p. 411-6.

124. Peng, Y.R., et al., *Coordinated changes in dendritic arborization and synaptic strength during neural circuit development.* Neuron, 2009. **61**(1): p. 71-84.

125. Kwan, K.M., et al., *The Tol2kit: a multisite gateway-based construction kit for Tol2 transposon transgenesis constructs.* Dev Dyn, 2007. **236**(11): p. 3088-99.